REPORT OF INVESTIGATION 36

MESOMETEOROLOGY PROJECT
DEPARTMENT OF METEOROLOGY
THE UNIVERSITY OF CHICAGO
5727 UNIVERSITY AVENUE
CHICAGO 37, ILLINOIS

STATE OF ILLINOIS
WILLIAM G. STRATTON, Governor

DEPARTMENT OF REGISTRATION AND EDUCATION
VERA M. BINKS, Director

Three-Dimensional Mesoanalysis of a Squall Line

BY T. FUJITA

This report appears also as Research Report 1, Contract No. DA-36-039 SC64656, Army Sub-Task 3-99-04-112 for the U. S. Army Signal Corps Engineering Laboratories, Fort Monmouth, New Jersey

ILLINOIS STATE WATER SURVEY
WILLIAM C. ACKERMANN, Chief
URBANA
1958

Printed by authority of State of Illinois
14 (76521—4-58)

ILLINOIS STATE WATER SURVEY

METEOROLOGIC LABORATORY

Urbana, Illinois

THREE-DIMENSIONAL MESOANALYSIS OF A SQUALL LINE

By

Tetsuya Fujita

A Cooperative Study
by
The University of Chicago
and
Illinois State Water Survey
with
Partial Support from the U. S. Weather Bureau

prepared as

RESEARCH REPORT NO. 1
under
Contract No. DA-36-039 SC-64656
with
U. S. Army Signal Engineering Laboratories
Fort Monmouth, New Jersey
Army Sub-Task 3-99-04-112
November 1957

Table of Contents

	Page
Abstract	1
Introduction	1
Synoptic Situation	2
Hourly Mesocharts	3
Preparation of 10-Minute Interval Charts	5
10-Minute Interval Charts	8
Composite Charts	13
Vertical Cross Section	15
Conclusions	17
Acknowledgments	18
References	19
Figures	20-80

THREE-DIMENSIONAL MESOANALYSIS OF A SQUALL LINE

by

Tetsuya Fujita
The University of Chicago

ABSTRACT

Using the surface and upper air observations taken on 29 June 1947, by the Thunderstorm Project in Ohio, composite charts covering an area of 130 by 100 miles were analyzed. The levels of analysis were: 980 (surface), 950, 850, 800, 700, 500, 400, 300 and 200 mb. This analysis revealed that the pressure surge line studied did not result from an upper disturbance, but was the leading edge of an outflowing cold air dome, the top of which did not reach the 700 mb level. A sharp ridge line, however, was found above the 400 mb level. No evidence of discontinuity in temperature and wind velocity was found at any level above the surface pressure surge line east of the cold dome.

INTRODUCTION

Knowledge regarding mesoscale systems over the Midwestern part of the United States has been increasing rapidly. Mesoanalyses of the area covered by the U. S. Weather Bureau's Severe Local Storm Network in Texas and Oklahoma revealed the important relationship existing between the development of mesosystems and the occurrence of severe storms. Fujita, Newstein

and Tepper[3] emphasized the importance of mesosystems through their study of the June 24, 1953 case. Rather small features of mesosystems have been studied by the Illinois State Water Survey in a careful analysis of the 1947 Thunderstorm Project data. Their results were summarized by Stout.[5]

Several authors have tried a theoretical approach to the three-dimensional structure and the movement of squall lines: Tepper[6] who explained pressure jumps by the gravitational wave hypothesis, and Newton, who considered the divergence and convergence fields generated by the activity of the squall line itself.[4]

Attempts to construct an upper air chart in the vicinity of any pressure jump proved unsuccessful because of the scarcity of radiosonde ascents made in storm areas. So far, no upper air data have been taken over a small area and at short time intervals, except those obtained by the Thunderstorm Project. The author tried to make the most of the observations taken by the Thunderstorm Project in Ohio, and the case of June 29, 1947 was selected as the most favorable, because of the large number of ascents available for that date.

The present study, begun in 1954, progressed intermittently with the development of mesoanalysis techniques by the author and his collaborators. The analysis was done with the use of base maps of three different sizes, covering respective areas of 1500 by 2000 miles, 200 by 300 miles, and 20 by 40 miles. The operating area of the Thunderstorm Project appears near the center of the base maps.

SYNOPTIC SITUATION

As shown in the surface chart for 2230 EST on June 29, 1947 (Fig. 1) a cold front extended from eastern Ontario to the center of a small low in Kansas. The mesosystem analyzed in this study started forming several hours prior to the map time. This formation took place inside the warm sector, approximately 30 miles east of the cold front. In four to five hours, the system reached its mature stage with dimensions of 100 by 200 miles. The rectangle in the chart indicates the area covered by the composite chart shown later. (Fig. 2)

The 850 mb chart at 2200 EST (Fig. 2) gives the impression that the mesosystem referred to as a mesohigh had moved out of the cold front. Examination of the chart shows that the mesosystem was almost vertical whereas the cold frontal surface was tilted westward, so that the front at the 850 mb surface was located considerably farther northwest. A cut-off low, off the East Coast, had circular isobars at this level with a developed circulation around its center.

The mesosystem existing over Ohio is not visible on the 700 mb chart (Fig. 3). The winds observed by the Thunderstorm Project at this level fit the large scale features very well. From this observation it may be postulated that the top of this mesoscale cold dome did not reach the 700 mb level. This will permit drawing a chart by smoothing out the contours inside the squall line area.

No basic difference appears in the height pattern between the 700 and the 500 mb charts. As may be seen in the 500 mb chart (Fig. 4), the winds recorded by the Thunderstorm Project also fit the larger pattern of the chart. At this level, the center of the anticyclone is located considerably farther to the west, while the axis of the cut-off low to the east remained vertical.

The 300 mb chart (Fig. 5) does not contain enough observations to permit an accurate analysis. If the analysis presented here is accepted, the south-southwesterly winds observed by the Thunderstorm Project after the passage of the pressure surge line were almost normal to the height contour. In any event, the radius of curvature of this anticyclonic stream line was so small that it must be explained in relation to a mesoscale disturbance.

HOURLY MESOCHARTS

On June 29, 1947, four mesosystems were seen within 200 miles of the area of the Thunderstorm Project. Isochrones of these mesosystems and of a cold front are shown in Figure 6. The systems were designated by numbers indicating the day and the hour of their first appearance. Each of the four systems originated in a small area inside the warm sector, 30 to 50 miles southeast of the cold front. They first appeared to the north, then their

location gradually shifted southward.

Mesosystem 917, which moved over the network, appeared 50 miles northwest of the radar station. Three hours after its initiation, it reached maturity and dissipated in another four hours.

The first chart of mesoanalysis (Fig. 7) shows the situation at 1700 EST when mesosystem 917 started developing in an area of 20 by 30 miles. On this chart and the following charts the stippled areas represent the precipitation during the hour preceding map time and the dashed line shows the boundary of the mesosystem. The double circle in the chart describes the maximum effective range of the radar at Wilmington Air Force Base. Over Lake Erie, mesosystem 913 had reached its mature stage. The pressure surge line of this system was accompanied by gusts as high as 30 mph.

In one hour mesosystem 917, in which solid echoes were observed, grew rapidly. The chart at 1800 EST (Fig. 8) indicates that the excess pressure had reached 3 mbs. Small echoes scattered outside the system were not organized, so that the thunderstorm high, beneath the echoes, was of negligible significance. Systems 916 and 917 produced an extensive rain area. Inside system 913, on the other hand, the rain area had considerably diminished, indicating that the weakened mesohigh had been overtaken by the developing wake low.

As can be seen in Figure 9, by 1900 EST systems 916 and 917 were merging. The solid echo northwest of the radar station was located above the areas of high wind which followed the pressure surge line. The southern portion of the line had moved out of the rain area, and a dry pressure surge line had formed. The excess pressure near the center of the system had reached 4 mb.

By this time, system 913 had dissipated further, and its southern portion was covered by the newly developed system 916. Small echo groups to the south of the radar station produced some rain on the ground, but the pressure field beneath the echoes was not organized. The patches of rain behind the cold front did not develop into mesosystems.

The chart for 2000 EST in Figure 10 shows the features of systems 916 and 917 in their early dissipating stage. This stage may be characterized by a weakening pressure surge line, a decrease in excess pressure, the disintegration of solid echoes into scattered ones, etc. As a rule, a pressure surge line moves away from rain areas. The high in the southern part of the mesosystem is related to the still active thunderstorm cell. This type of high with a horizontal dimension of one to ten miles may be termed "cellular high" and usually moves with the main cell.

The last system, 919, started to develop in Kentucky about 50 miles southeast of the cold front. Its detailed features are not known due to the large distances between reporting stations.

Figure 11, the last hourly chart at 2100 EST, represents systems 916 and 917 in their dissipating stage. Some squall line activity still exists west of the pressure surge line near the center of the systems, but it has greatly diminished elsewhere. The echoes within the effective radar range are disintegrating cells that are no longer in a line,

PREPARATION OF 10-MINUTE INTERVAL CHARTS

The basic data used for the analysis of surface charts are the original traces from the Thunderstorm Project. In addition, traces and visual observations from the stations in the vicinity of the Network were supplied by the National Weather Records Center, Asheville, North Carolina.

The area analyzed at every 10-minute interval appears in Figure 12. The Thunderstorm Project Network consisted of numbered interior and lettered exterior stations. The radar was located to the north of the Network at B.

The following surface weather elements were recorded at the Network stations. A description of the instruments at the Network stations is given in The Thunderstorm.[1]

1. Temperature and relative humidity
2. Pressure
3. Wind direction and wind speed

4. Precipitation

5. Visual observation and cloud photographs: Observations were taken at stations 39, A, B, C and F

The time check of the clocks was done once a day when the recording sheets were changed, but after the fast or slow moving clocks had presumably been corrected, some time discrepancies were still found among the traces. The rain gauge trace showed that the pen recorded the oscillations of the gauge itself as well as the accumulated rain amount. The oscillations were found to coincide with periods of strong gusty winds. Figure 13 shows an example of the relationship existing between high winds and the rain gauge. It is evident that gusts A and B correspond to oscillations A' and B'.

As the rain gauge and the wind instrument were standing very close to each other, the time of their two records could be adjusted. The amount of correction thus established is: 0 min for 15 stations, 1 min for 5 stations, 2 min for 10 stations, 3 min for 5 stations, 4 min for 1 station, 5 min for 2 stations. No station needed any correction larger than 6 min and 9 stations showed no indication of rain gauge oscillation.

After careful time checks, the time sections for all the network and regular Weather Bureau stations in the vicinity were prepared. Figure 14 shows examples of such time sections.

The technique used for making surface charts from the time sections thus prepared is exactly the same as that indicated in previous papers published by the writer.(2)(3)

On June 29, 1947, upper air observations were taken at the 11 available stations. The rawin equipment at station A, C, F, G and H, Radio Set SCR-584, was a micro-wave radar set with a wind measurement accuracy of 2 degrees in direction and 2 mph in speed. The rawinsonde equipment used at station 7, 19, 39, 47, D and E consisted of a Radio Set SCR-658 and of an AN/FMQ-1 Cycloray Recorder. The distribution of upper air stations appears in Figure 15.

In regular upper air analysis little consideration is given to either the time or the location of the balloons, but in an analysis done on the present scale, "one minute" and "one mile" are no longer negligible. Fortunately, the location of the balloon, the time of observation and the wind velocity, tabulated by the Thunderstorm Project analysts, were available for every 1000 ft; these data were plotted for each ascent.

Now the upper air chart is ready for plotting, but the level best suited for analysis at a given time must still be chosen. Figure 16 shows the number of balloons available for every 10-minute interval at each 100 mb level. The slanted lines represent the time-height curve of each balloon released during the entire period. The figures in circles give the number of balloons passing through each pressure level within the 10 minutes before and after a given time. Two consecutive levels are selected in order to analyze the winds at both levels on a single chart.

Figure 17 demonstrates how winds at two levels were plotted on one chart. The symbols representing the wind at the higher level are made larger than the ones showing those at the lower level. The numbers near the wind symbol refer to the time at which the balloon penetrated that particular level. The radar echoes are plotted in the upper air chart for every 10-minute interval. In order to indicate whether the balloon is inside or outside the echo, the location of the balloons must be adjusted with respect to echo movement. The upper right section of the figure represents the vector of echo movement for 10-minute periods before and after the map time. Using this vector, a balloon penetrating the constant pressure surface at 1820 EST, 10 minutes after the map time, for example, is shifted a half inch to the left. The location of each balloon in the 10-minute interval charts gives the spatial relationship between balloons and echoes.

An analysis of maps made at 10-minute intervals was completed for an area of 44 by 53 statute miles. This analysis consists of sets of two maps each, covering the same area at the same map time. In the right hand chart analyses of the distribution of surface winds (long barbs = 5 mph), sea level isobars for every 0.2 mb, isotherms of station temperature for

every 2°F, and radar echoes are shown. The left hand chart represents upper winds at consecutive 100 mb levels (upper level in red, long barbs = 5 mph), temperature and relative humidity, surface rain intensity contoured for every 1.0 inch per hour, and radar echoes with their movement in knots. The location of each balloon is adjusted with respect to echo movement to indicate whether or not the balloon is inside an echo.

10-MINUTE INTERVAL CHARTS

The first chart at 1630 EST (Fig. 18) shows the winds in the warm sector, roughly 100 miles from the cold front which was approaching the Network at a speed of 20 knots. Surface winds of 5 to 10 mph over the Network increased in speed to 15 to 20 knots at the 900 mb level. Surface and 900 mb winds had the same direction; however, from the 900 to the 800 mb level, a shift from south-southwest to southwest was observed.

At 1640 EST (Fig. 19) the upper winds which had shifted sharply to the west-northwest at the 700 mb level, returned due west at the 600 mb level. Surface winds show no variation from the previous chart.

The 500 and 400 mb chart at 1650 EST (Fig. 20) shows winds similar in both speed and direction to those of the 600 mb level. Such a wind field in deep layers is capable of steering embedded echoes and it favors the development of cumulus clouds.

The 300 and 200 mb level chart at 1700 EST (Fig. 21) pictures winds quite different from those of the underlying flow pattern. A marked decrease in speed at the higher levels is noticed.

The surface winds of the Project area remained unchanged until 1710 EST (Fig. 22) when the surface isobars started curving under the influence of the approaching trough.

The first radar echo formed inside the analysis area at 1718 EST; it can be seen at the northwest corner of the 1720 EST chart (Fig. 23). It was followed one minute later by a second echo appearing 5 miles to its northwest. Both were moving east-northeast at a speed of 21 knots.

Ten minutes later at 1730 EST (Fig. 24) the first echo in the previous chart grew to 4 by 4 miles and two bright spots were seen in it. The second echo also developed rapidly. A small trough passing over the Network had not disturbed the surface winds. The cloud base at this time was 3,000 ft above ground, and the top of scattered cumuli over the Network reached 5,000 to 6,000 feet.

Echoes appearing to the north in the 1740 EST chart (Fig. 25) were identified by the observer at the radar station as very dark and heavy cumuli. A new development was taking place 10 miles west of the Network; its top reached 9,000 ft and its base rested at 3,000 ft. It had not yet appeared on the radar screen.

Ten minutes later the top of the cumulus observed to the west had risen to 20,500 ft, and the radar picked up the echo associated with it. As shown in the 1750 EST chart (Fig. 26), this echo was moving east northeast at a speed of 19 knots. Visual observation showed its diameter to be two miles and indicated that it was part of a larger cloud, ten miles in diameter.

A second group of balloons was released slightly before the 1800 EST map time, (Fig. 27). Wind, temperature and humidity for both the 900 and 800 mb levels are plotted in the chart under discussion. Surface temperature values are plotted in the vicinity of radar echoes on the surface chart. The cumulus which appeared to the west had reached the northwest corner of the Network. Its top had already become inactive and the diameter of the visible cloud had considerably decreased. Thunder was heard and precipitation was visible in the dark cloud to the north of the Network. To the south, on the other hand, a large cumulonimbus top was moving toward the southwest corner of the Network.

The 1810 EST chart (Fig. 28) represents winds and temperatures at the 700 and 600 mb levels. A balloon caught in a cloud, at the lower left of the Network, was moving with a larger southerly component than the general flow pattern. It is not known whether or not this movement is related to a mesoscale phenomenon. The top of the cloud under discussion reached 22,000 ft

and its visible diameter was five miles; beneath it, a light surface rain as well as a cool area were observed. Another cloud over the northwest corner of the Network produced a few raindrops on the ground.

The top of the cumulonimbus over the southern part of the Network reached 18,000 ft by 1820 EST. A cirrus streamer drifted as far as ten miles from its top, and was embedded in the westerly flow which reached the 450 mb level (see Fig. 29). At this time, the weather stations observed heavy precipitation and thunder to the north. The pressure surge line and the mesosystem appeared in the upper left corner of the chart.

At 1830 EST (Fig. 30) the pressure surge line was moving southeastward at a speed of 20 knots. Station C located northwest of the Network reported stratocumuli at 2500 ft; they were moving from the west-southwest. Although the exact location of the clouds was not given, they should be east of the line, where the wind direction was west-southwest. Huge scattered cumuli were sighted to the south; one of them was producing light rain and considerable cooling. At the time of the storm passage, however, the increase in pressure beneath the cloud was only a fraction of a millibar. Winds at the 300 and 200 mb levels were northwesterly, with an average speed of 15 to 20 mph.

The echo over the lower right of the Network was in its dissipating stage; the top of the visible cloud reached 15,000 ft. Intense rain occurred under the echo. As may be seen in the chart for 1840 EST (Fig. 31), a field of diverging winds formed directly below this cloud. The pressure surge line reached Station C. Heavy rain and lightning were reported to the north of the station. No particular phenomenon occurred aloft. A break in the storm at the surface was observed to the north, between the forerunning echo and the main ones.

At 1850 EST (Fig. 32) the pressure surge line had moved four miles southeastward beyond Station C. No rain had reached the station yet, and the leading edge of Sc, St, Fs, and Fc, which later mushroomed over the station, was still three miles away to the northwest. Scattered echoes to the south were moving eastward at 21 to 22 knots. Some of them were

accompanied by thunder. Other storm cells were not large enough to produce cellular highs which would merge into a mesoscale thunderstorm high.

The 1900 EST (Fig. 33) chart gives an idea of the pressure line as it passed across the main part of the Project area. It was located as far as ten miles southwest of the edge of the rain areas. Most of the stations it reached recorded a pressure jump of considerable magnitude, followed shortly afterward by a sharp drop in temperature. No significant cloud change was noticed with the jump; but Fc, Sc, St, part of which formed a scud roll, moved over the stations some 10 minutes after the passage of the line.

Small cells of radar echoes appeared west of the Network. The largest echo in the 1910 EST chart (Fig. 34) was accompanied by a small cellular high and possible surface rain. At Station F southwest of the Network, low fibrous clouds with billowing bottoms appeared overhead to the east. The speed of the surface winds which followed the surge line increased to 25 mph with gusts of 30 to 40 mph. To the north of the Network a large radar echo was observed. As the cells developed, they joined to form a line of showers.

The 1920 EST chart (Fig. 35) shows the relationship existing between precipitation and the cellular highs beneath the clouds. A future attempt might be made to relate winds and isobars, as is done in regular synoptic charts, but in the present scale no simple relationship between them is known. In a section west of the surge line the wind is blowing toward an area of high pressure.

The showers, lined up near the center of the chart, reached their mature stage at 1930 EST (see Fig. 36), a time when the pressure surge line had already swept the entire Network area. A new cell was rapidly developing south of the shower line. A balloon released from Station 47, exactly under this developing cell, ascended through the 900 and 800 mb levels. The 800 mb wind, inside the echo, formed an angle of 45 degrees with the general flow pattern. No explanation of this peculiarity has been attempted.

At about 1940 EST (Fig. 37) Station 47, located directly under the storm cell, measured a rain intensity of 8 inches per hour. It had a smaller cellular high which was about to merge with the one approaching from the west.

It is interesting to note that these cellular highs were blocking the path of the straight northerly wind, thus creating a comparatively calm area beneath the cells. The cooling on the ground associated with the cellular highs was not appreciable. The balloon released from Station 47 went up to the 640 mb level, then dropped to the 880 mb level, and rose again to the 760 mb level where it could no longer be followed. The line of showers seen in the previous chart was dissipating, with a maximum rain intensity of one inch per hour. The chart also shows the velocity of the radar echoes to be very close to that of the 700 and 600 mb level winds.

By 1950 EST (Fig. 38) the line of showers had disintegrated, but the storm over the southern portion of the network was still in its mature stage. As the cellular high to the south intensified, southerly winds started blowing into the Network area. A huge thunderstorm to the west seemed to be accompanied by heavy rain and a pronounced cellular high. Its detailed features, however, were not yet discernible.

At 2000 EST (Fig. 39) the huge echo from the west was covering the southwestern half of the Network. A new field of divergence accompanied by the cellular high beneath the echo pushed the northerly wind away from the Network area. This cell was still in its mature stage with two heavy rain spots. At this time, the 300 and 200 mb wind data were available; they will be discussed in the section dealing with the composite chart.

The intense echo discussed above, with an unusually large cellular high moved directly over the Network. The center of the diverging winds at 2010 EST (Fig. 40) appeared in the southern part of the Network. Several cells of heavy rain were analyzed in the chart without disclosing any definite relationship between them and the surface wind pattern. Three 900 mb winds, in the left chart, show a rather simple northwesterly flow over the area and do reveal a relationship between the wind at that level and the mesoscale pattern.

An interesting feature becoming visible in the 2020 EST chart (Fig. 41) is a small low to the rear of the high. This high has now developed into a mesohigh. The precipitation beneath the cloud had weakened, but it still showed

an intensity of two and a half inches per hour.

The low initiated in the previous chart appeared to be a wake depression of a very small scale. In the 2030 EST chart (Fig. 42), the low had not yet been surrounded by circulation, but it had induced a light shifting of the winds.

Attention should be paid to the 180 degree difference between the direction of the surface and of the 900 mb winds seen in the 2040 EST chart (Fig. 43). The surface winds do not seem to fit the pressure gradient, especially as they pass through the center of the low. The reason for such an odd phenomenon in mesometeorology remains an open question.

The velocity of the 700 and 600 mb winds analyzed in the 2050 EST chart (Fig. 44) is similar to the velocity of the echo. These winds seem to be steering winds of the radar echoes. Most of these echoes are now scattered, and thunderstorm activity is rapidly decreasing.

At 2100 EST (Fig. 45) the low which now has the characteristics of a wake depression deforms the wind pattern. Thunderstorms have left the Network area.

The last chart of the series (Fig. 46) presents the analysis of the 300 and 200 mb winds at 2110 EST. Only one medium size echo is still visible near the edge of the chart. The wake depression has moved off the Network, leaving surface winds of less than 5 mph. Most of the squall line activity has disappeared.

COMPOSITE CHARTS

The 10-minute interval charts discussed in the previous section reveal the meteorological features found within a small area, 40 by 50 miles in size. Since these charts were analyzed at close time intervals, they can properly be organized into a composite chart covering a much larger area.

The composite surface chart (Fig. 47) is made by shifting the stations with respect to the pressure surge line. The stream line analysis in the figure gives the detailed features of the wind field. To the east of the pressure surge line, southwesterly winds prevail, except in the small area of outflow of a local thunderstorm. Strong northwesterly winds exist to the

northwest of the pressure surge line; in that direction, strong divergence fields are visible beneath the radar echoes. In connection with the mesohigh, the temperature went from 86°F to 68°F: a drop of 18 degrees.

The 950 mb composite chart (Fig. 48) is constructed by shifting the upper winds in the 10-minute interval charts with respect to the pressure surge line. Heavy short arrows along the reference line indicate the time when balloons penetrated the illustrated pressure level. At this level, the pressure surge line is located above the line in the surface chart. This indicates that the surface of discontinuity is vertical. A very strong gust reaching 30 to 40 mph is seen in a 20 to 30 mile zone west of the pressure surge line. To the northwest, away from the pressure surge line, the southern part of the wake depression is visible. The temperature inside the mesohigh is about 20°C, approximately 9°C cooler than the warm air.

A wind pattern similar to that of the 950 mb level is seen in the 900 mb chart (Fig. 49). At this level, the mesohigh is only 4°C cooler than its environment. This evidence leads to the conclusion that a mesoscale pressure surge results from cooling at low levels.

The pressure surge line, at the 850 mb level (Fig. 50), is located eight miles toward the northwest. From this datum, the tangent to the surface of the cold dome was computed to be 1/20, which is very steep. Winds inside the cold dome shifted to the west-northwest. The temperature inside the dome is still 3°C below that of the warm air to the east.

At the 800 mb level, the surface of the cold dome is located ten miles farther to the northwest. Because of the small temperature difference between the warm and the cold air, the wind shift at the pressure surge line (Fig. 51) is only 30 degrees, with a slight surge in wind speed. It should be noted that the component of cold air velocity which is normal to the pressure surge line is only 10 miles per hour. Without any source of cold air above this level, the dome must subside and spread over the ground.

Figure 52 shows the 700 mb composite chart. The pressure surge line is completely gone at this level, and the winds blow from the west, except those in the southeast corner of the chart.

Winds blow from the west throughout the 600 mb chart (Fig. 53). A careful study of the winds inside and outside of the echoes forming the squall line leads us to conclude that the horizontal wind velocity, at this level, is not disturbed by clouds. Any attempt to work out an organized divergence and convergence pattern in mesoscale would prove rather difficult.

At the 500 mb level, winds slowed down slightly from the 25 mph reached at 600 mb. Thus we notice a similarity in both direction and speed from the 700 to the 500 mb level winds. Since the velocity of the radar echoes is very close to the wind velocity, it is reasonable to locate their steering level between 700 and 500 mb.

Stream lines in the 400 mb level chart (Fig. 55) started curving, and the wind decreased considerably near the echoes. These facts indicate that at this level the air temperature was higher in the immediate vicinity of the squall line than in the surrounding area. This difference must result from the heat released through condensation inside the clouds.

The effect of the released heat, integrated with height, results in the sharp ridge observed at the 300 mb level (Fig. 56). As already indicated, (Fig. 5), the winds inside the composite chart do not at all fit a larger pattern.

Figure 57 shows the ridge at the 200 mb level, the highest level analyzed in mesoscale. A wind pattern similar to that observed in the 300 mb chart exists.

VERTICAL CROSS SECTION

The composite upper air charts presented in the previous section have characteristics of both time and space section charts. These characteristics permit us to make a vertical cross section along a given line.

In Figure 58, a vertical cross section of temperature was made along the straight line passing through Stations 19, 7, and D. The rectangular chart to the right is a part of the adiabatic diagram referring to the temperature curves in the cross section. It will be seen that inversions inside the warm sector at the 4,000 and 18,000 ft levels do not reach above

the mesosystem. The surface of the cold dome associated with the mesosystem is similar to that of a rapidly moving cold front, except that the dome remains below the 700 mb level. Cooling of the air in the dome is appreciable throughout a very shallow layer above the ground.

The distribution of relative humidity in the same vertical plane as the one used for the temperature cross section is given in Fig. 59. At the 2,000 ft level, dry air of a relative humidity as low as 55 percent exists inside the dome. This is the level of maximum temperature at the inversion top. The initiation of this dry air accompanied by the inversion is explained by strong descending motions, inside the dome, which do not reach the ground. The "humidity dip" discovered by the Thunderstorm Project, a drop in relative humidity occurring at the time of intense thundershowers, can be explained by assuming that the dry air is brought down by the drag of large raindrops.

A layer of dry air found 2,000 ft above the bottom of each of three inversions, east of the pressure surge line, probably results from the fact that the underlying inversion layers prevent descending motions.

The vertical cross section of the winds aloft is constructed in Figure 60. In the warm sector, underneath the lower inversion surface, there appears a frictional layer in which the wind direction is mostly southwest. Rather slow and variable winds are visible above 28,000 ft; they blow north-northwestward east of the surge line, and southwestward above the mesohigh. Following the line, high speed northwesterly gusts are observed on the ground for a short while; then they slow down and change into easterly winds.

At the level labeled "steering level of radar echoes," the mean echo velocity is of the same order of magnitude as that of the winds; these are represented by large wind symbols. The echoes themselves are drawn with the help of RHI pictures.

Based upon the analyses of this paper, a schematic vertical motion of the atmosphere in and out of the squall line of June 29, 1947 is constructed (Fig. 61). The increase in height of the frictional layer and the disappearance of the inversion layers a few miles east of the pressure surge line give support to the existence of an upward current above the surface of the

cold dome. The formation of dry air accompanied by the temperature maxima 2,000 ft above the bottom of each inversion is explained by the introduction of the layers of subsidence shown in the figure.

Downdrafts, which supply cold air to the underlying cold dome, are accompanied by a cellular high and a cellular surge line on the ground. These cellular features measure from one to ten miles and move with the rain cells aloft. The dome itself subsides under its own weight while it receives cold air. When the surrounding air does not converge quickly enough to compensate the space thus created, the dome's falling produces the subsidence of overriding layers.

CONCLUSIONS

The three-dimensional mesoanalysis of a squall line, June 29, 1947, was made with the use of data from the Thunderstorm Project. This study revealed features and characteristics of a squall line and of mesosystems known only through assumption or imagination, until now.

Special techniques were developed in analyzing complicated features of temperature, wind, and pressure fields. Upper air data are the most difficult to utilize. Instead of treating the rawinsonde and pibal observations in the manner usual in climatology, careful coordination of the location of each balloon with time was necessary. Observations were then reorganized into 10 min and 100 mb interval charts. Techniques of construction of a composite upper air chart made it possible to analyze an area of 200 by 300 miles at any height up to the 200 mb level.

One of the most important aspects of this work was the investigation of the height of this mesosystem. It was generally assumed that such systems reached 20,000 ft or more, but the top of the cold dome in this case was found to be far below the 700 mb level. Above 700 mb there existed neither temperature nor wind discontinuities associated with the boundary of the mesosystem.

Evidence was offered that the component of cold air velocity which is normal to the pressure surge line was large enough to permit cold air to

advect with the velocity of the line. Thus, the assumption of a gravitational wave in the atmosphere proved inadequate to explain the pressure surge line of this case study.

The author hopes to carry out more case studies using the data of the Thunderstorm Project or some other proper material. In this respect the present paper will help in planning future severe storm research networks.

ACKNOWLEDGMENTS

This research was accomplished under the general direction of Dr. Horace R. Byers, Chairman of Department of Meteorology, University of Chicago, and William C. Ackermann, Chief of the Illinois State Water Survey, and under the general guidance of Glenn E. Stout, Head of Meteorology Section, Illinois State Water Survey on the campus of the University of Illinois.

Sincere appreciation should be expressed to Roy H. Blackmer, Jr., J. B. Holleyman and Harold M. Gibson, meteorologists, Mesometeorology Project, Illinois State Water Survey, for their kind suggestions and comments.

The writer is also very grateful to Miss Juliette Rey, University of Chicago; Toshiyuki Ishimatsu, Kyushu Institute of Technology; and Kimio Katow, and T. N. Krishnamurti, Illinois State Water Survey, for their assistance in organizing and plotting a large amount of the data.

Credit is due Dr. D. M. Swingle and Dr. R. Schrott of the U. S. Army Signal Laboratories for encouraging this research and reviewing this report. Credit is also due the U. S. Weather Bureau for their cooperation in permitting the author to carry out this investigation.

REFERENCES

1. Byers, H. R. and Braham, R. R. Jr., 1949: The Thunderstorm, Report of the Thunderstorm Project, 1946 and 1947. Government Printing Office, Washington, D. C.

2. Fujita, T., 1955: Results of Detailed Synoptic Studies of Squall Lines, Tellus Vol. 7, No. 4, pp. 405-436

3. Fujita, T., Newstein H. and Tepper, M., 1956: Mesoanalysis, An Important Scale in the Analysis of Weather Data. Research Paper No. 39, U. S. Weather Bureau

4. Newton, C. W., 1950: Structure and Mechanism of the Prefrontal Squall Line. Journal of Meteorology, Vol. 7, pp. 210-222

5. Stout, G. E., 1957: Mesometeorological System for a Dense Network of Stations. Presented at IUGG Meeting in Toronto, Sept. 1957

6. Tepper, M., 1950: A Proposed Mechanism of Squall-Lines: The Pressure Jump Line. Journal of Meteorology, Vol. 7, pp. 21-29

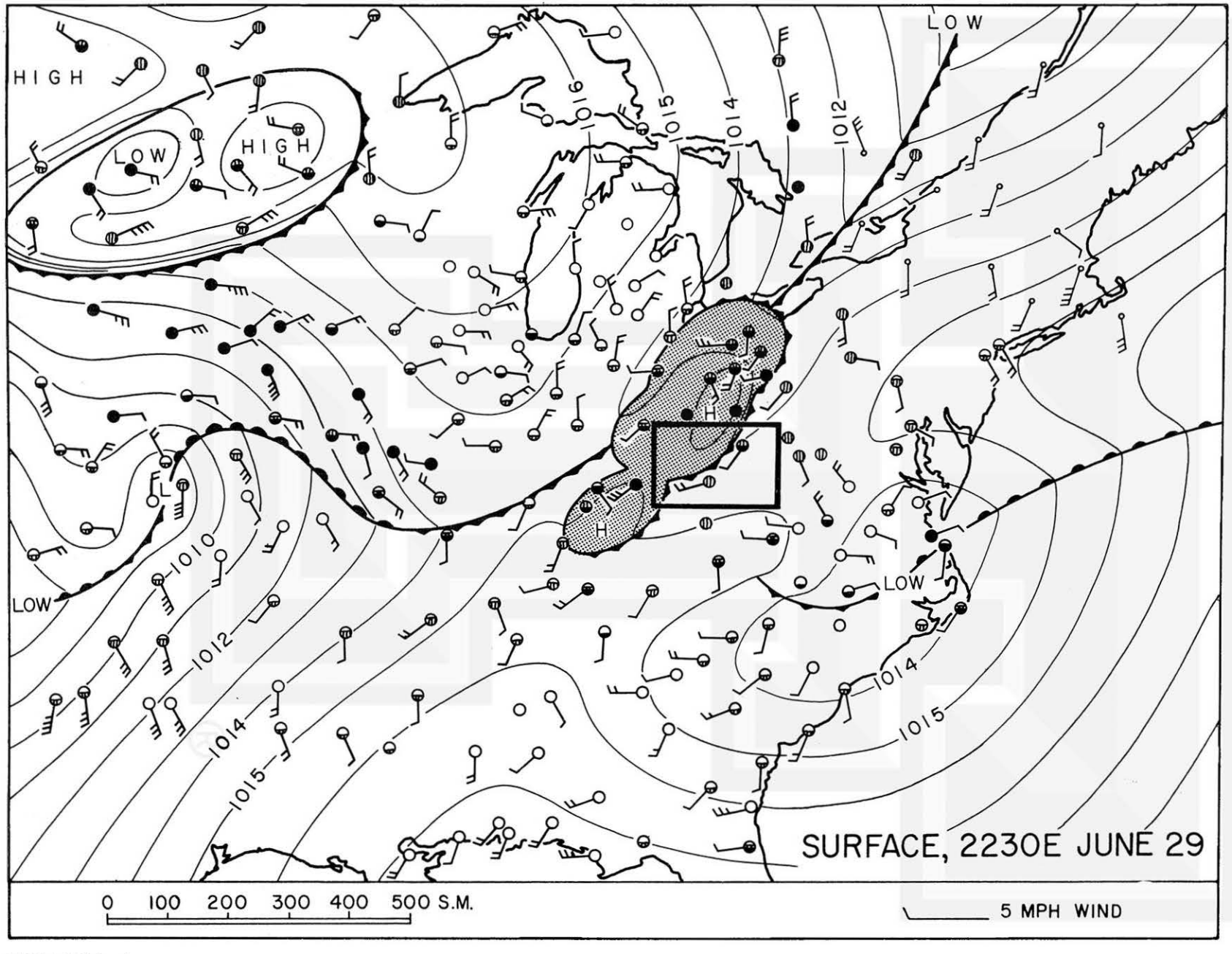
HIGH
LOW
HIGH
LOW
1016
1015
1014
1012
H
H
L
LOW
1010
1012
1014
1015
LOW
1014
1015
SURFACE, 2230E JUNE 29
0 100 200 300 400 500 S.M.
5 MPH WIND

FIGURE 1

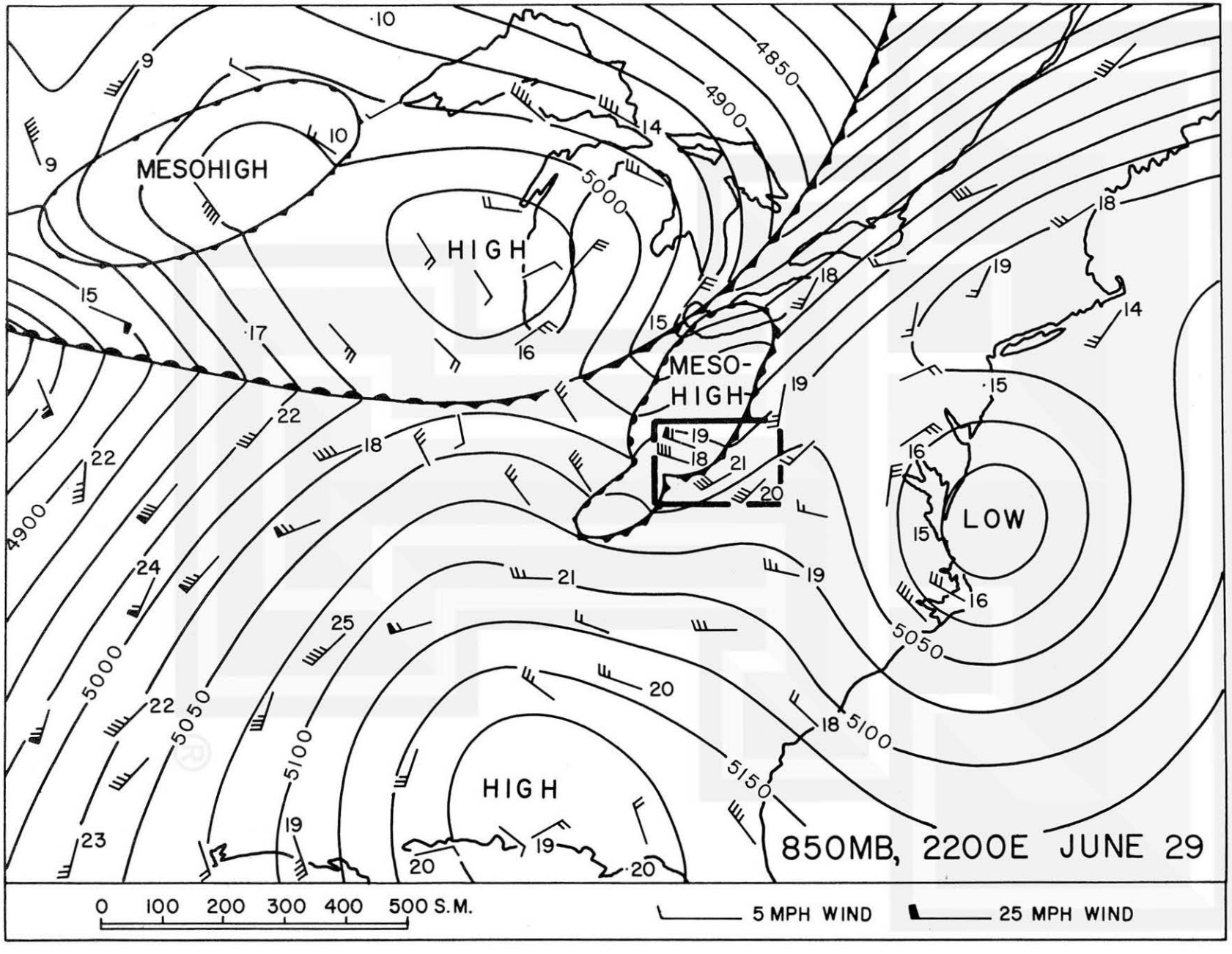
MESOHIGH
HIGH
MESO-
HIGH
LOW
HIGH
4850
4900
5000
5050
5100
5150
850MB, 2200E JUNE 29
0 100 200 300 400 500 S.M.
5 MPH WIND
25 MPH WIND

FIGURE 2

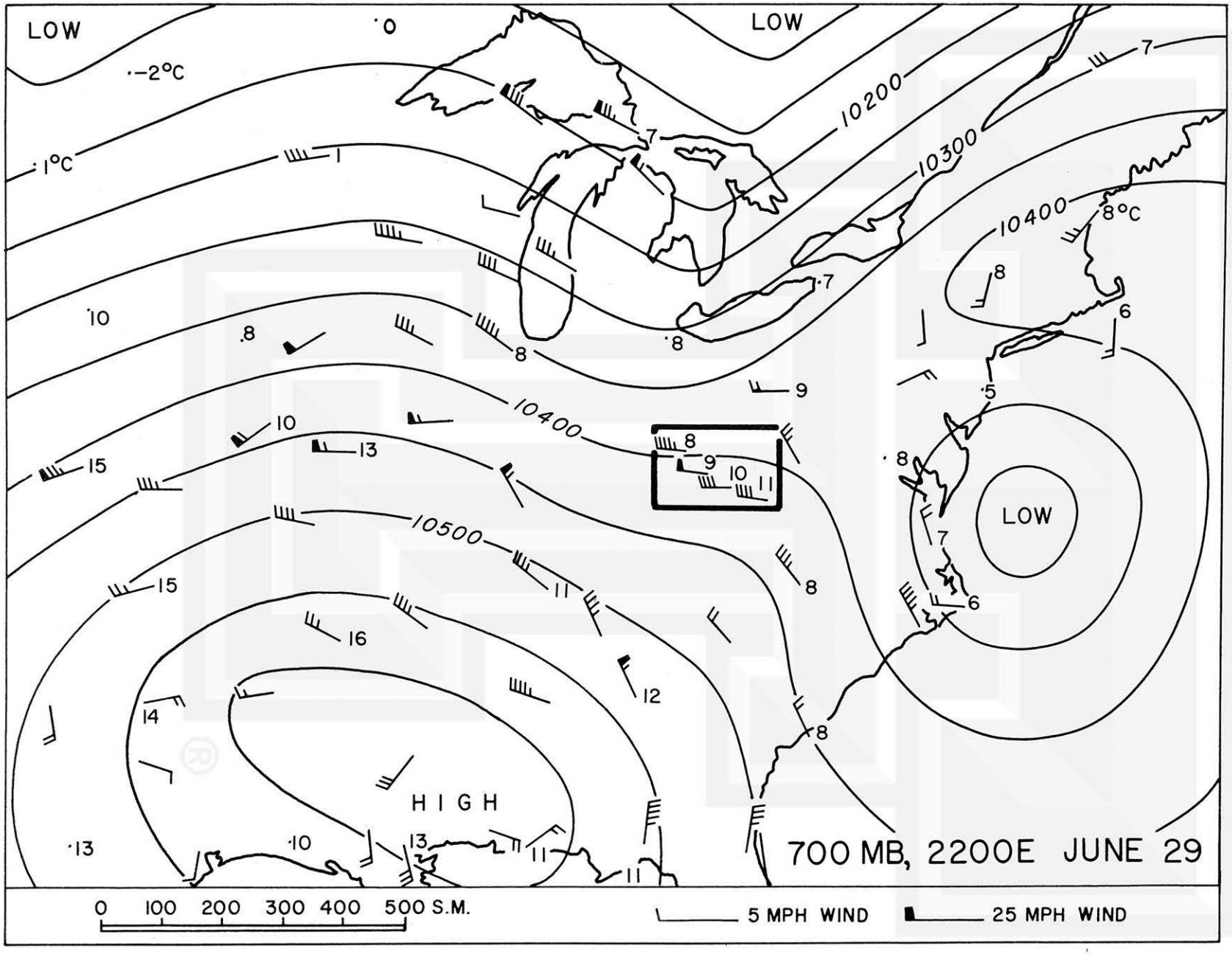
LOW
LOW
0
-2°C
-1°C
10200
10300
10400
10500
8°C
LOW
HIGH
700 MB, 2200E JUNE 29
0 100 200 300 400 500 S.M.
5 MPH WIND
25 MPH WIND

FIGURE 3

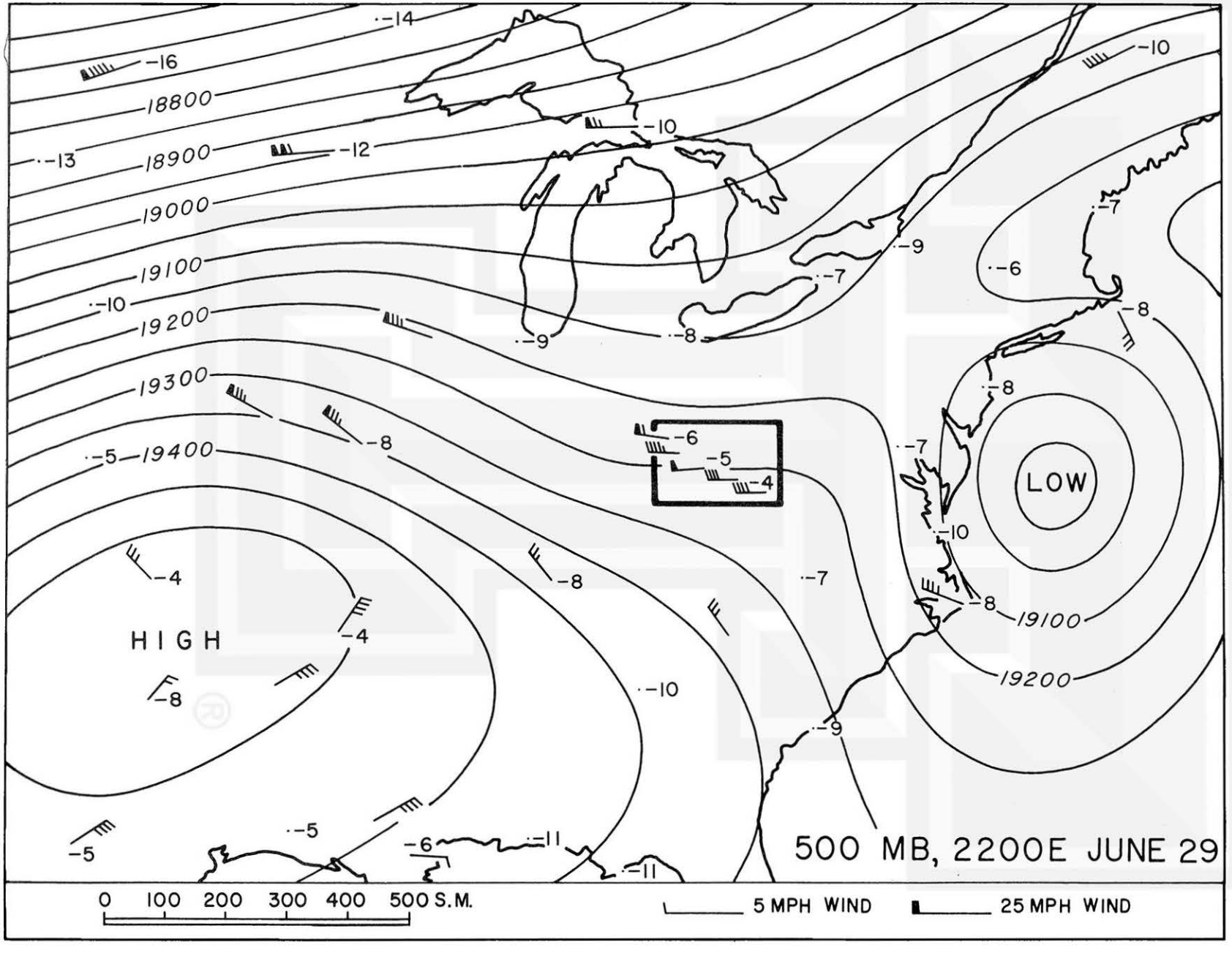
18800
18900
19000
19100
19200
19300
19400
HIGH
LOW
500 MB, 2200E JUNE 29
0 100 200 300 400 500 S.M.
5 MPH WIND
25 MPH WIND

FIGURE 4

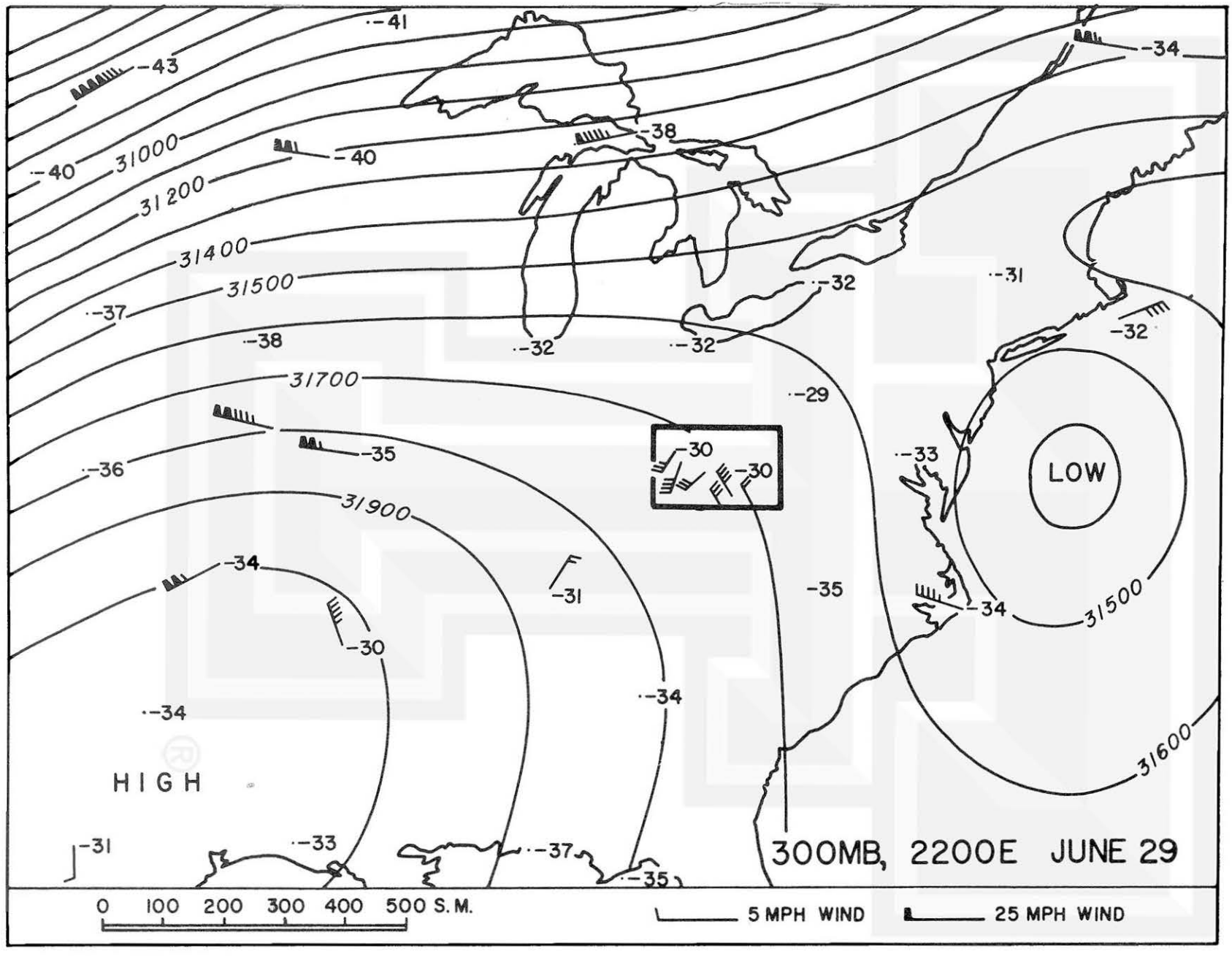
-41
-43
-40
31000
-40
31200
-38
-34
31400
31500
-37
-38
-32
-32
-32
-31
-32
31700
-29
-30
-30
-36
-35
-33
LOW
31900
-34
-31
-35
-34
31500
-30
-34
-34
31600
HIGH
-31
-33
-37
-35
300MB, 2200E JUNE 29
0 100 200 300 400 500 S.M.
5 MPH WIND
25 MPH WIND

FIGURE 5

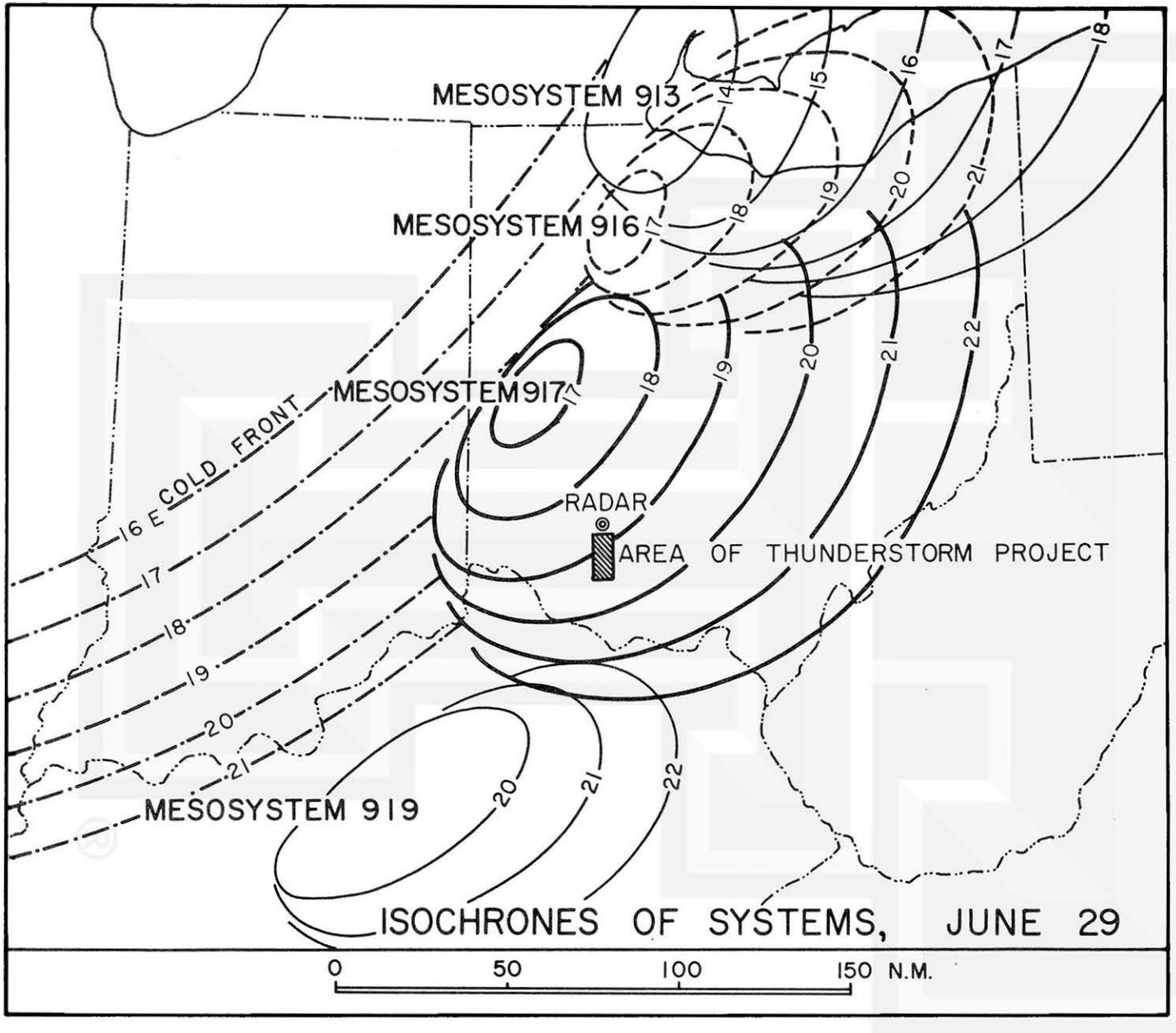
MESOSYSTEM 913
MESOSYSTEM 916
MESOSYSTEM 917
MESOSYSTEM 919
COLD FRONT
16 E
17
18
19
20
21
22
RADAR
AREA OF THUNDERSTORM PROJECT
ISOCHRONES OF SYSTEMS, JUNE 29
0
50
100
150 N.M.

FIGURE 6

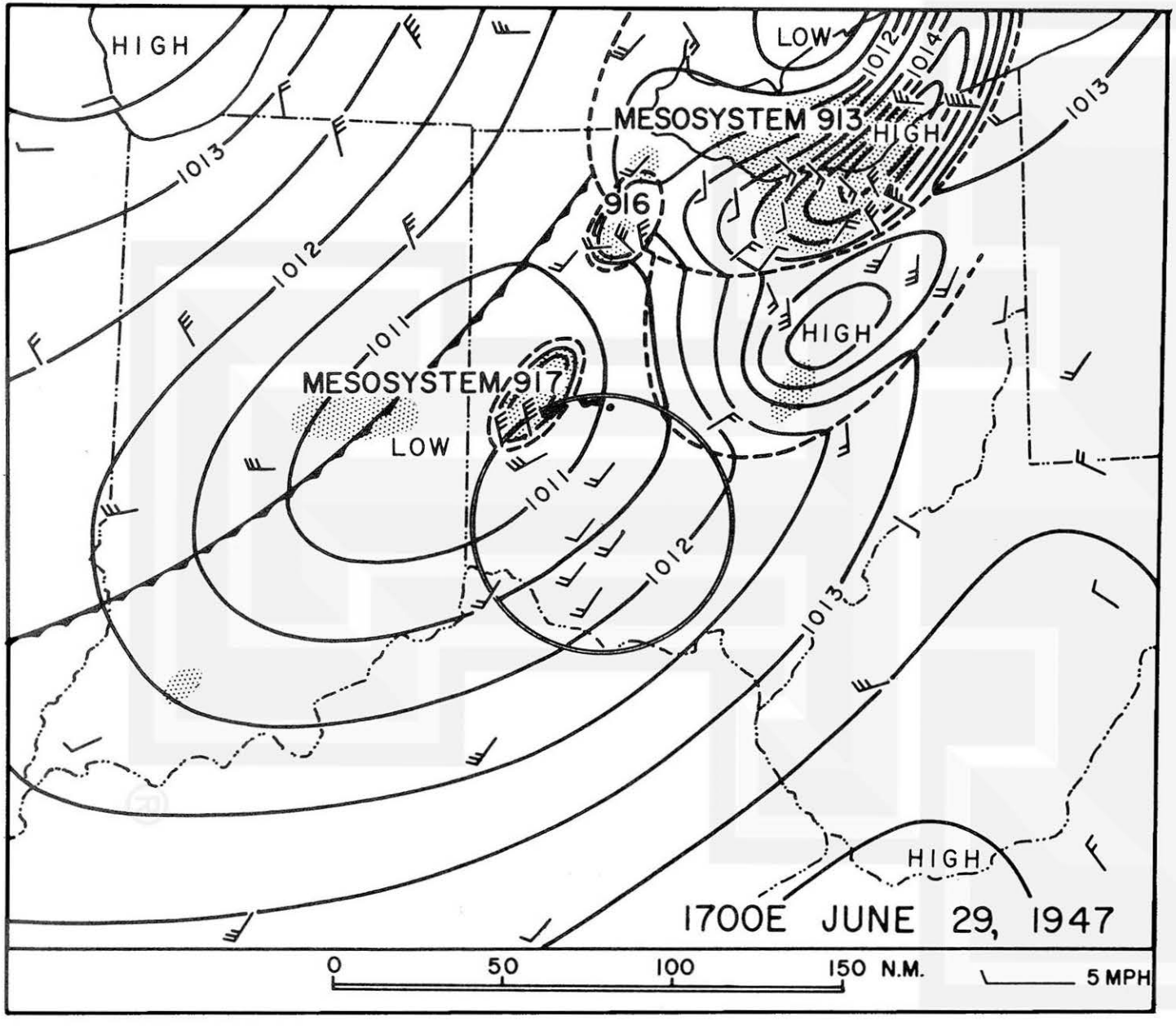
HIGH
LOW
1012
1014
1013
MESOSYSTEM 913
HIGH
916
1013
1012
1011
HIGH
MESOSYSTEM 917
LOW
1011
1012
1013
HIGH
1700E JUNE 29, 1947
0
50
100
150 N.M.
5 MPH

FIGURE 7

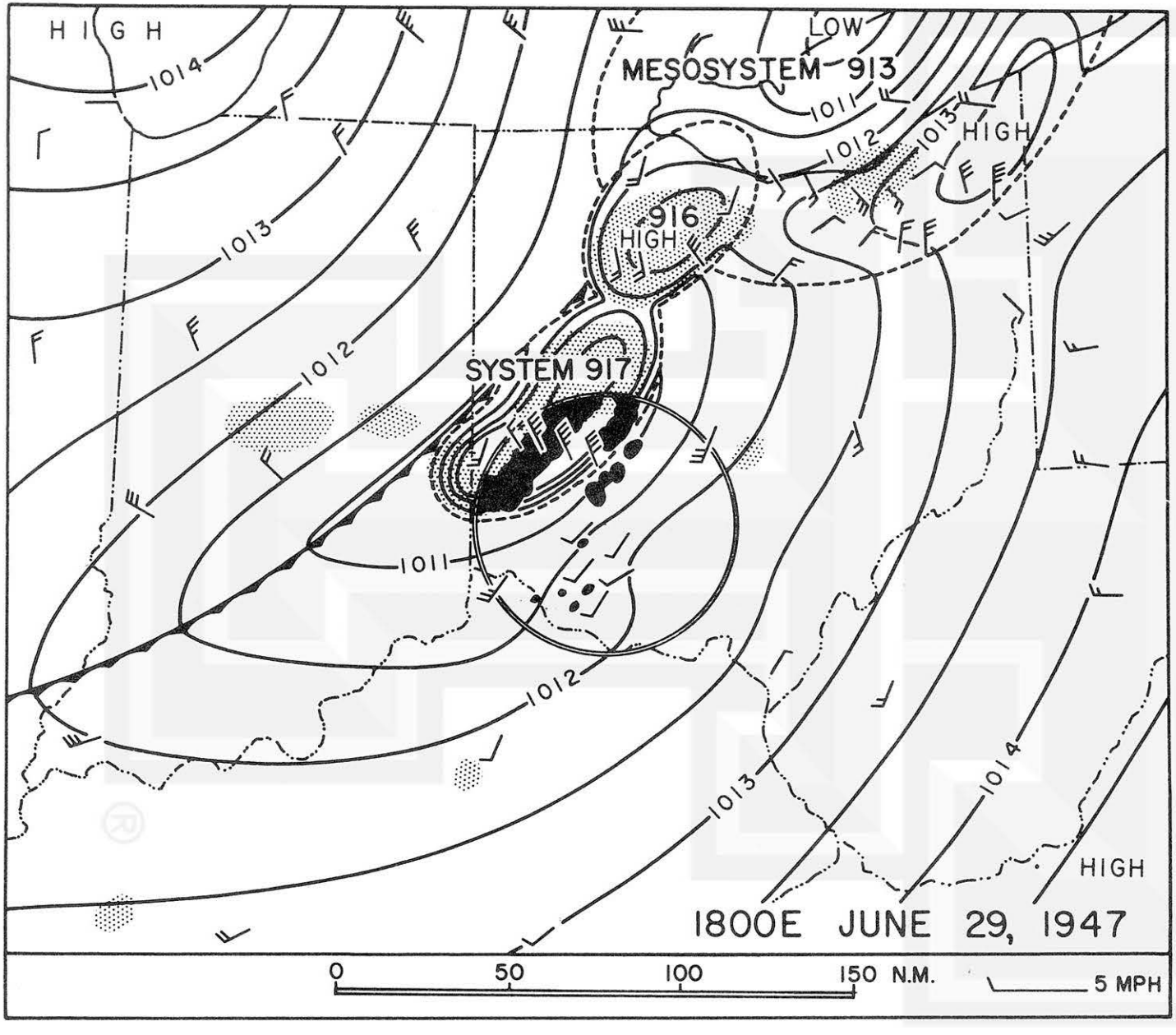
HIGH
1014
1013
1012
1011
LOW
MESOSYSTEM 913
1012
1013
HIGH
916
HIGH
SYSTEM 917
1011
1012
1013
1014
HIGH
1800E JUNE 29, 1947
0
50
100
150 N.M.
5 MPH

FIGURE 8

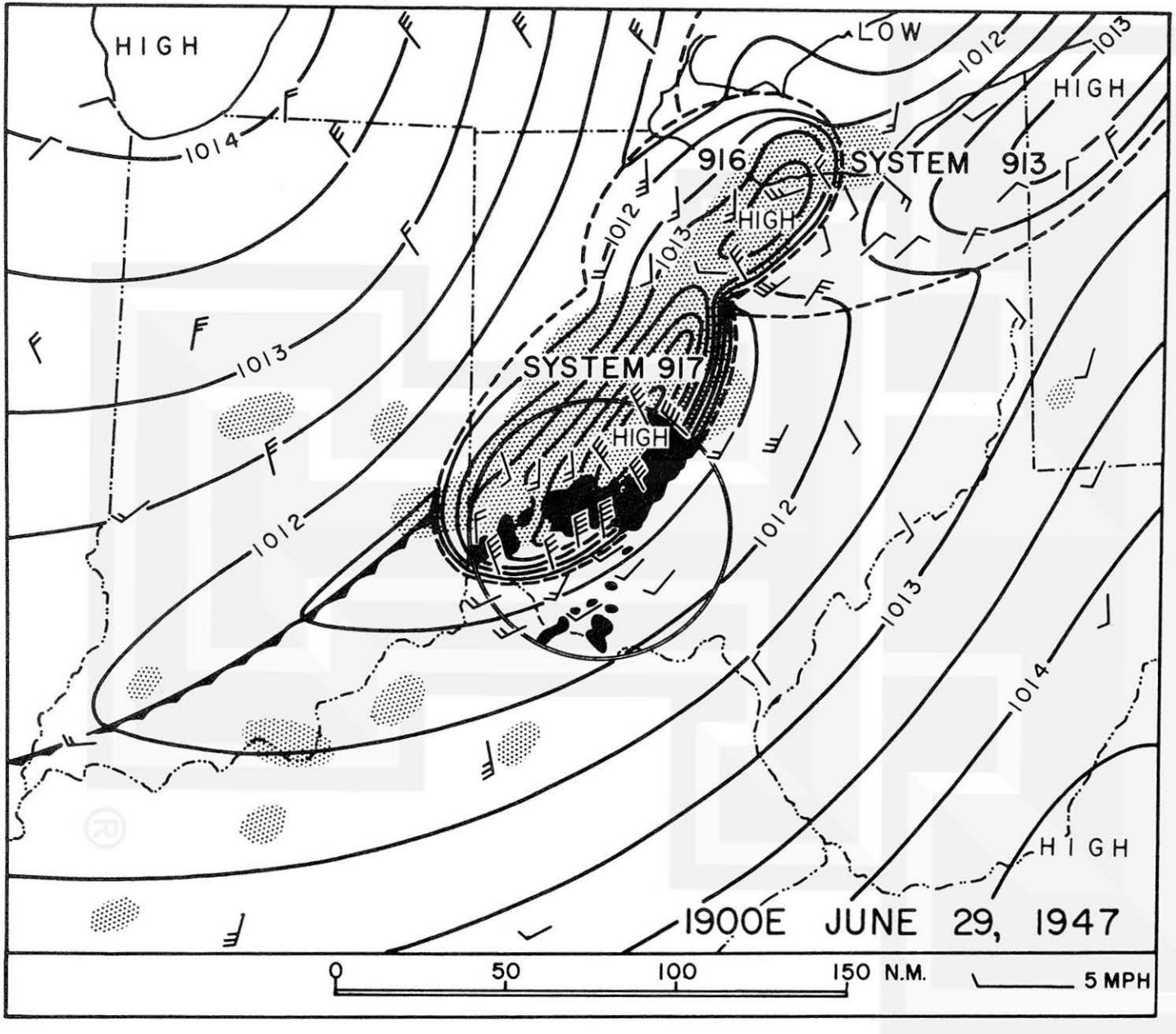
HIGH
1014
LOW
1012
1013
HIGH
916
SYSTEM 913
HIGH
1012
1013
1013
SYSTEM 917
HIGH
1012
1012
1013
1014
HIGH
1900E JUNE 29, 1947
0
50
100
150 N.M.
5 MPH

FIGURE 9

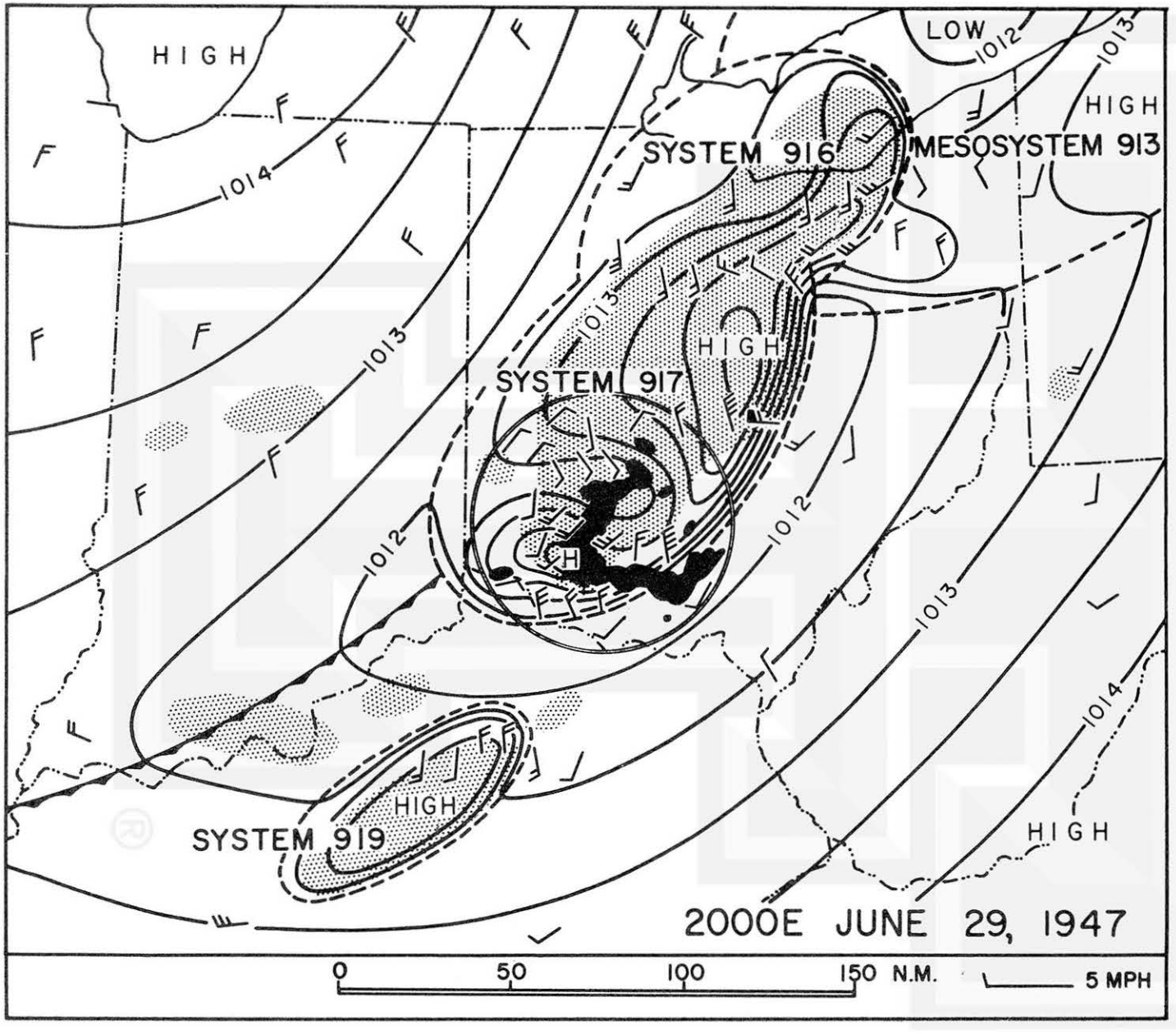
HIGH
LOW
1012
1013
HIGH
SYSTEM 916
MESOSYSTEM 913
1014
1013
HIGH
SYSTEM 917
1012
1012
1013
1014
HIGH
SYSTEM 919
HIGH
2000E JUNE 29, 1947
0
50
100
150 N.M.
5 MPH

FIGURE 10

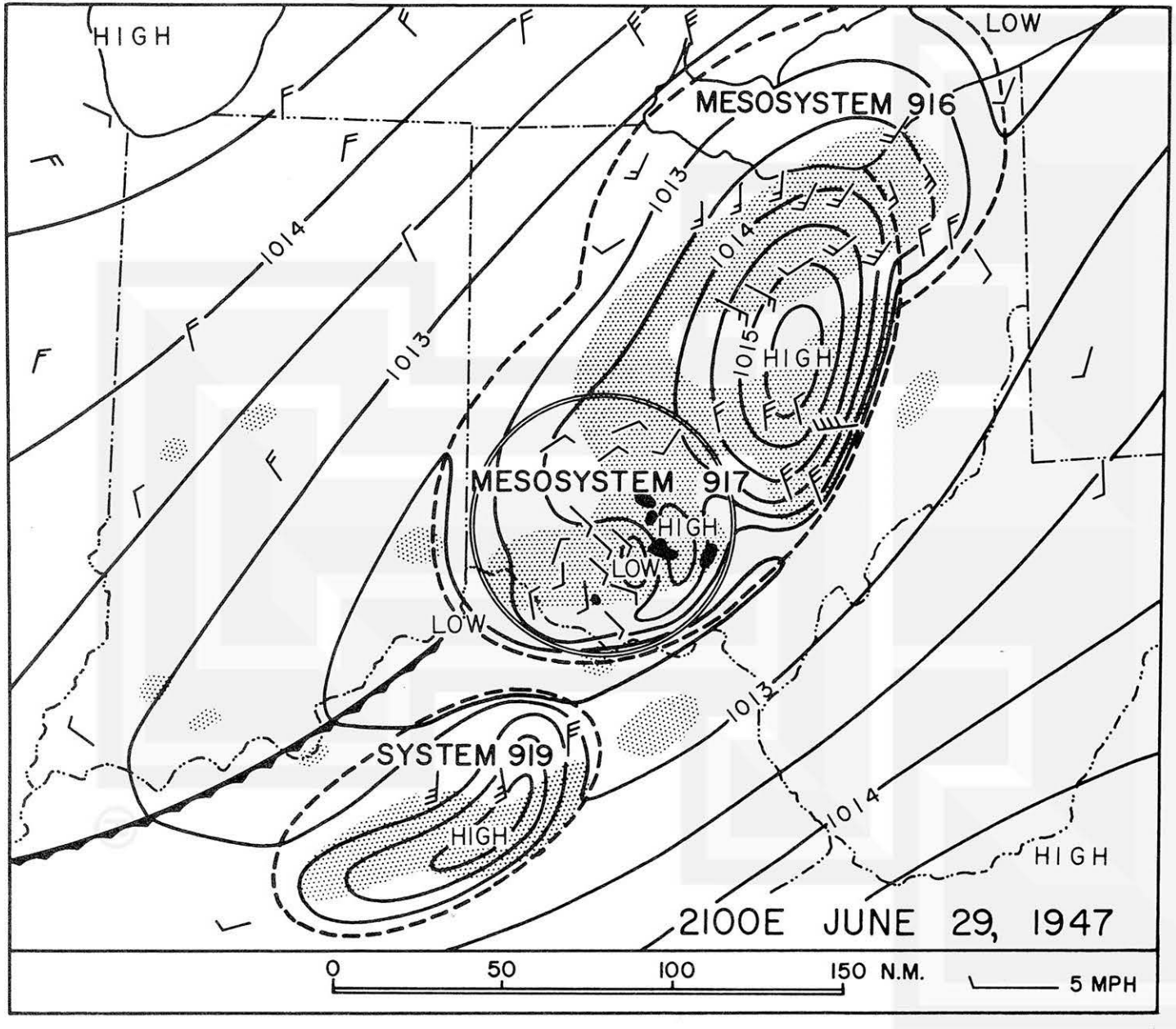
HIGH
LOW
MESOSYSTEM 916
1013
1014
1015
HIGH
MESOSYSTEM 917
HIGH
LOW
LOW
1013
SYSTEM 919
HIGH
1014
HIGH
2100E JUNE 29, 1947
0
50
100
150 N.M.
5 MPH

FIGURE 11

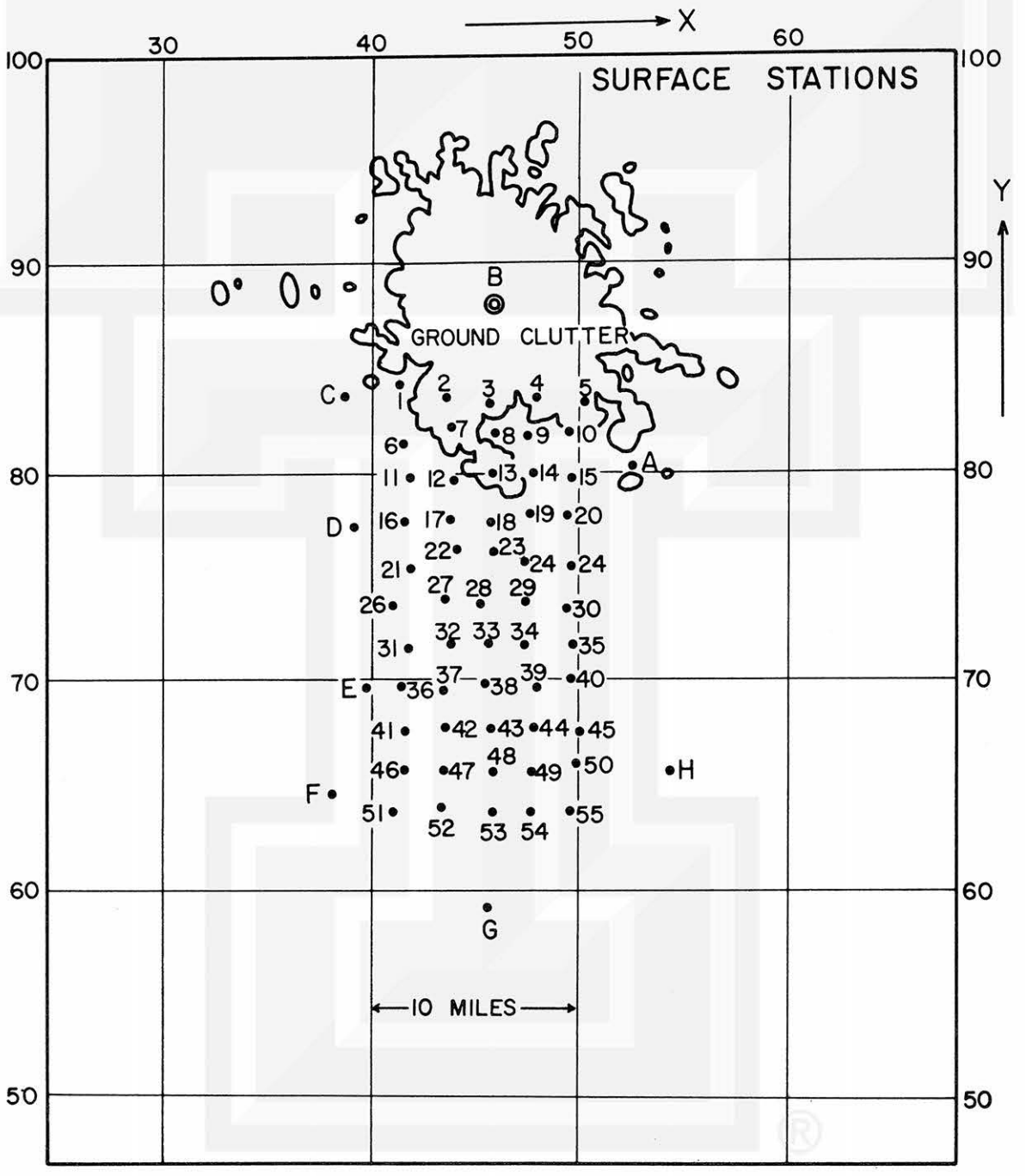
X
Y
30
40
50
60
100
90
80
70
60
50
SURFACE STATIONS
GROUND CLUTTER
A
B
C
D
E
F
G
H
1
2
3
4
5
6
7
8
9
10
11
12
13
14
15
16
17
18
19
20
21
22
23
24
24
26
27
28
29
30
31
32
33
34
35
36
37
38
39
40
41
42
43
44
45
46
47
48
49
50
51
52
53
54
55
10 MILES

FIGURE 12

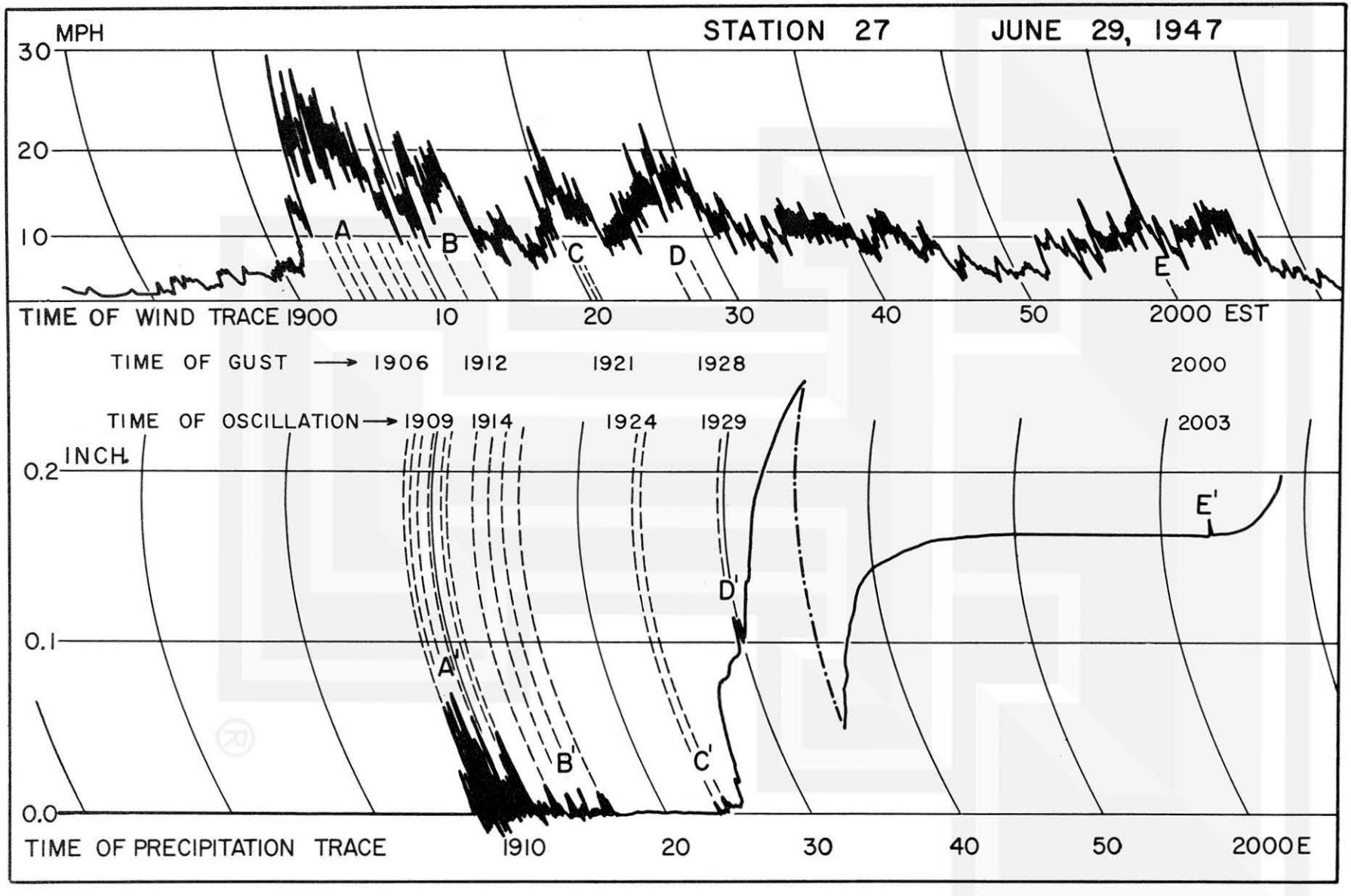
MPH
STATION 27
JUNE 29, 1947
30
20
10
A
B
C
D
E
TIME OF WIND TRACE 1900
10
20
30
40
50
2000 EST
TIME OF GUST → 1906
1912
1921
1928
2000
TIME OF OSCILLATION → 1909
1914
1924
1929
2003
INCH.
0.2
0.1
0.0
A'
B'
C'
D'
E'
TIME OF PRECIPITATION TRACE
1910
20
30
40
50
2000E

FIGURE 13

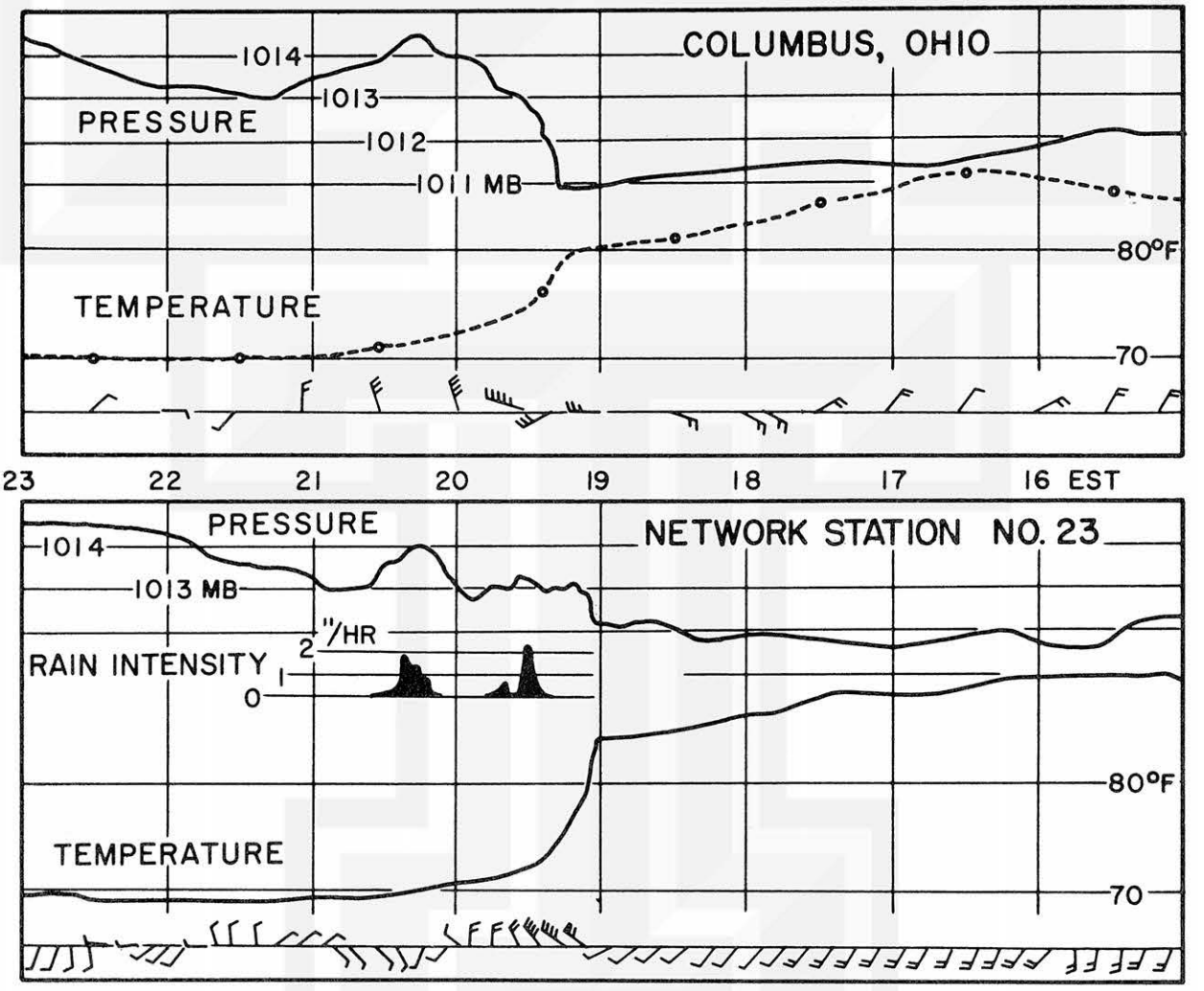
COLUMBUS, OHIO
1014
1013
PRESSURE
1012
1011 MB
80°F
TEMPERATURE
70
23
22
21
20
19
18
17
16 EST
PRESSURE
NETWORK STATION NO. 23
1014
1013 MB
"/HR
2
RAIN INTENSITY
1
0
80°F
TEMPERATURE
70

FIGURE 14

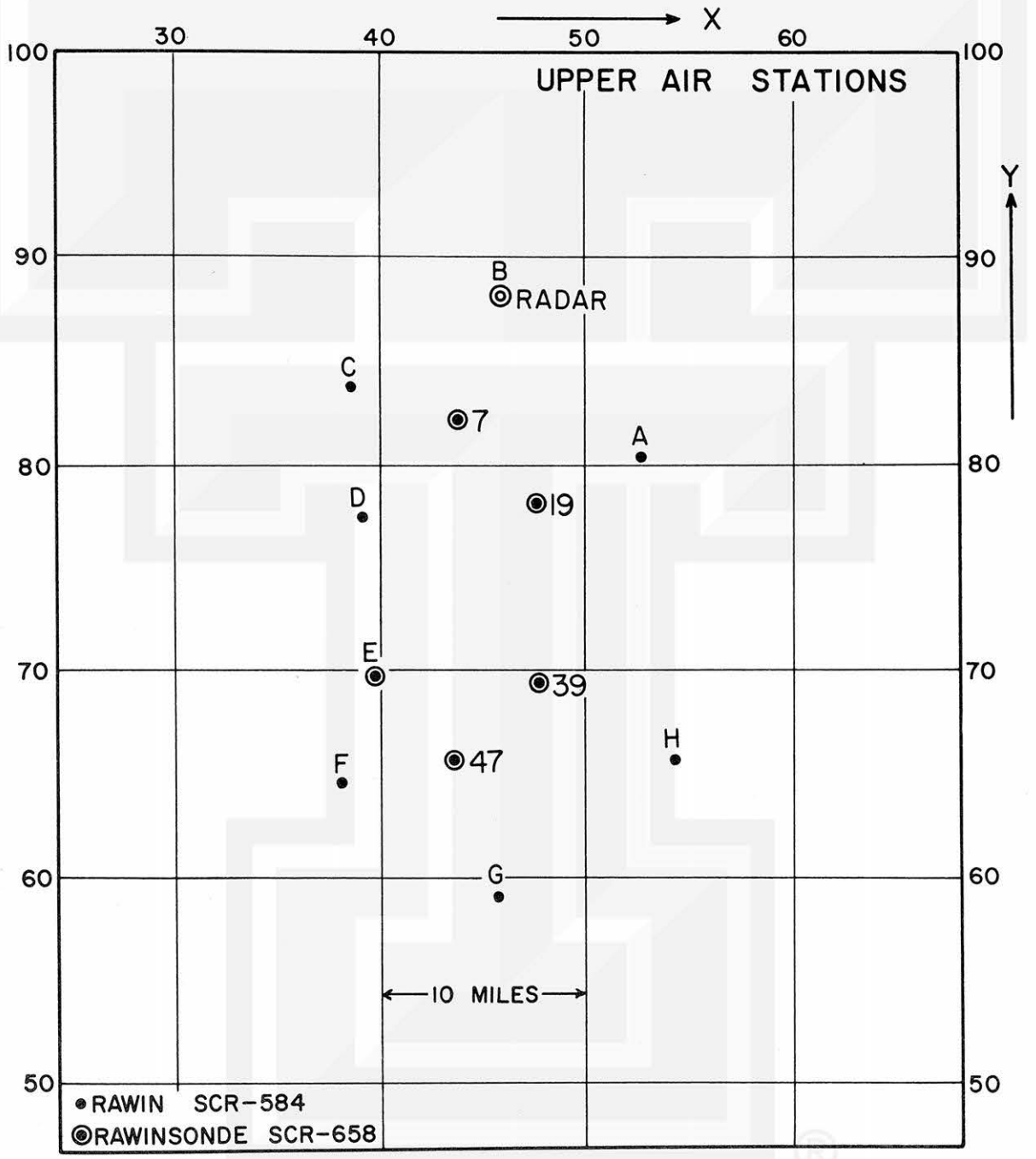
X
30
40
50
60
100
90
80
70
60
50
Y
UPPER AIR STATIONS
B
RADAR
C
7
A
D
19
E
39
H
F
47
G
10 MILES
RAWIN SCR-584
RAWINSONDE SCR-658

FIGURE 15

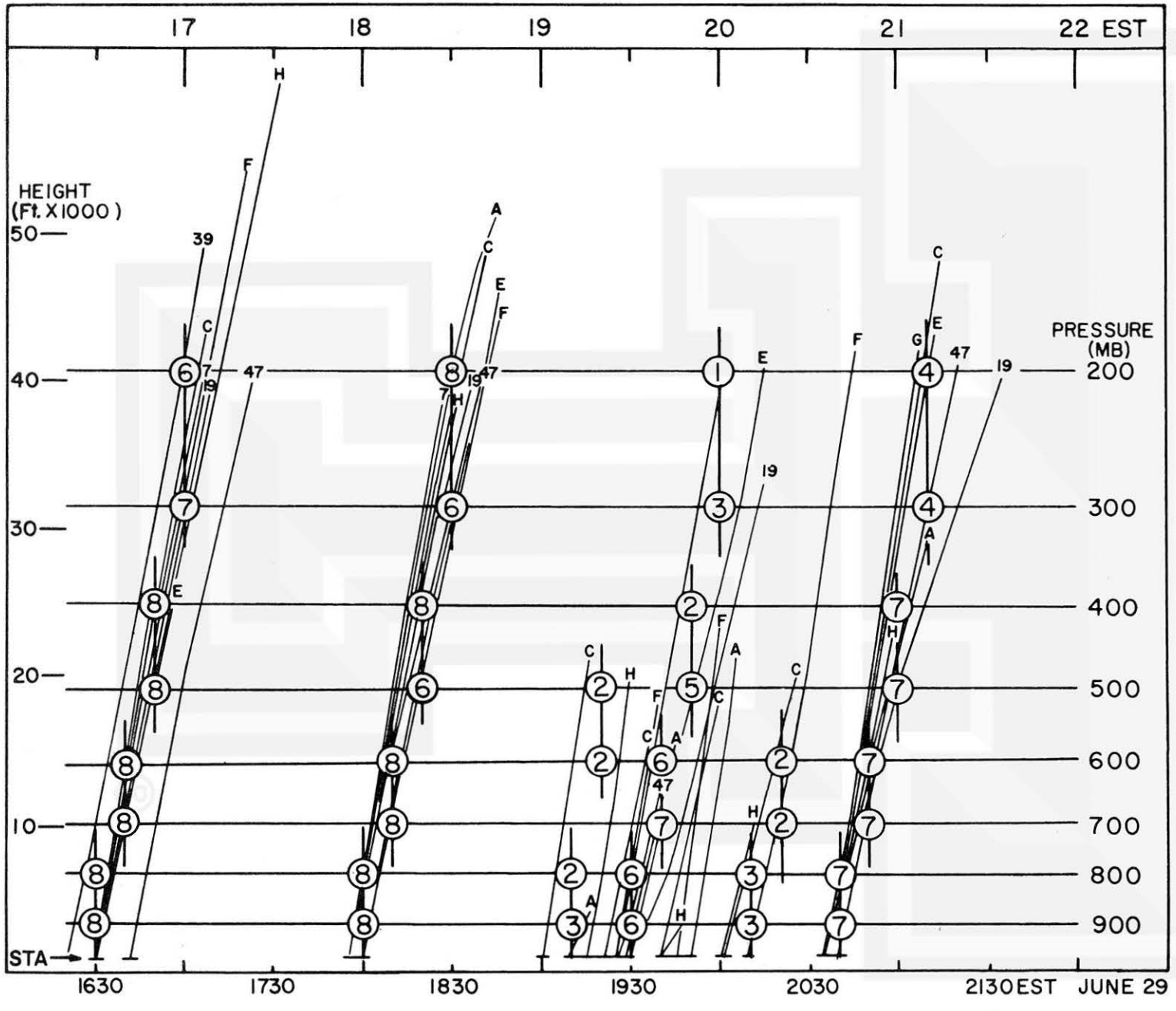
17
18
19
20
21
22 EST
HEIGHT
(Ft. X1000)
50
40
30
20
10
PRESSURE
(MB)
200
300
400
500
600
700
800
900
STA
1630
1730
1830
1930
2030
2130EST JUNE 29

FIGURE 16

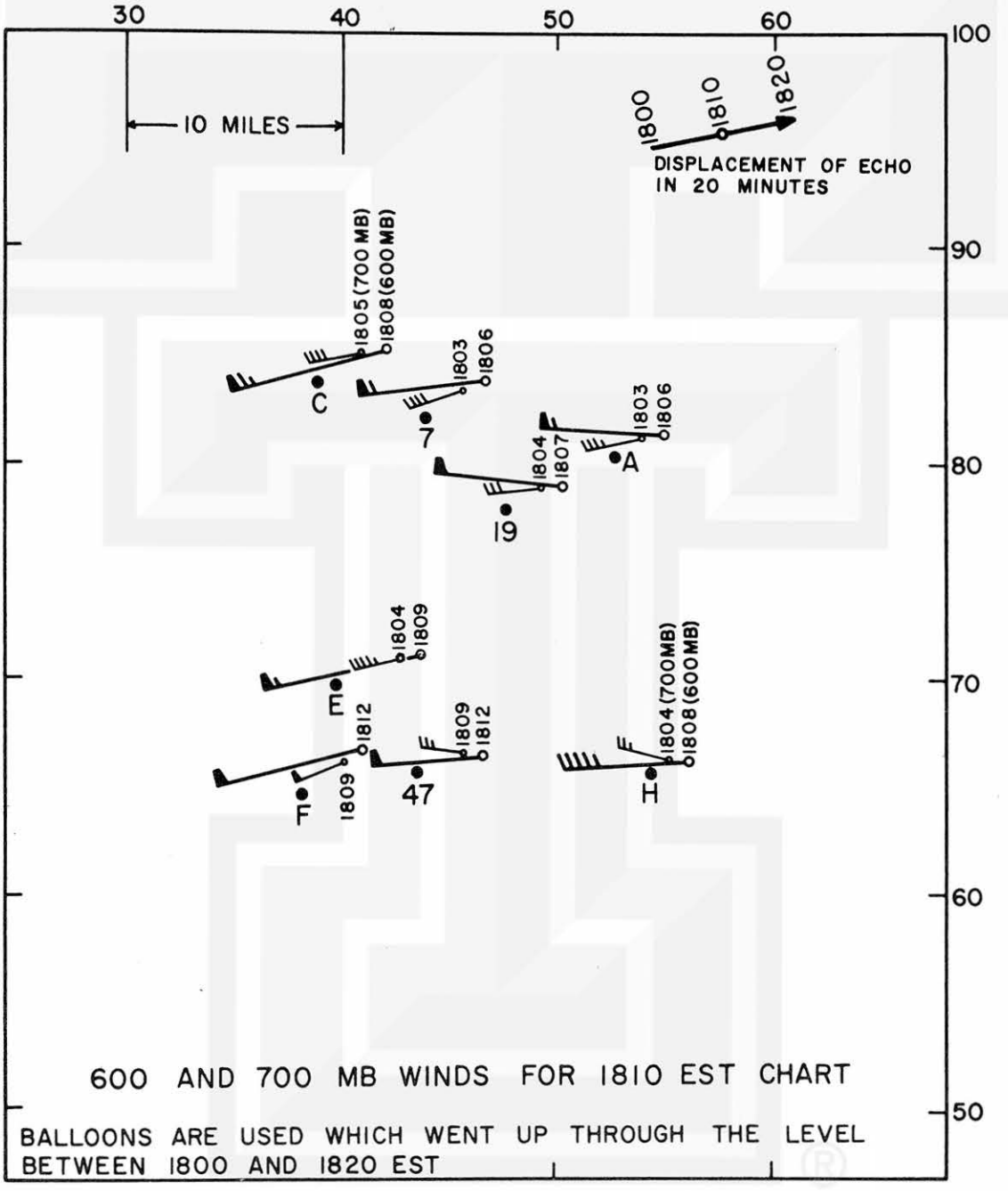
30
40
50
60
100
90
80
70
60
50
10 MILES
1800
1810
1820
DISPLACEMENT OF ECHO
IN 20 MINUTES
1805 (700 MB)
1808 (600 MB)
C
1803
1806
7
1804
1807
19
1803
1806
A
1804
1809
E
1812
1809
1812
F
1809
47
1804 (700 MB)
1808 (600 MB)
H
600 AND 700 MB WINDS FOR 1810 EST CHART
BALLOONS ARE USED WHICH WENT UP THROUGH THE LEVEL
BETWEEN 1800 AND 1820 EST

FIGURE 17

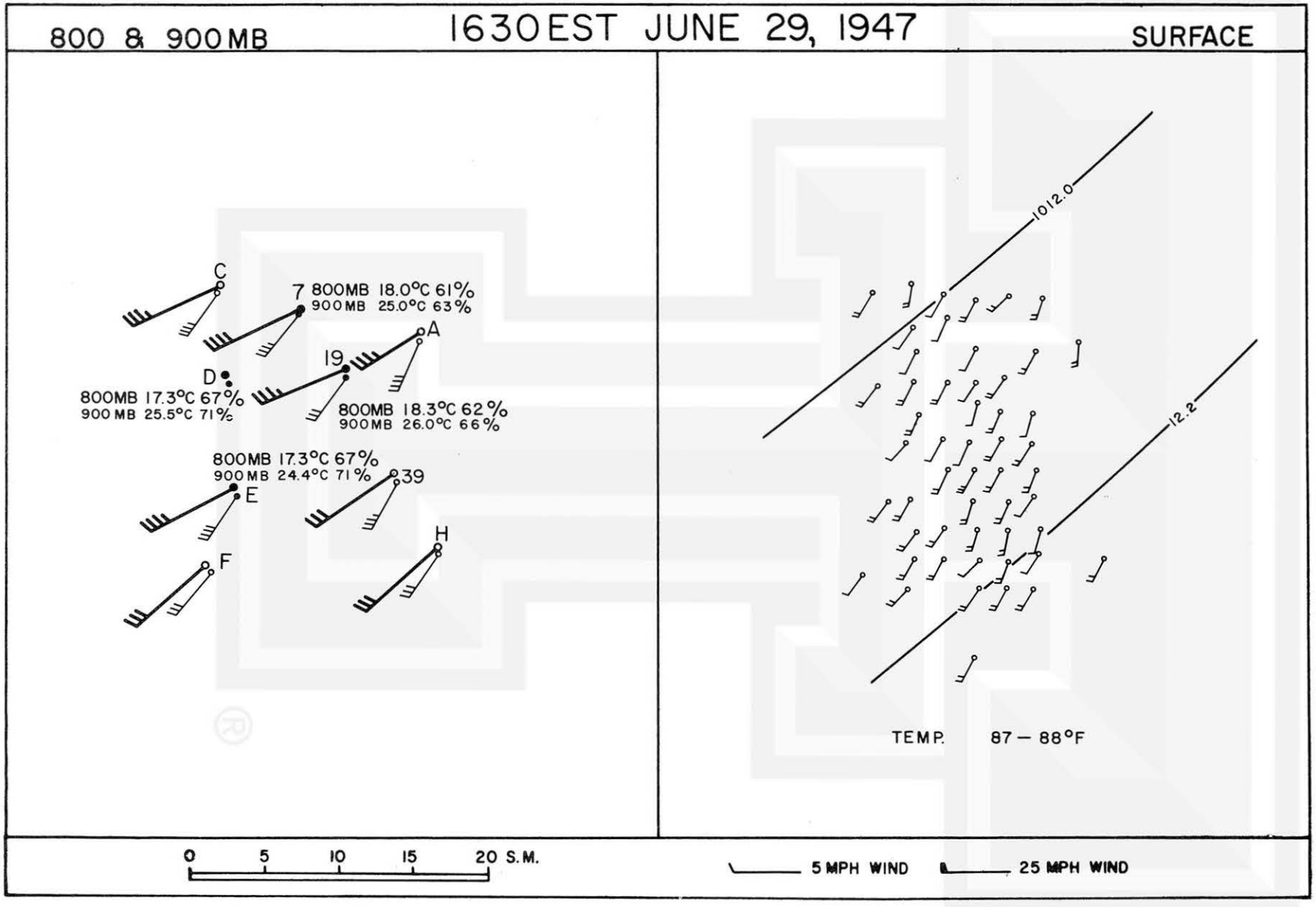
800 & 900 MB
1630 EST JUNE 29, 1947
SURFACE
C
7
800MB 18.0°C 61%
900MB 25.0°C 63%
A
19
D
800MB 17.3°C 67%
900 MB 25.5°C 71%
800MB 18.3°C 62%
900MB 26.0°C 66%
800MB 17.3°C 67%
900 MB 24.4°C 71%
39
E
F
H
1012.0
12.2
TEMP. 87 — 88°F
0 5 10 15 20 S.M.
5 MPH WIND
25 MPH WIND

FIGURE 18

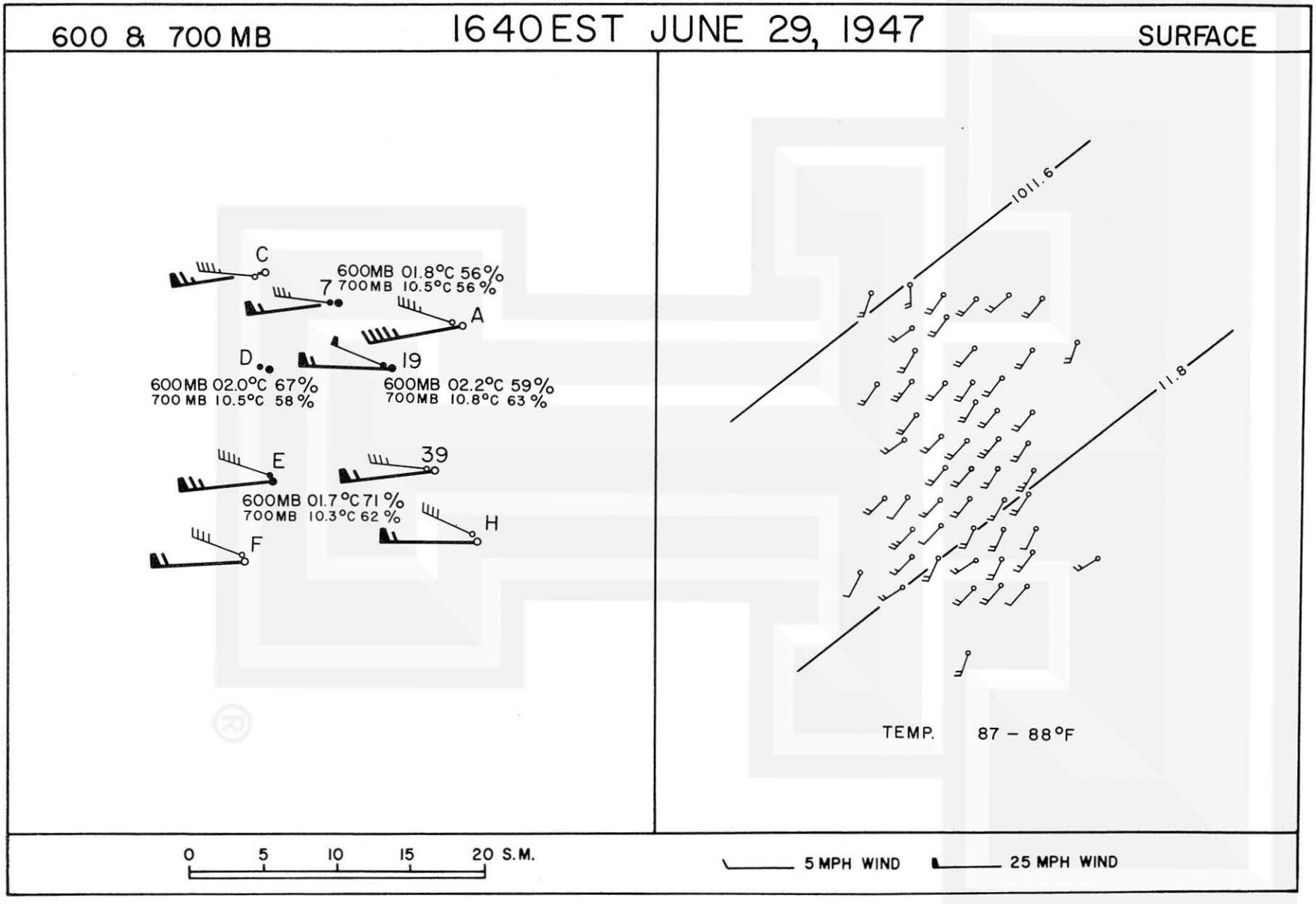
600 & 700 MB
1640 EST JUNE 29, 1947
SURFACE
C
600MB 01.8°C 56%
7 700MB 10.5°C 56%
A
D
19
600MB 02.0°C 67%
700 MB 10.5°C 58%
600MB 02.2°C 59%
700MB 10.8°C 63%
E
39
600MB 01.7°C 71%
700MB 10.3°C 62%
H
F
1011.6
11.8
TEMP. 87 – 88°F
0 5 10 15 20 S.M.
5 MPH WIND
25 MPH WIND

FIGURE 19

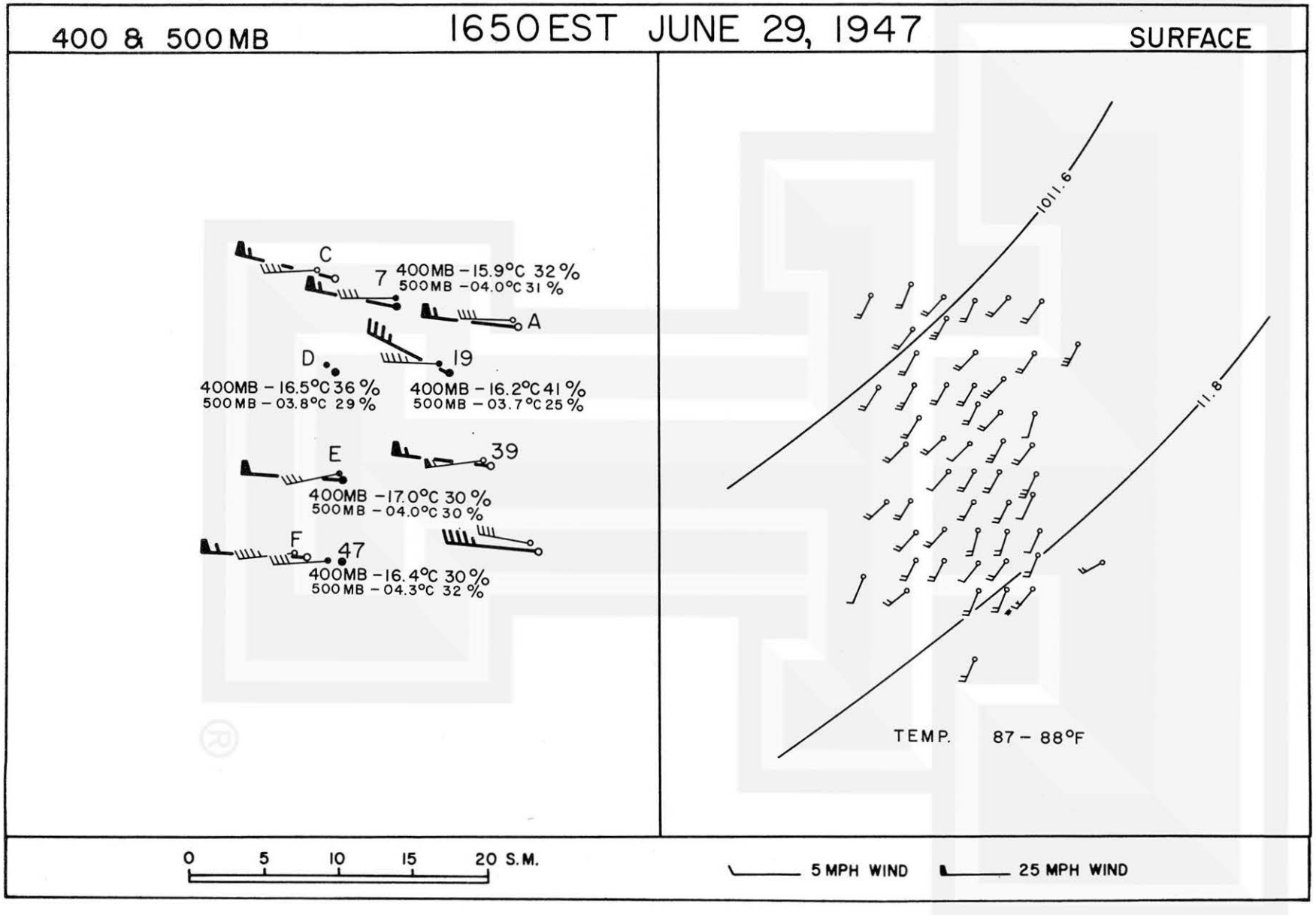
400 & 500 MB
1650 EST JUNE 29, 1947
SURFACE
C
7
400MB – 15.9°C 32 %
500MB – 04.0°C 31 %
A
D
19
400MB – 16.5°C 36 %
500MB – 03.8°C 29 %
400MB – 16.2°C 41 %
500MB – 03.7°C 25 %
E
39
400MB – 17.0°C 30 %
500MB – 04.0°C 30 %
F
47
400MB – 16.4°C 30 %
500MB – 04.3°C 32 %
1011.6
11.8
TEMP. 87 – 88°F
0 5 10 15 20 S.M.
5 MPH WIND
25 MPH WIND

FIGURE 20

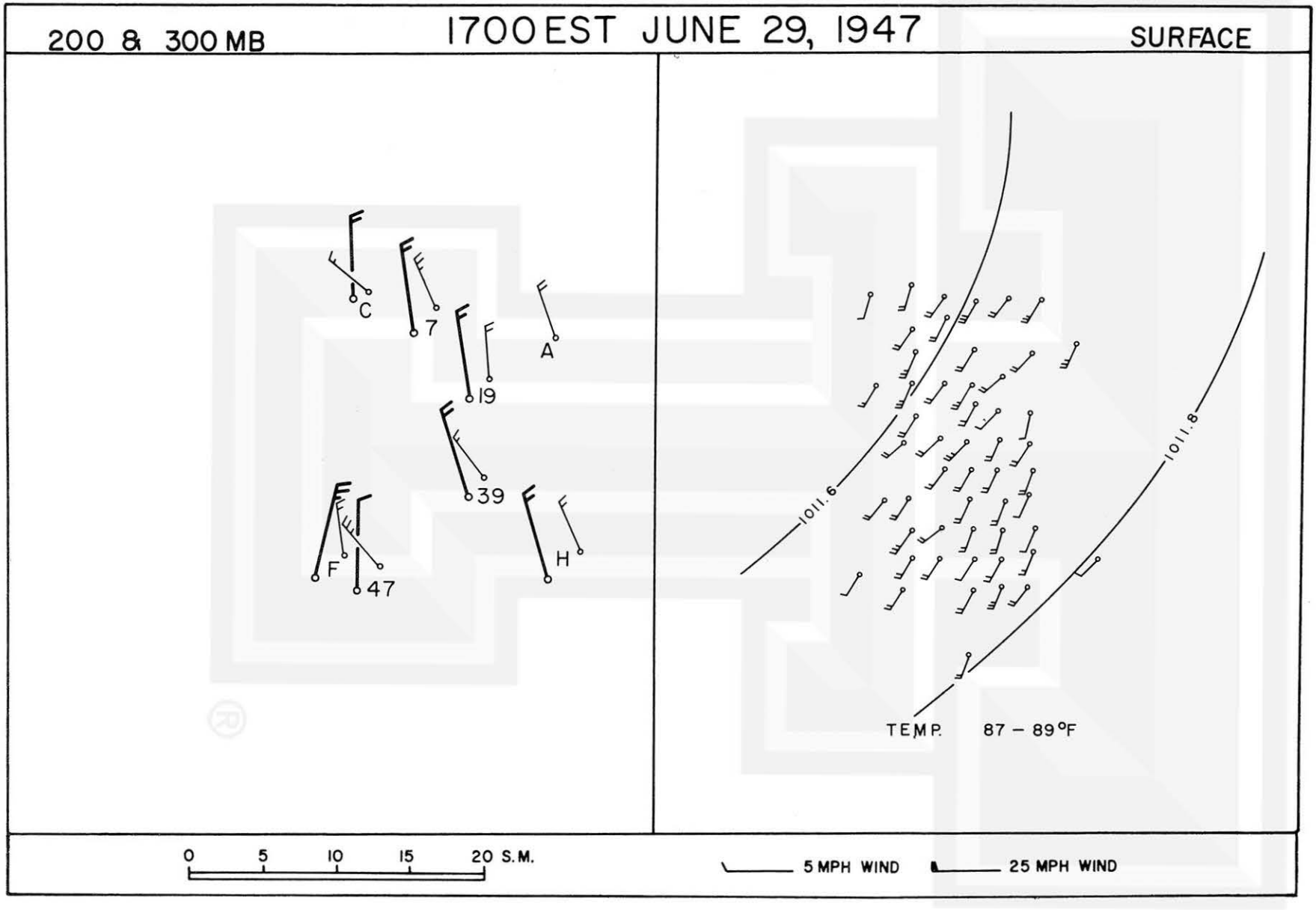
200 & 300 MB
1700 EST JUNE 29, 1947
SURFACE
C
7
A
19
39
F
47
H
1011.6
1011.8
TEMP. 87 – 89°F
0 5 10 15 20 S.M.
5 MPH WIND
25 MPH WIND

FIGURE 21

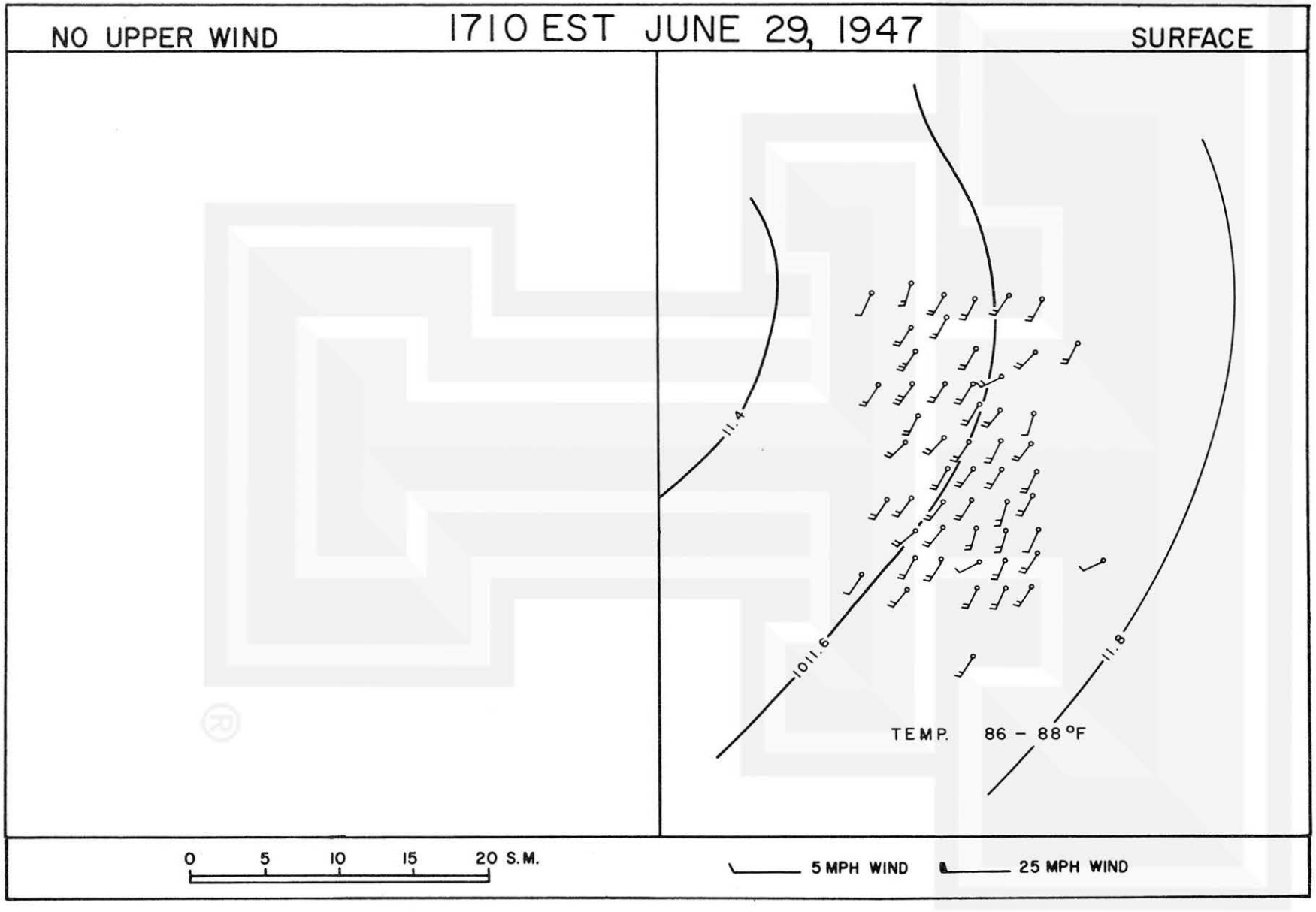
NO UPPER WIND
1710 EST JUNE 29, 1947
SURFACE
11.4
1011.6
11.8
TEMP. 86 – 88 °F
0 5 10 15 20 S.M.
5 MPH WIND
25 MPH WIND

FIGURE 22

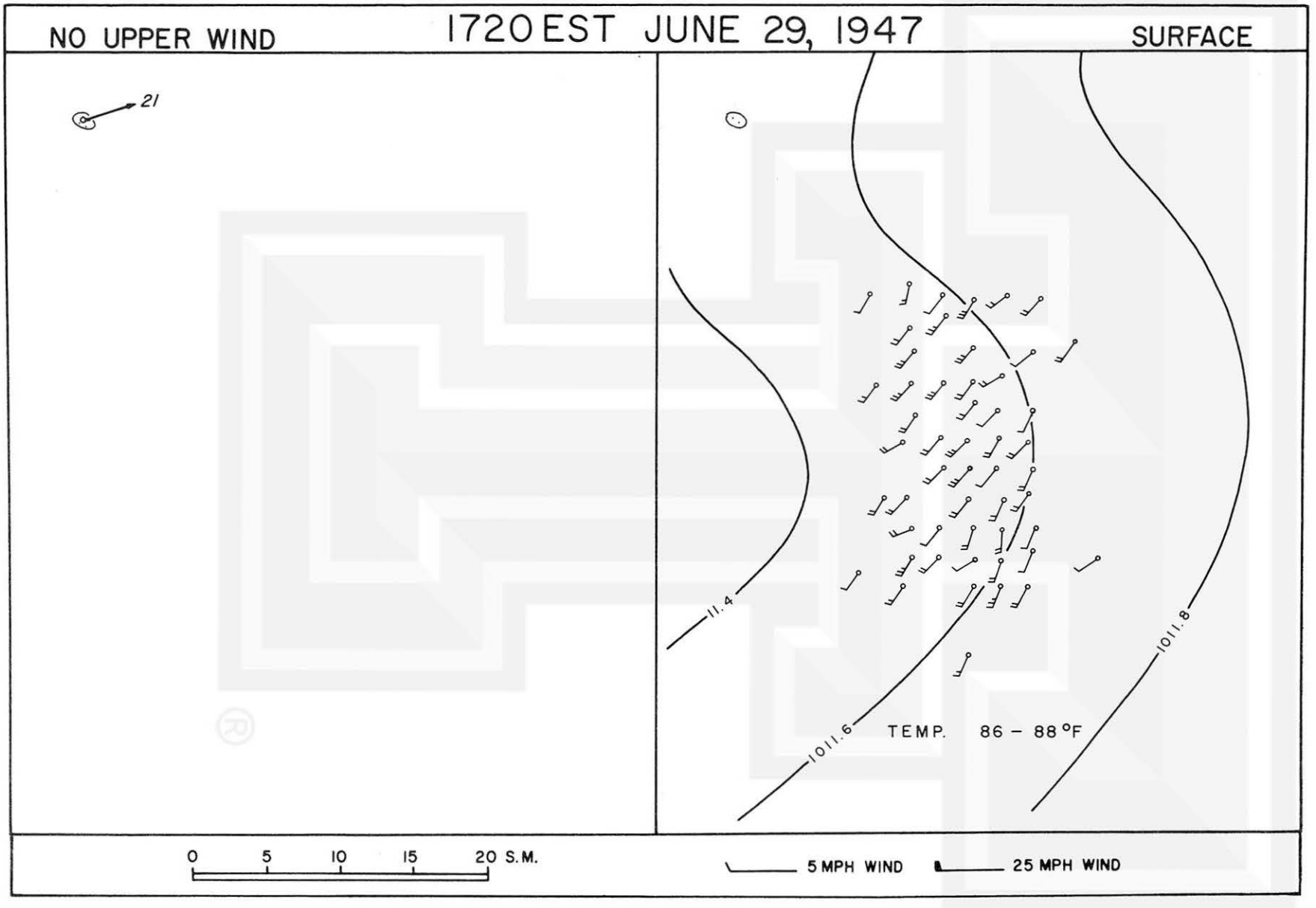
NO UPPER WIND
1720 EST JUNE 29, 1947
SURFACE
21
1011.4
1011.6
1011.8
TEMP. 86 – 88 °F
0 5 10 15 20 S.M.
5 MPH WIND
25 MPH WIND

FIGURE 23

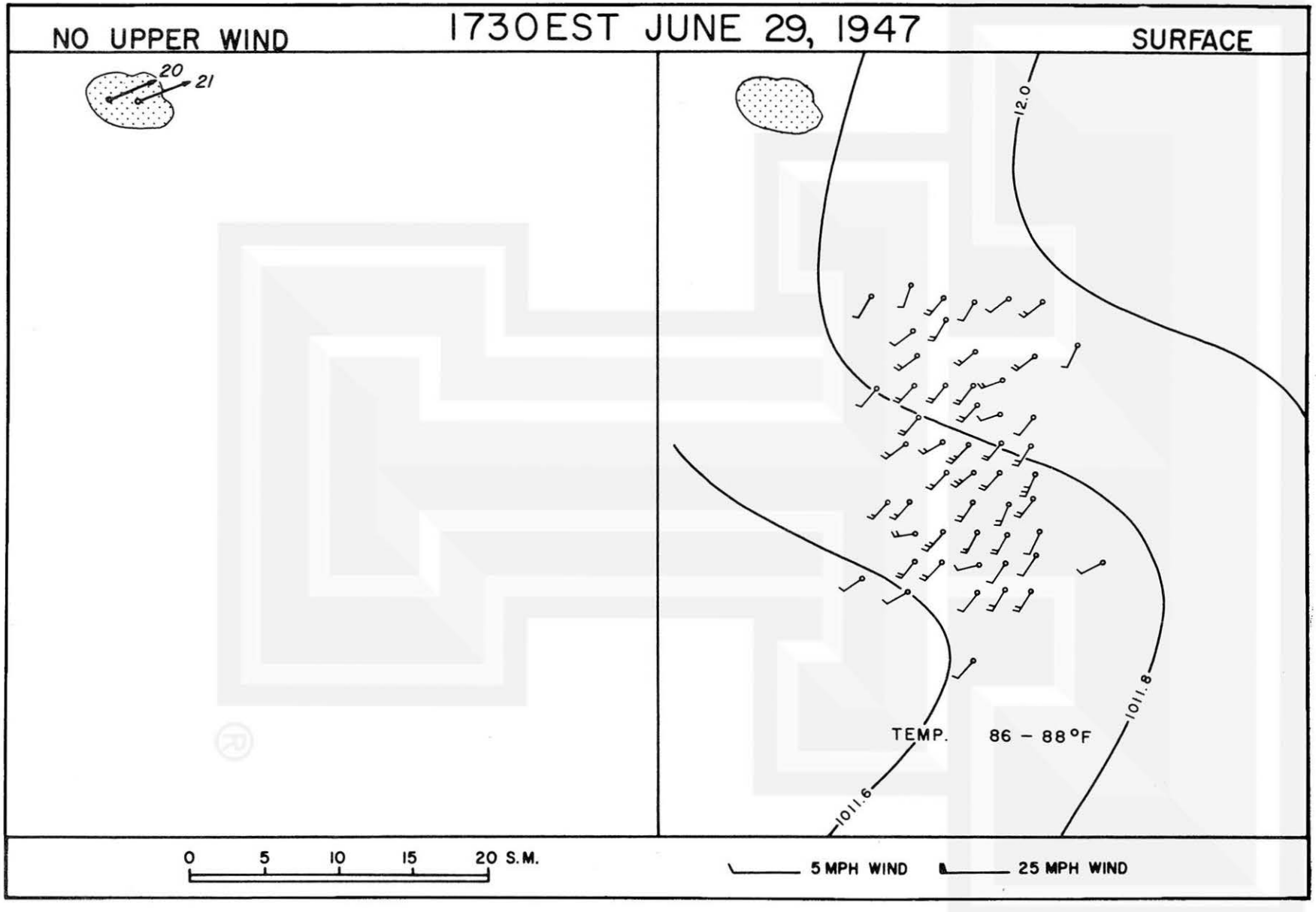
NO UPPER WIND
1730EST JUNE 29, 1947
SURFACE
20
21
12.0
TEMP. 86 – 88°F
1011.8
1011.6
0 5 10 15 20 S.M.
5 MPH WIND
25 MPH WIND

FIGURE 24

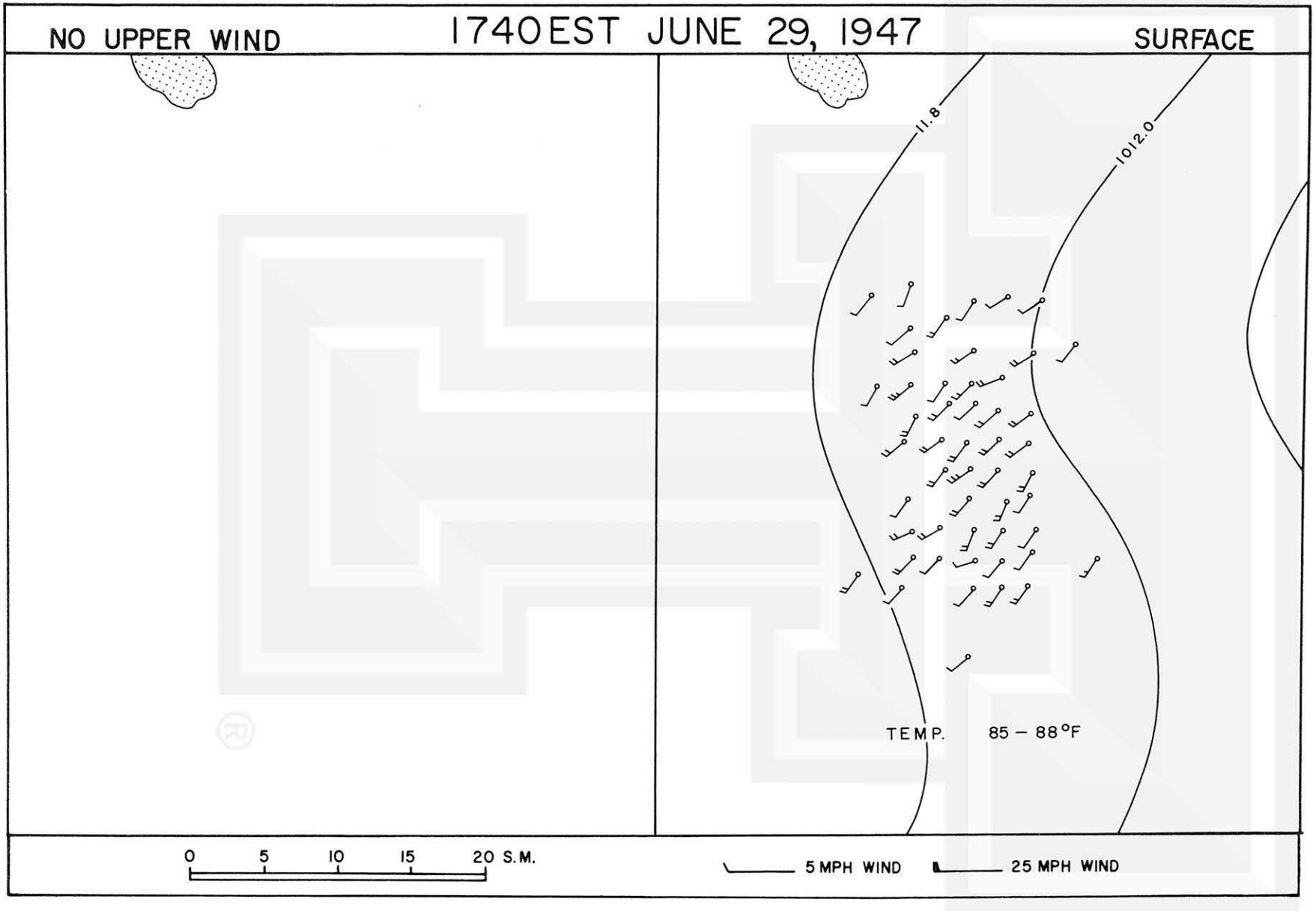
NO UPPER WIND
1740 EST JUNE 29, 1947
SURFACE
1011.8
1012.0
TEMP. 85 – 88°F
0 5 10 15 20 S.M.
5 MPH WIND
25 MPH WIND

FIGURE 25

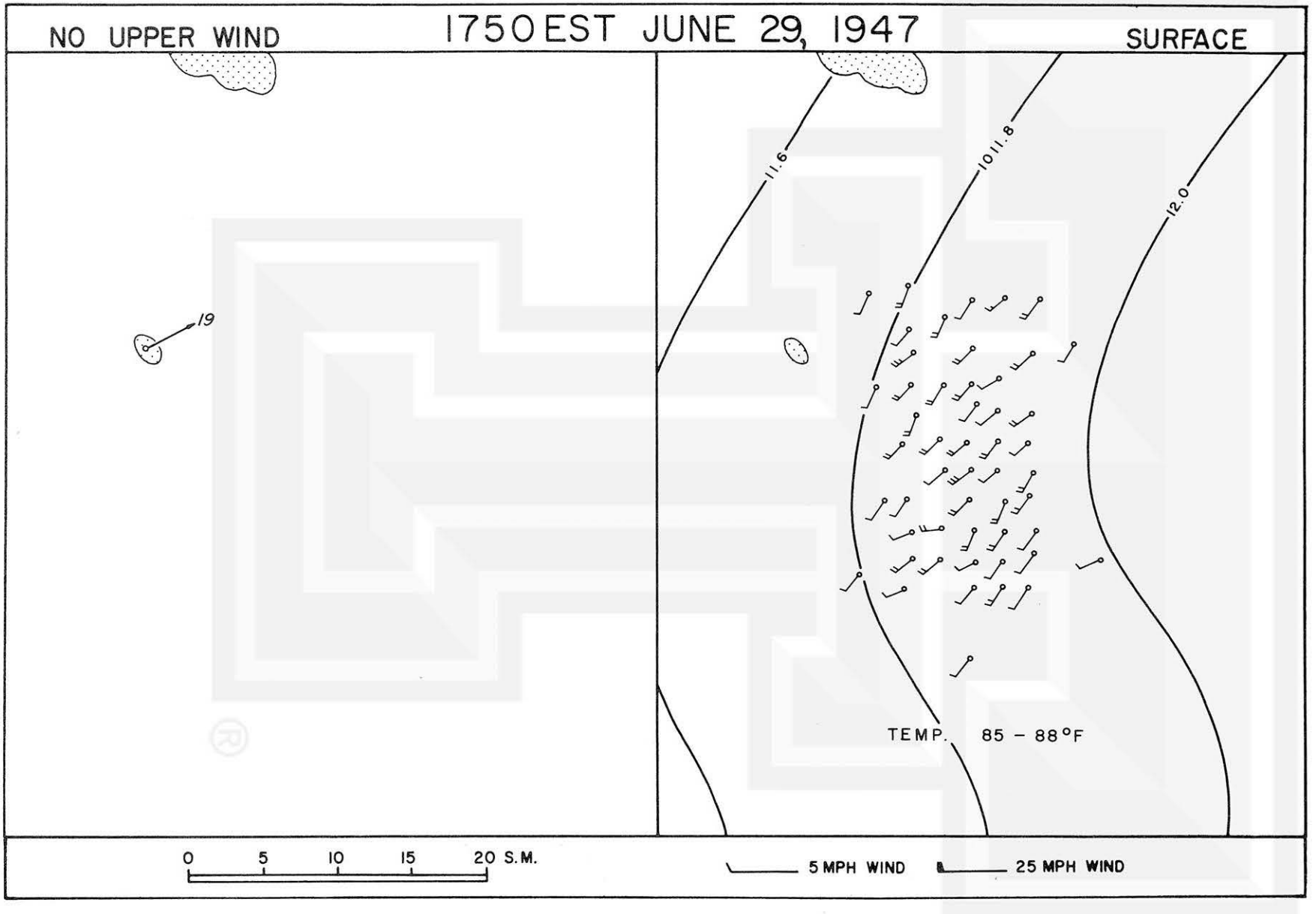
NO UPPER WIND
1750 EST JUNE 29, 1947
SURFACE
19
1011.6
1011.8
1012.0
TEMP. 85 – 88°F
0 5 10 15 20 S.M.
5 MPH WIND
25 MPH WIND

FIGURE 26

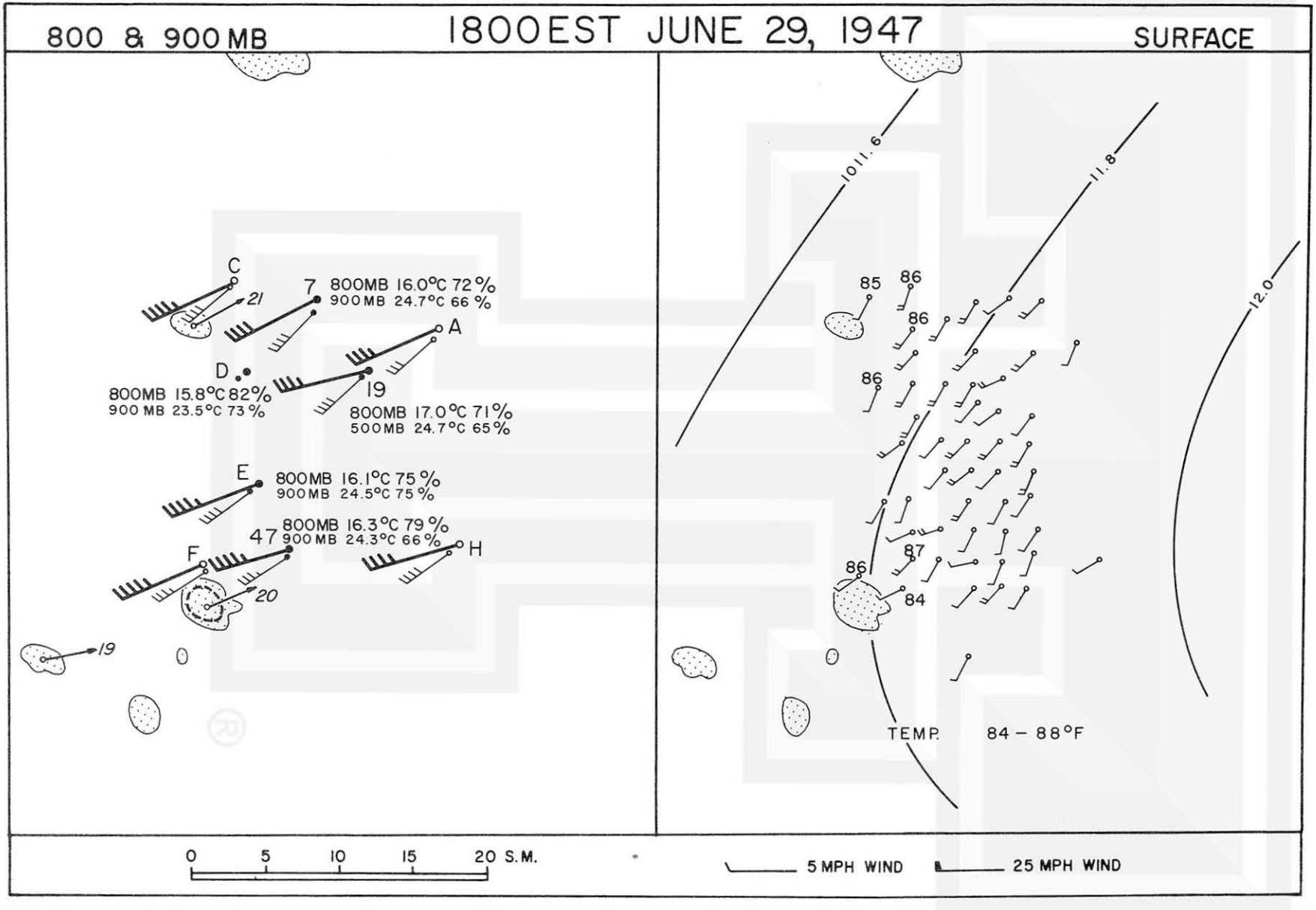
800 & 900 MB
1800 EST JUNE 29, 1947
SURFACE
C
21
7
800MB 16.0°C 72%
900MB 24.7°C 66%
A
D
800MB 15.8°C 82%
900 MB 23.5°C 73%
19
800MB 17.0°C 71%
500MB 24.7°C 65%
E
800MB 16.1°C 75%
900MB 24.5°C 75%
47
800MB 16.3°C 79%
900MB 24.3°C 66%
F
H
20
19
1011.6
11.8
12.0
85
86
86
86
87
86
84
TEMP. 84 – 88°F
0 5 10 15 20 S.M.
5 MPH WIND
25 MPH WIND

FIGURE 27

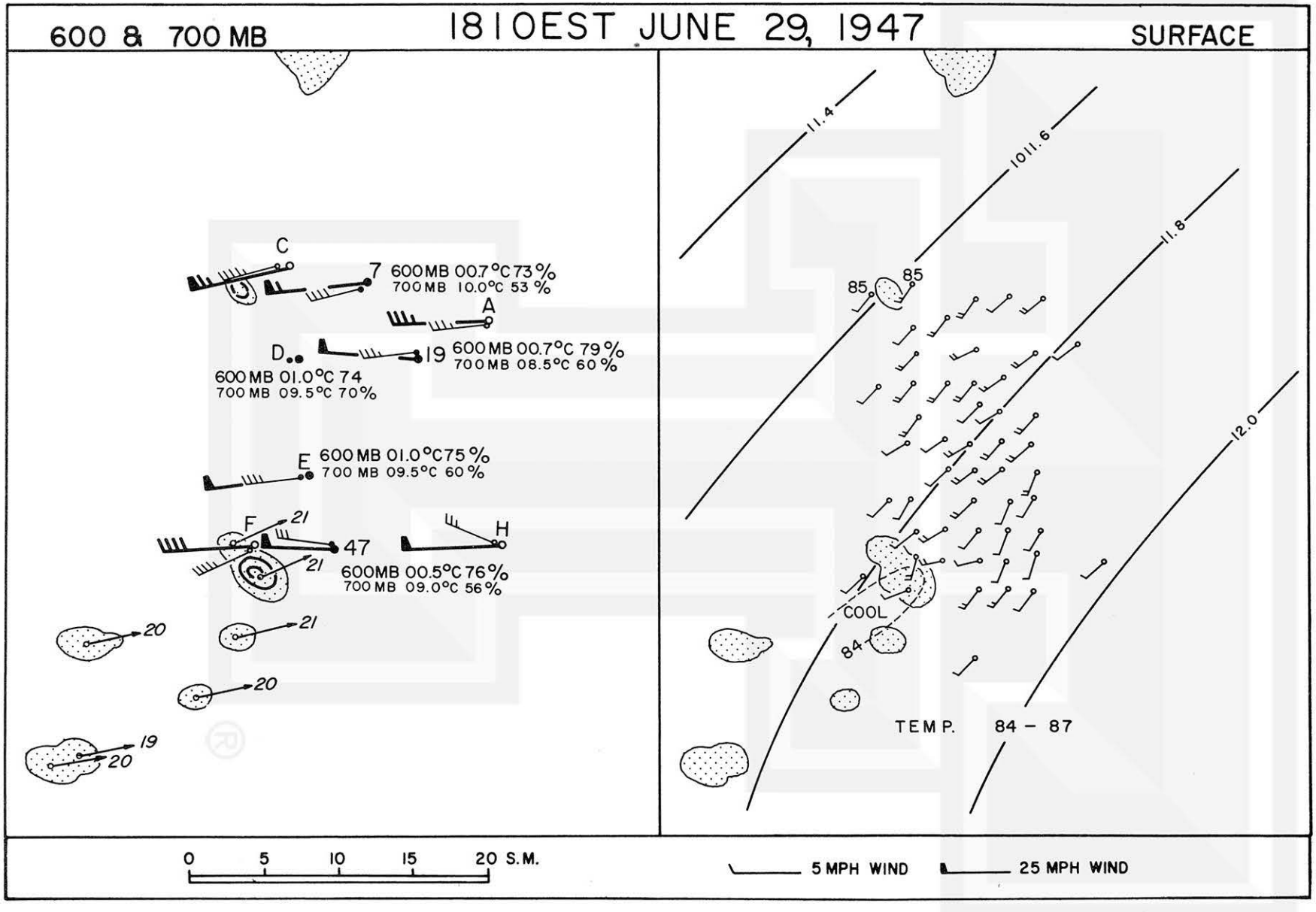
600 & 700 MB
1810EST JUNE 29, 1947
SURFACE
C
7
600MB 00.7°C 73%
700MB 10.0°C 53%
A
D
19
600MB 00.7°C 79%
700MB 08.5°C 60%
600MB 01.0°C 74
700MB 09.5°C 70%
E
600MB 01.0°C 75%
700 MB 09.5°C 60%
F
21
47
H
21
600MB 00.5°C 76%
700MB 09.0°C 56%
20
21
20
19
20
11.4
1011.6
11.8
12.0
85
85
COOL
84
TEMP. 84 – 87
0 5 10 15 20 S.M.
5 MPH WIND
25 MPH WIND

FIGURE 28

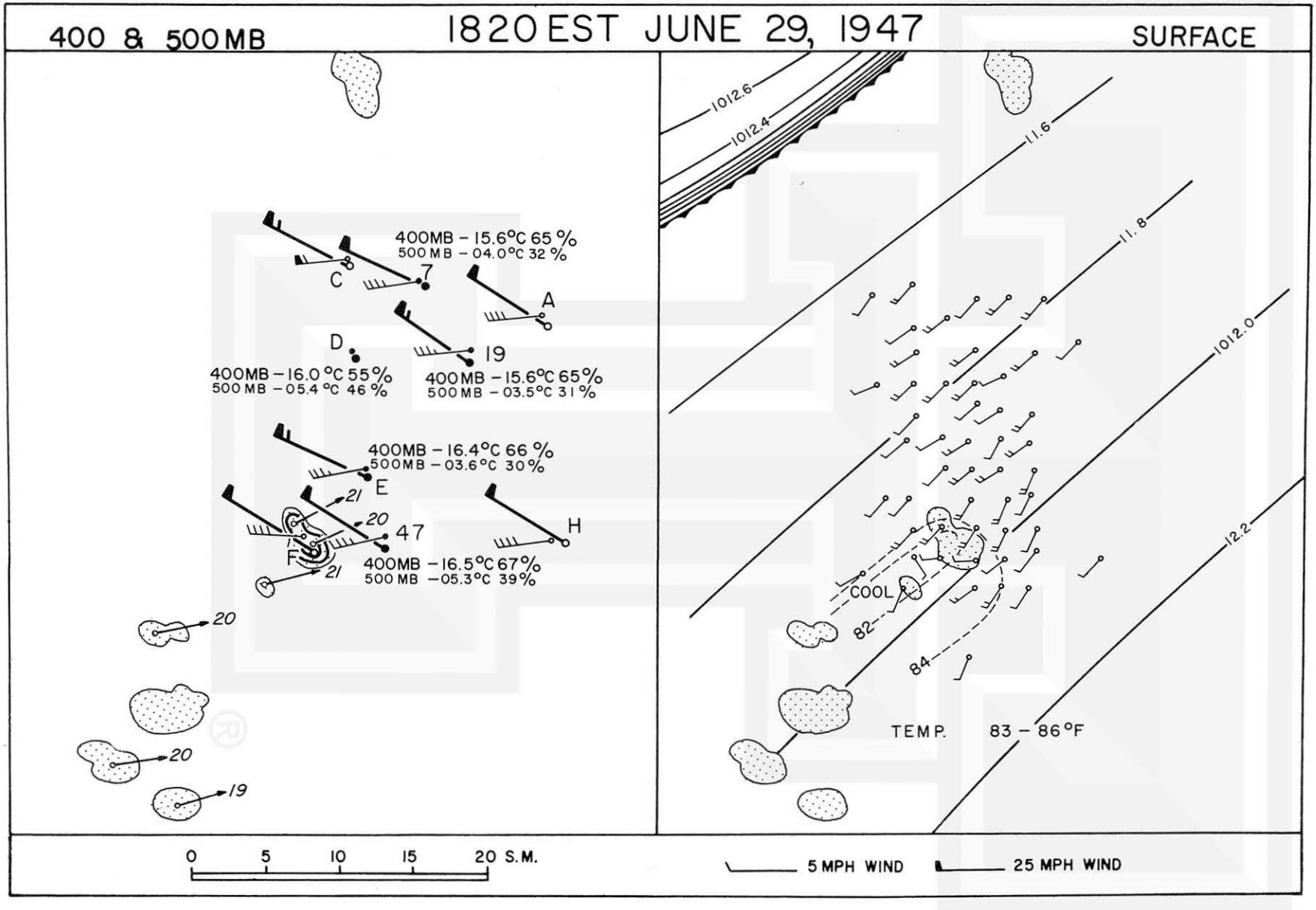
400 & 500 MB
1820 EST JUNE 29, 1947
SURFACE
400MB – 15.6°C 65 %
500 MB – 04.0°C 32 %
C
7
A
D
19
400MB – 16.0 °C 55%
500 MB – 05.4 °C 46 %
400MB – 15.6°C 65%
500 MB – 03.5°C 31 %
400MB – 16.4°C 66 %
500MB – 03.6°C 30 %
E
21
20
47
H
F
400MB – 16.5°C 67%
500 MB – 05.3°C 39%
21
20
20
19
1012.6
1012.4
11.6
11.8
1012.0
12.2
COOL
82
84
TEMP. 83 – 86°F
0 5 10 15 20 S.M.
5 MPH WIND
25 MPH WIND

FIGURE 29

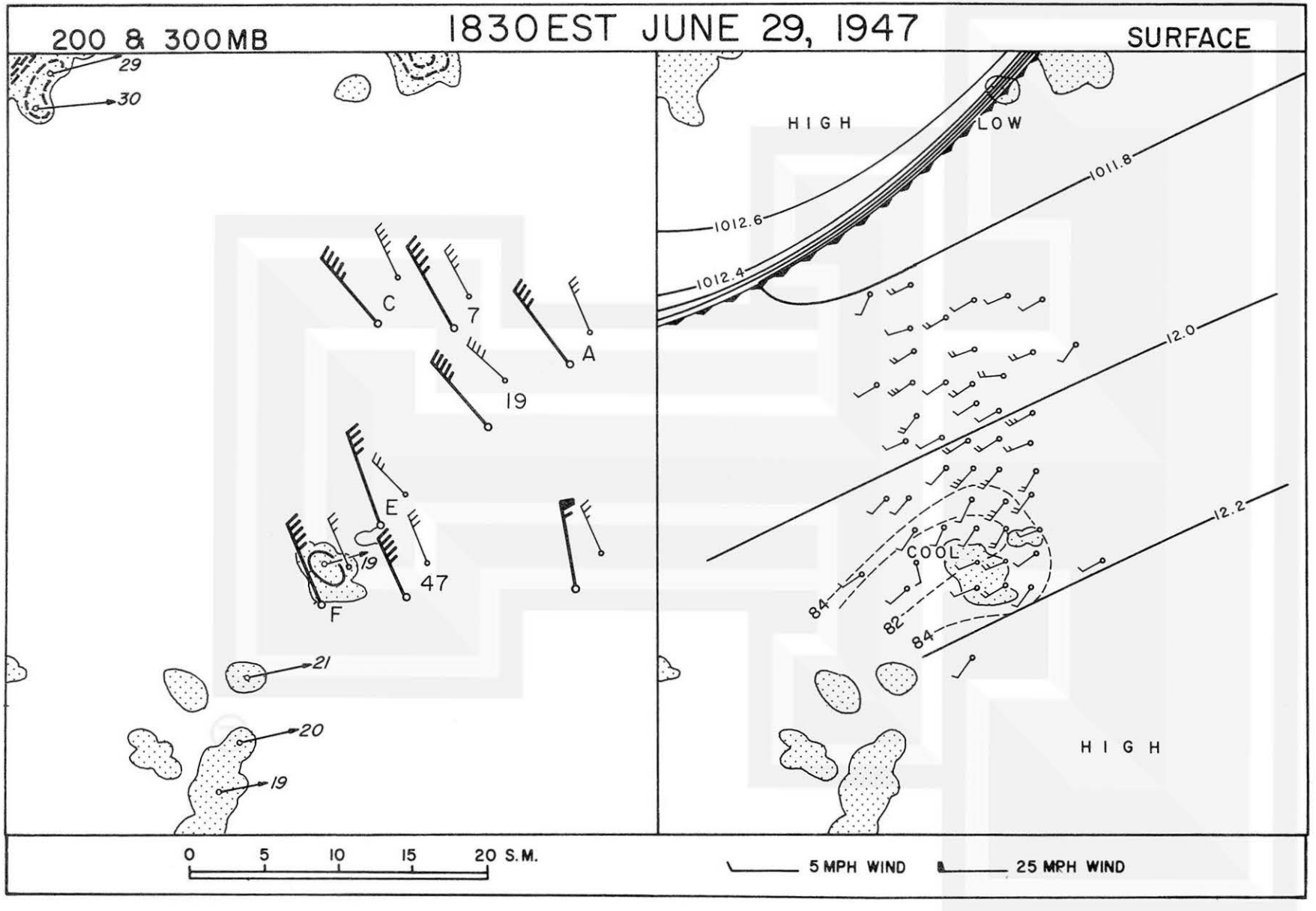
200 & 300MB
1830EST JUNE 29, 1947
SURFACE
29
30
C
7
A
19
E
19
47
F
21
20
19
HIGH
LOW
1011.8
1012.6
1012.4
12.0
12.2
COOL
84
82
84
HIGH
0 5 10 15 20 S.M.
5 MPH WIND
25 MPH WIND

FIGURE 30

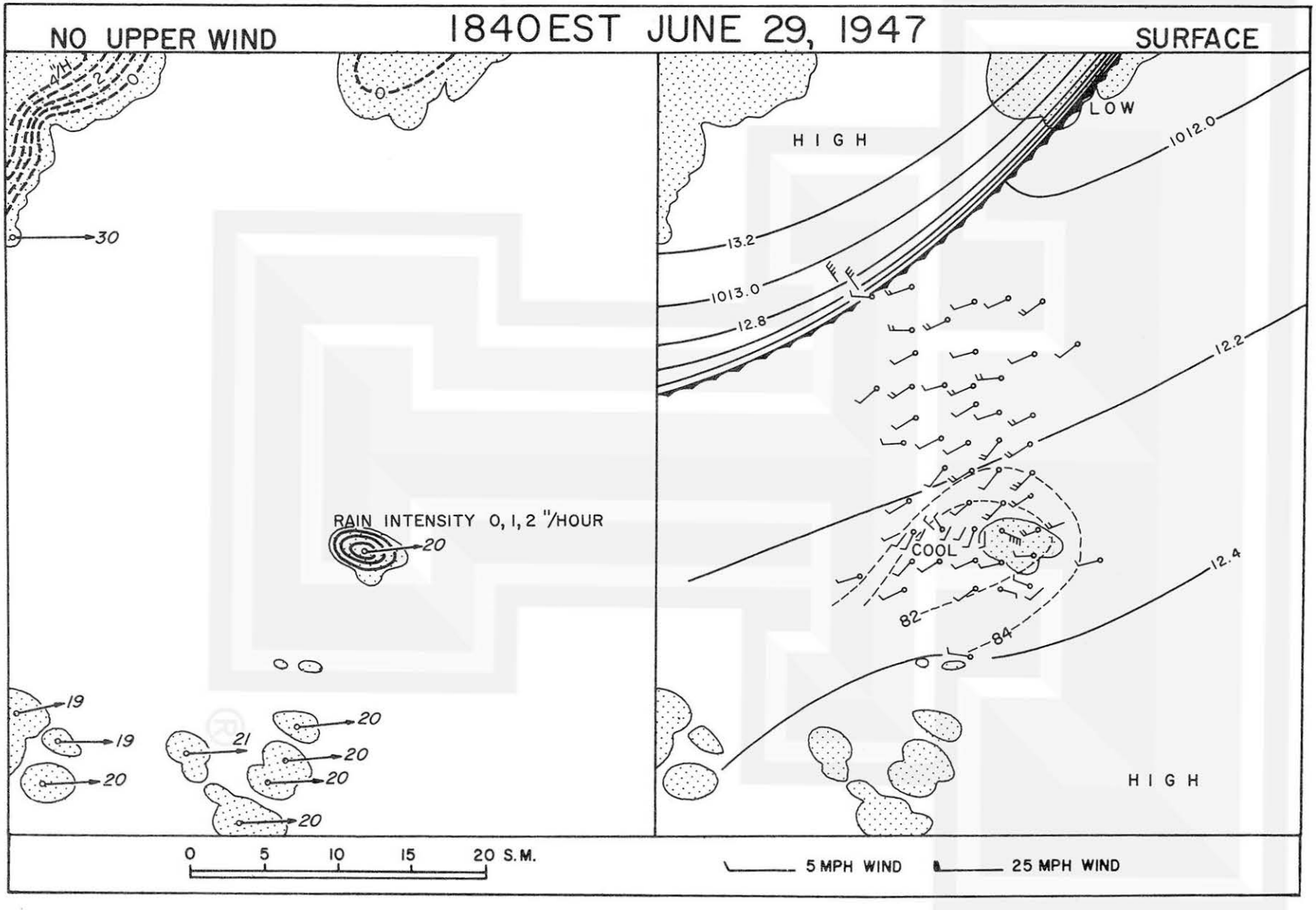
NO UPPER WIND
1840 EST JUNE 29, 1947
SURFACE
4"
2
0
30
0
HIGH
LOW
1012.0
13.2
1013.0
12.8
12.2
RAIN INTENSITY 0, 1, 2 "/HOUR
20
COOL
82
84
12.4
19
19
20
21
20
20
20
20
HIGH
0 5 10 15 20 S.M.
5 MPH WIND
25 MPH WIND

FIGURE 31

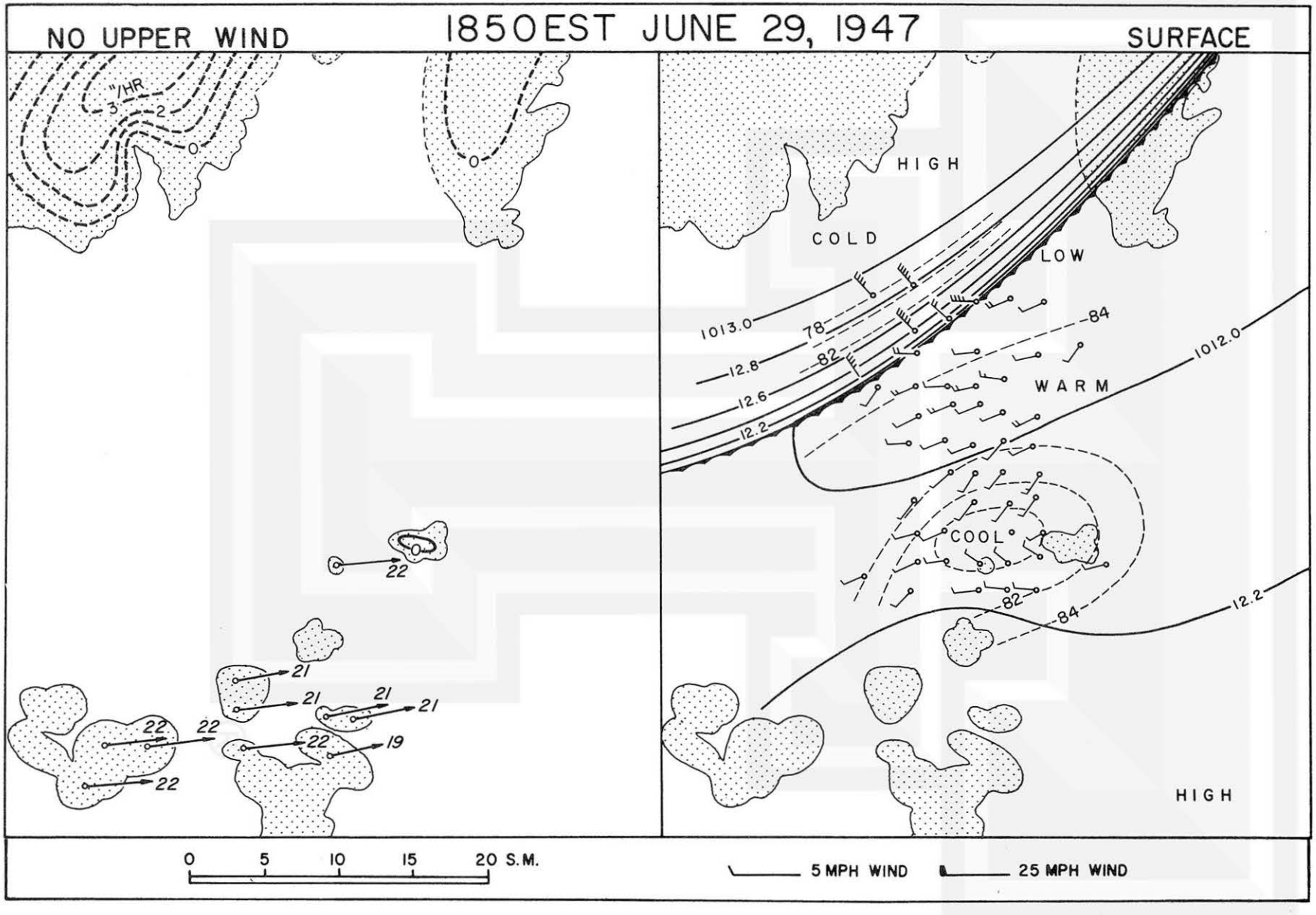
NO UPPER WIND
1850 EST JUNE 29, 1947
SURFACE
"/HR
3
2
0
0
HIGH
COLD
LOW
1013.0
78
84
12.8
82
1012.0
12.6
WARM
12.2
COOL
82
84
12.2
22
21
21
21
21
22
22
22
19
22
HIGH
0 5 10 15 20 S.M.
5 MPH WIND
25 MPH WIND

FIGURE 32

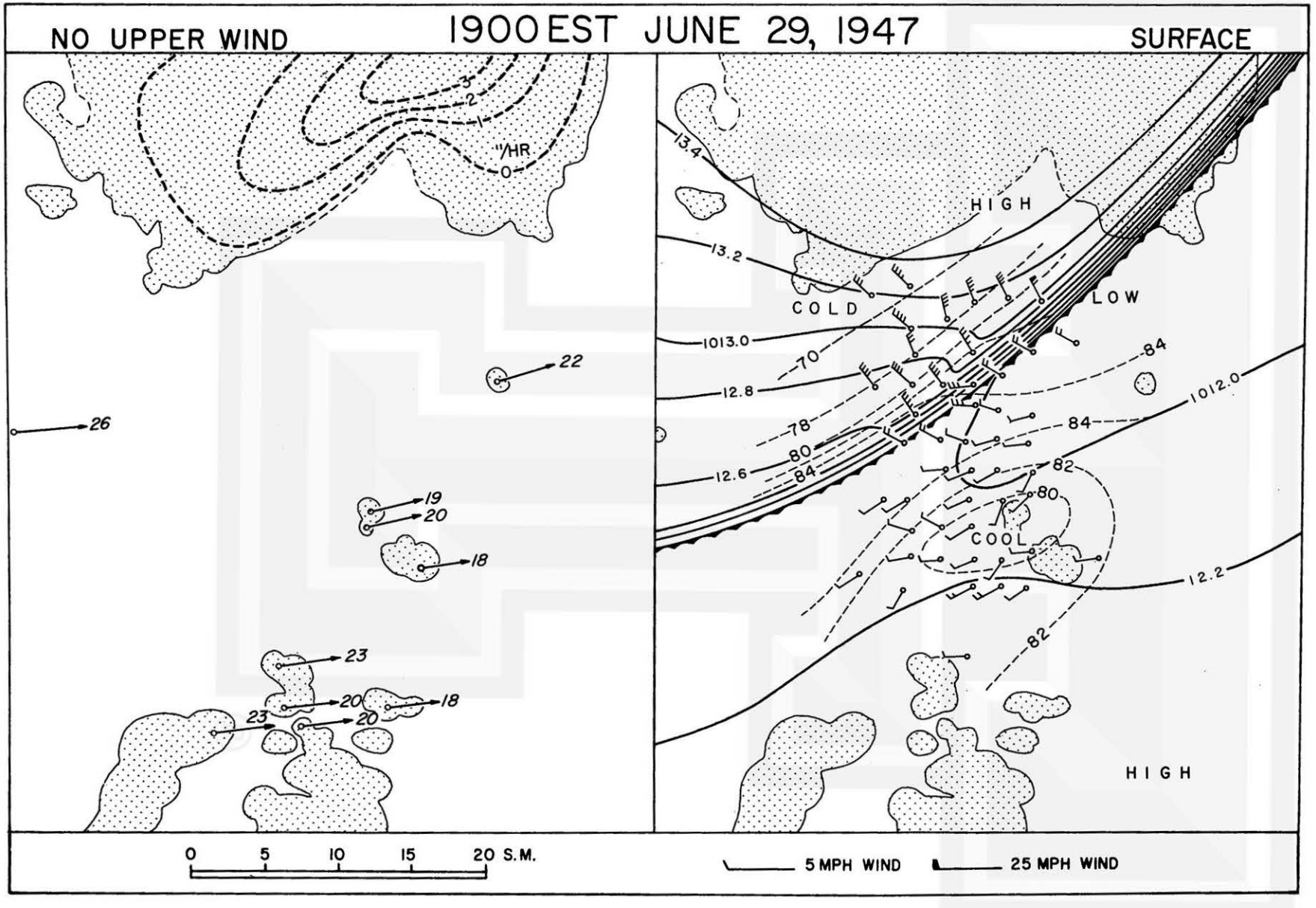
NO UPPER WIND
1900 EST JUNE 29, 1947
SURFACE
3
2
1
"/HR
0
22
26
19
20
18
23
20
18
23
20
13.4
HIGH
13.2
COLD
LOW
1013.0
70
84
12.8
78
84
1012.0
80
12.6
84
82
80
COOL
12.2
82
HIGH
0 5 10 15 20 S.M.
5 MPH WIND
25 MPH WIND

FIGURE 33

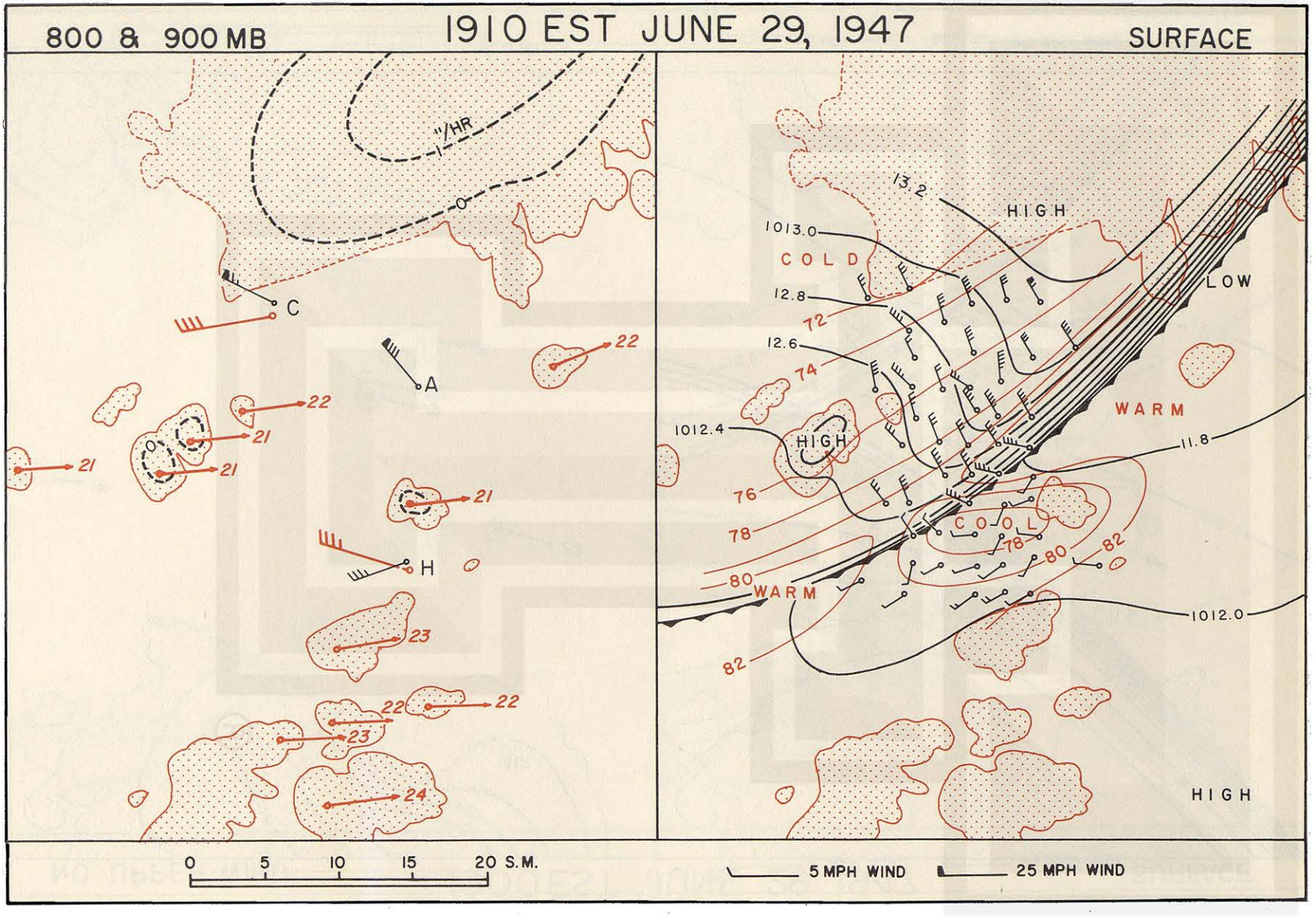
800 & 900 MB
1910 EST JUNE 29, 1947
SURFACE
"/HR
1
0
C
A
H
22
21
23
24
13.2
HIGH
1013.0
COLD
12.8
72
12.6
74
LOW
WARM
1012.4
HIGH
11.8
76
78
COOL
78
80
82
80
WARM
82
1012.0
HIGH
0 5 10 15 20 S.M.
5 MPH WIND
25 MPH WIND

FIGURE 34

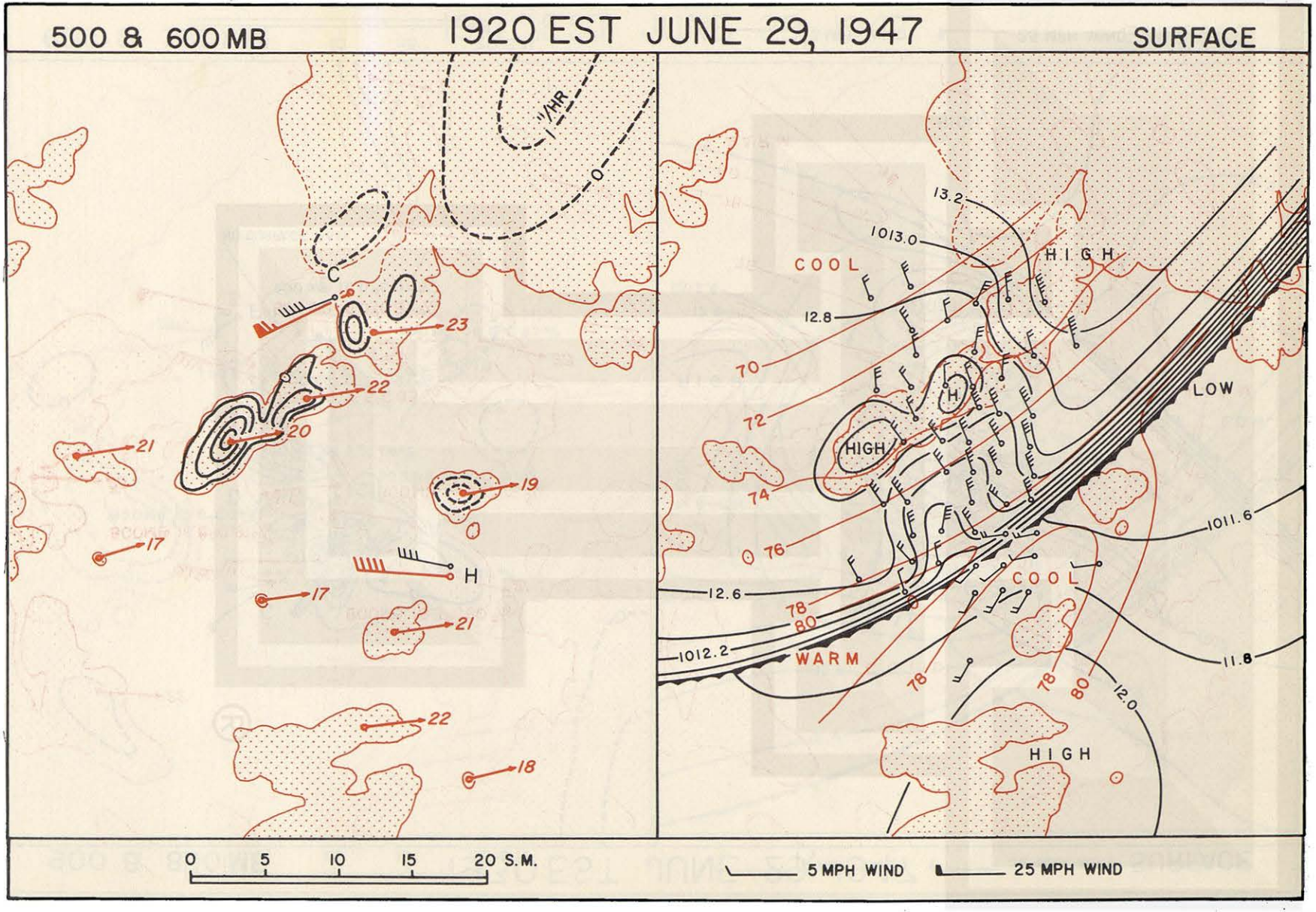
500 & 600 MB
1920 EST JUNE 29, 1947
SURFACE
1"/HR
1
0
C
23
22
20
21
19
17
17
H
21
22
18
13.2
1013.0
COOL
HIGH
12.8
70
72
74
76
H
HIGH
LOW
1011.6
12.6
78
80
1012.2
WARM
COOL
11.8
78
78
80
12.0
HIGH
0 5 10 15 20 S.M.
5 MPH WIND
25 MPH WIND

FIGURE 35

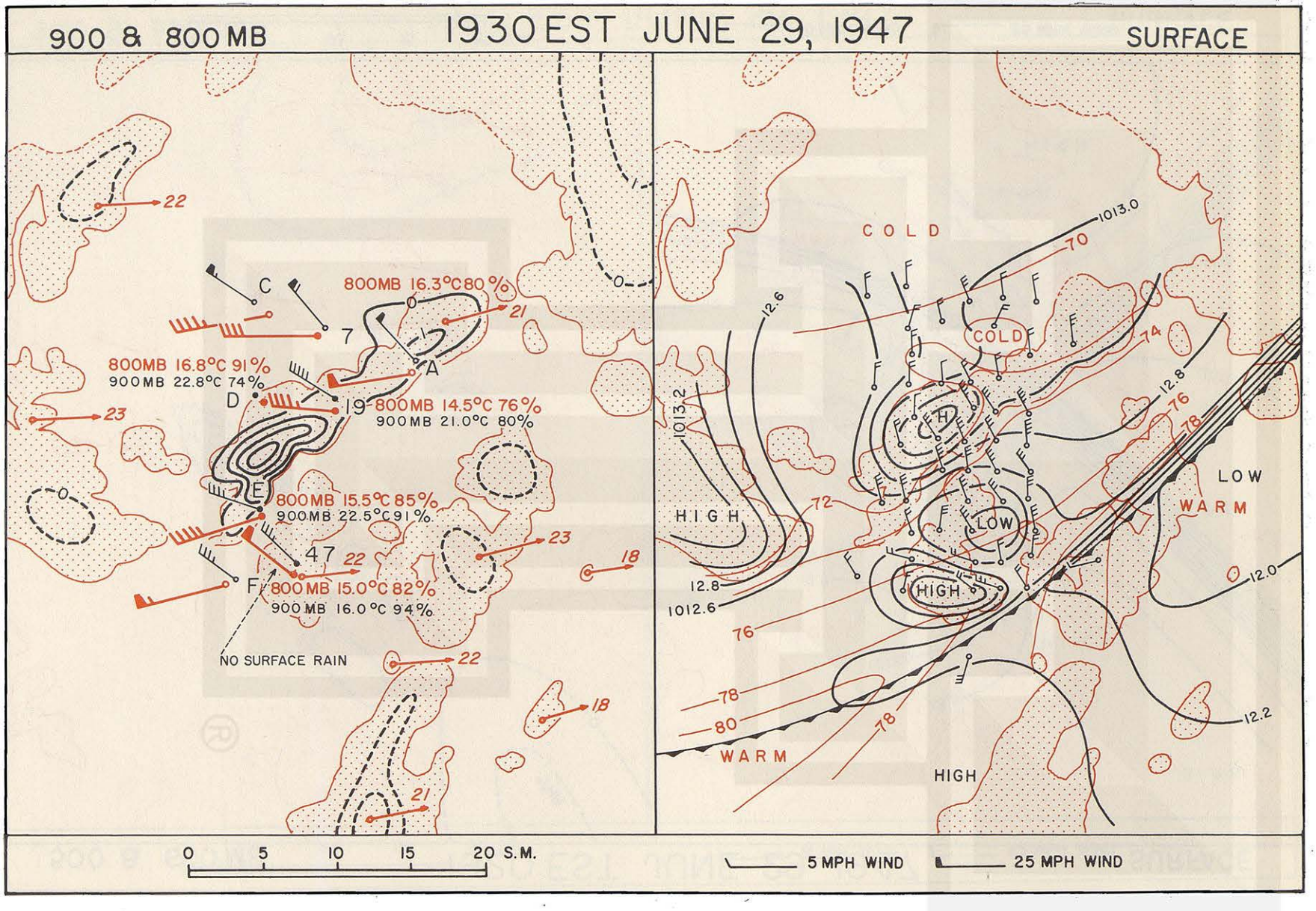
900 & 800 MB
1930 EST JUNE 29, 1947
SURFACE
800MB 16.3°C 80%
800MB 16.8°C 91%
900MB 22.8°C 74%
800MB 14.5°C 76%
900MB 21.0°C 80%
800MB 15.5°C 85%
900MB 22.5°C 91%
800MB 15.0°C 82%
900MB 16.0°C 94%
NO SURFACE RAIN
COLD
COLD
WARM
WARM
HIGH
HIGH
LOW
LOW
1013.0
1013.2
1012.6
12.6
12.8
12.0
12.2
0 5 10 15 20 S.M.
5 MPH WIND
25 MPH WIND

FIGURE 36

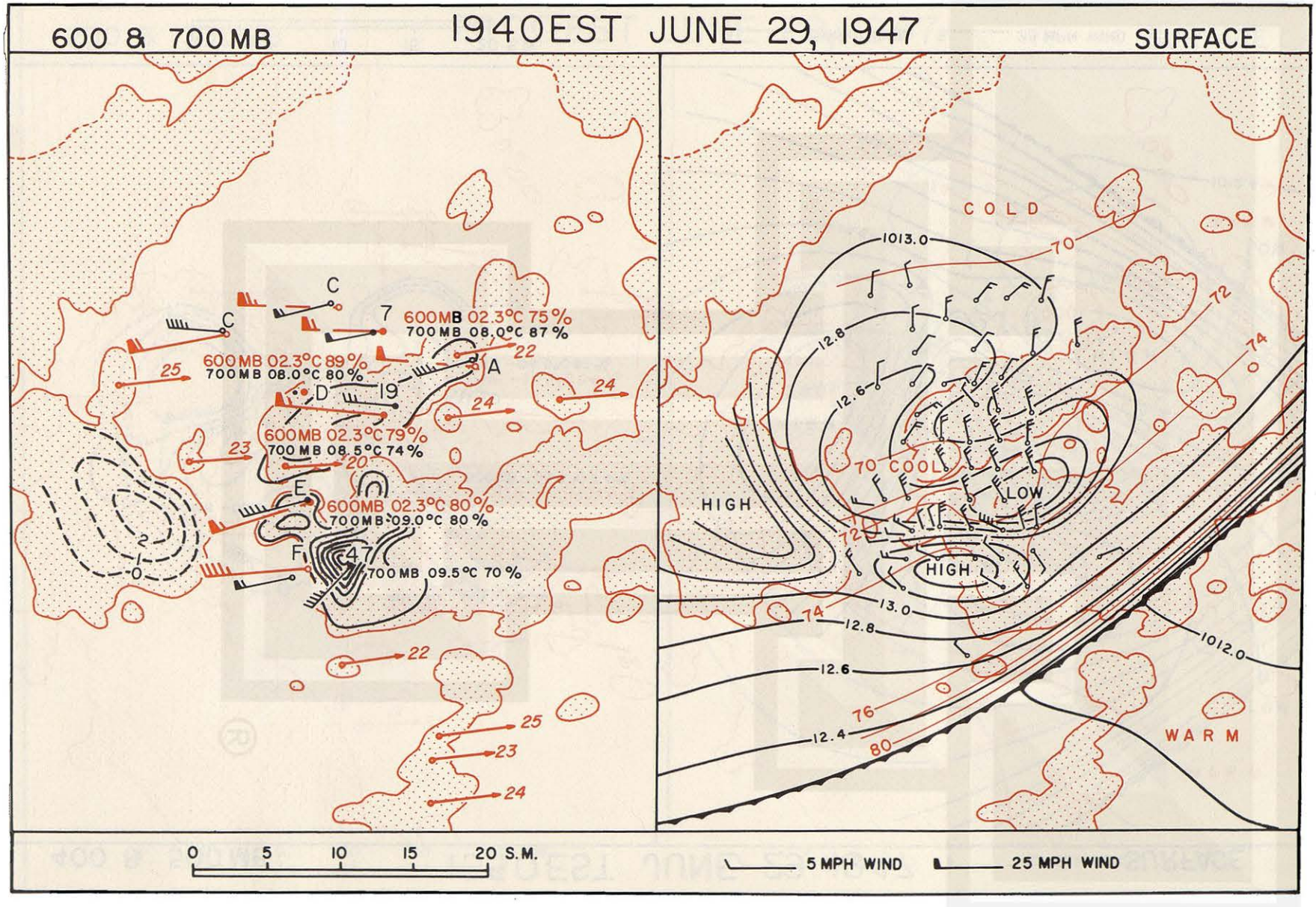
600 & 700 MB
1940 EST JUNE 29, 1947
SURFACE
600MB 02.3°C 75%
700MB 08.0°C 87%
600MB 02.3°C 89%
700MB 08.0°C 80%
600MB 02.3°C 79%
700MB 08.5°C 74%
600MB 02.3°C 80%
700MB 09.0°C 80%
700MB 09.5°C 70%
COLD
1013.0
70
72
12.8
12.6
74
70 COOL
HIGH
LOW
HIGH
13.0
12.8
1012.0
12.6
76
12.4
80
WARM
0 5 10 15 20 S.M.
5 MPH WIND
25 MPH WIND

FIGURE 37

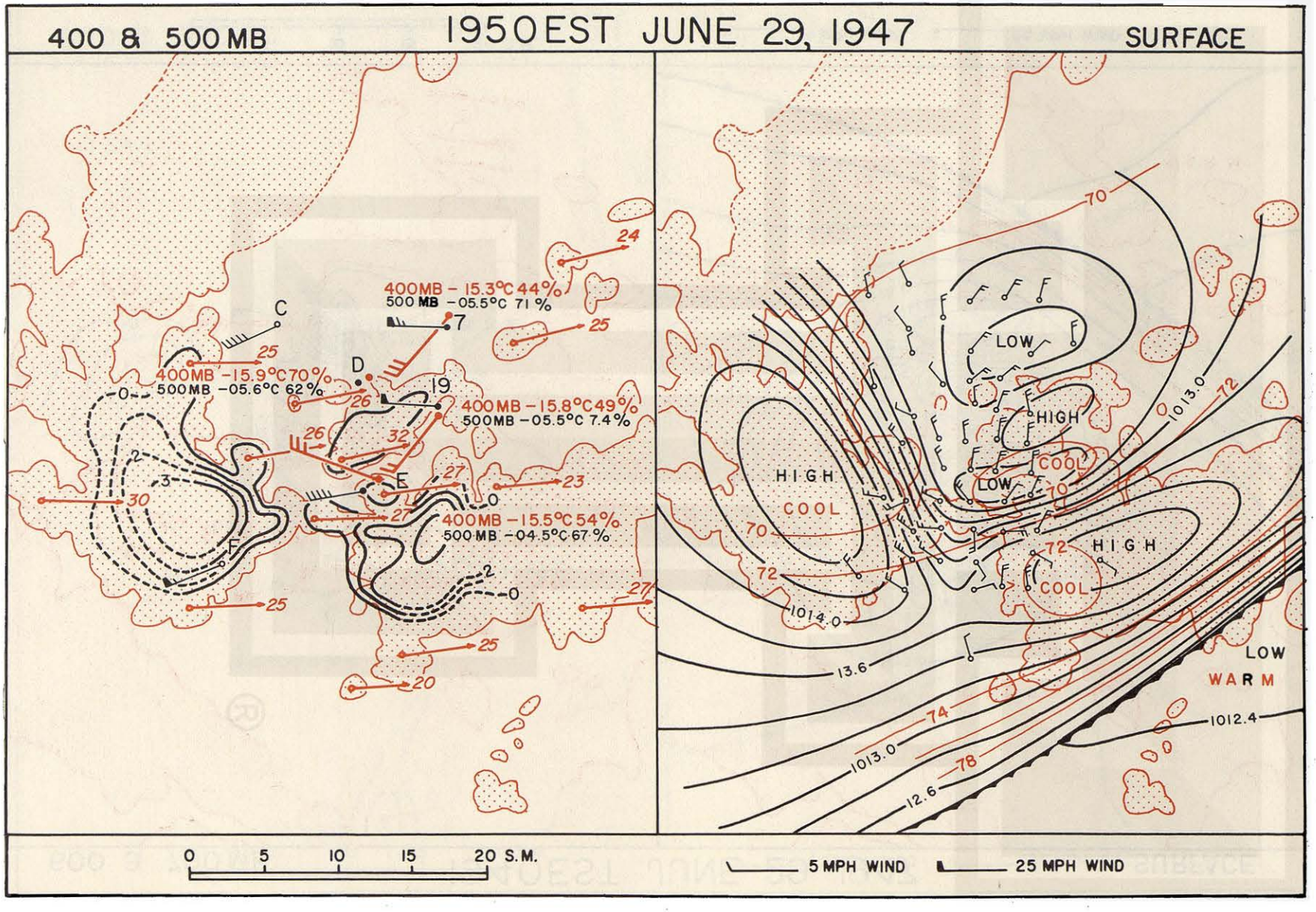
400 & 500 MB
1950 EST JUNE 29, 1947
SURFACE
400MB - 15.3°C 44%
500 MB -05.5°C 71 %
400MB -15.9°C 70%
500MB -05.6°C 62 %
400MB - 15.8°C 49%
500MB -05.5°C 7.4 %
400MB - 15.5°C 54%
500 MB -04.5°C 67 %
C
D
E
F
HIGH
COOL
LOW
WARM
1013.0
1014.0
1012.4
13.6
12.6
0 5 10 15 20 S.M.
5 MPH WIND
25 MPH WIND

FIGURE 38

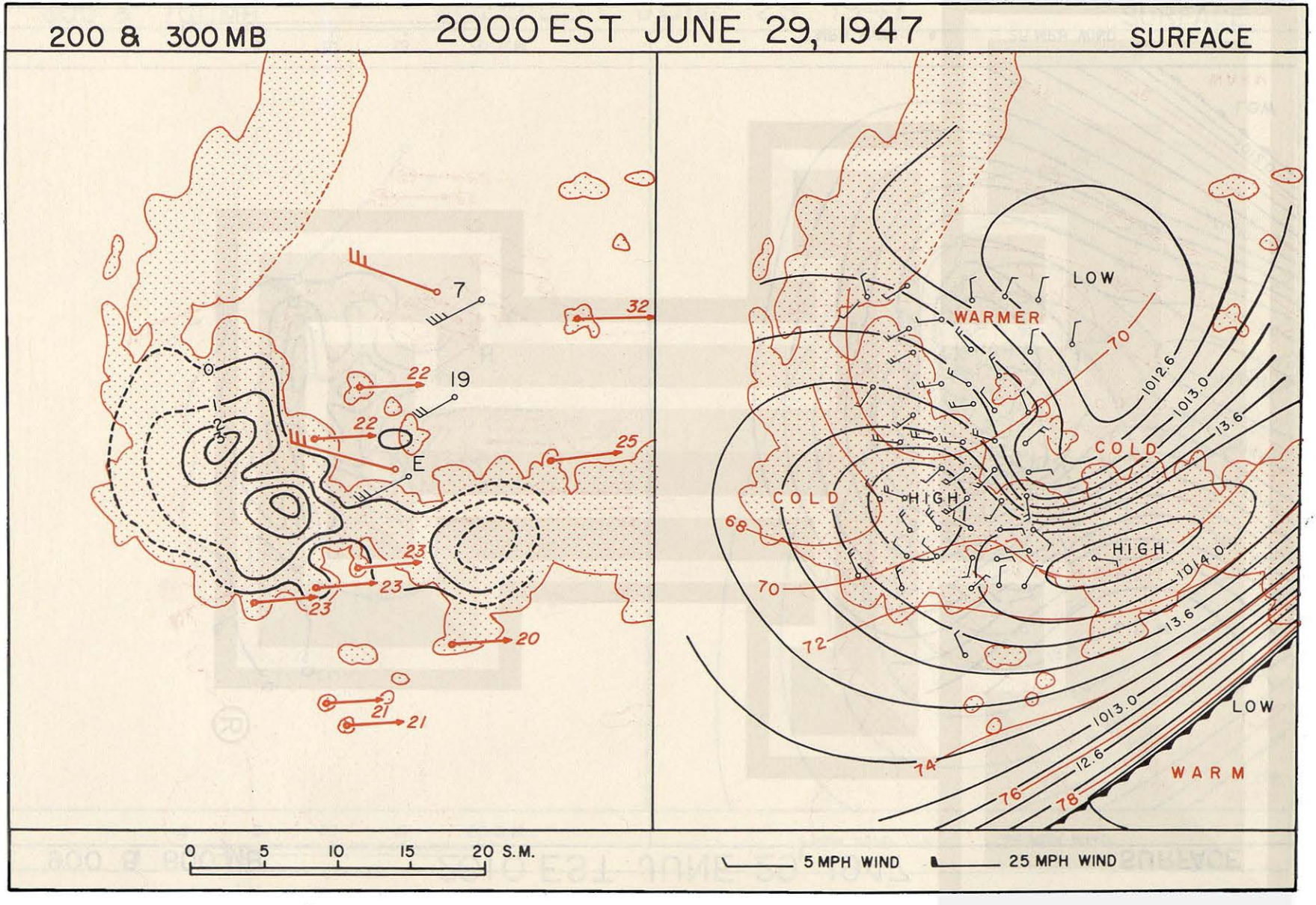
200 & 300 MB
2000 EST JUNE 29, 1947
SURFACE
7
32
22
19
22
25
E
0
1
2
3
23
23
23
20
21
21
LOW
WARMER
70
1012.6
1013.0
13.6
COLD
COLD
HIGH
HIGH
68
70
72
1014.0
13.6
1013.0
LOW
74
12.6
WARM
76
78
0 5 10 15 20 S.M.
5 MPH WIND
25 MPH WIND

FIGURE 39

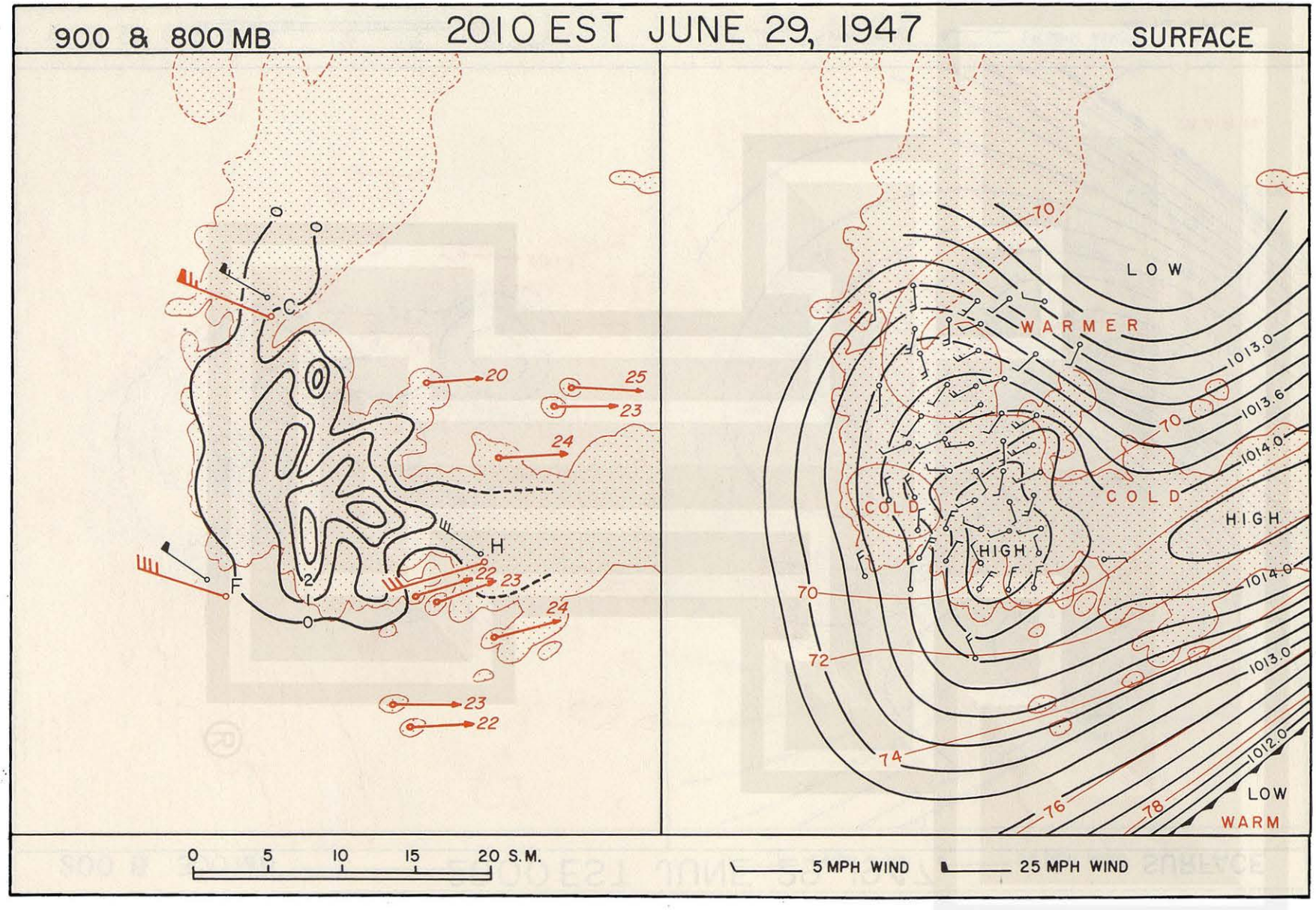
900 & 800 MB
2010 EST JUNE 29, 1947
SURFACE
C
F
H
20
25
23
24
22
23
24
23
22
LOW
WARMER
70
1013.0
1013.6
70
1014.0
COLD
COLD
HIGH
HIGH
1014.0
70
72
1013.0
74
1012.0
76
78
LOW
WARM
0 5 10 15 20 S.M.
5 MPH WIND
25 MPH WIND

FIGURE 40

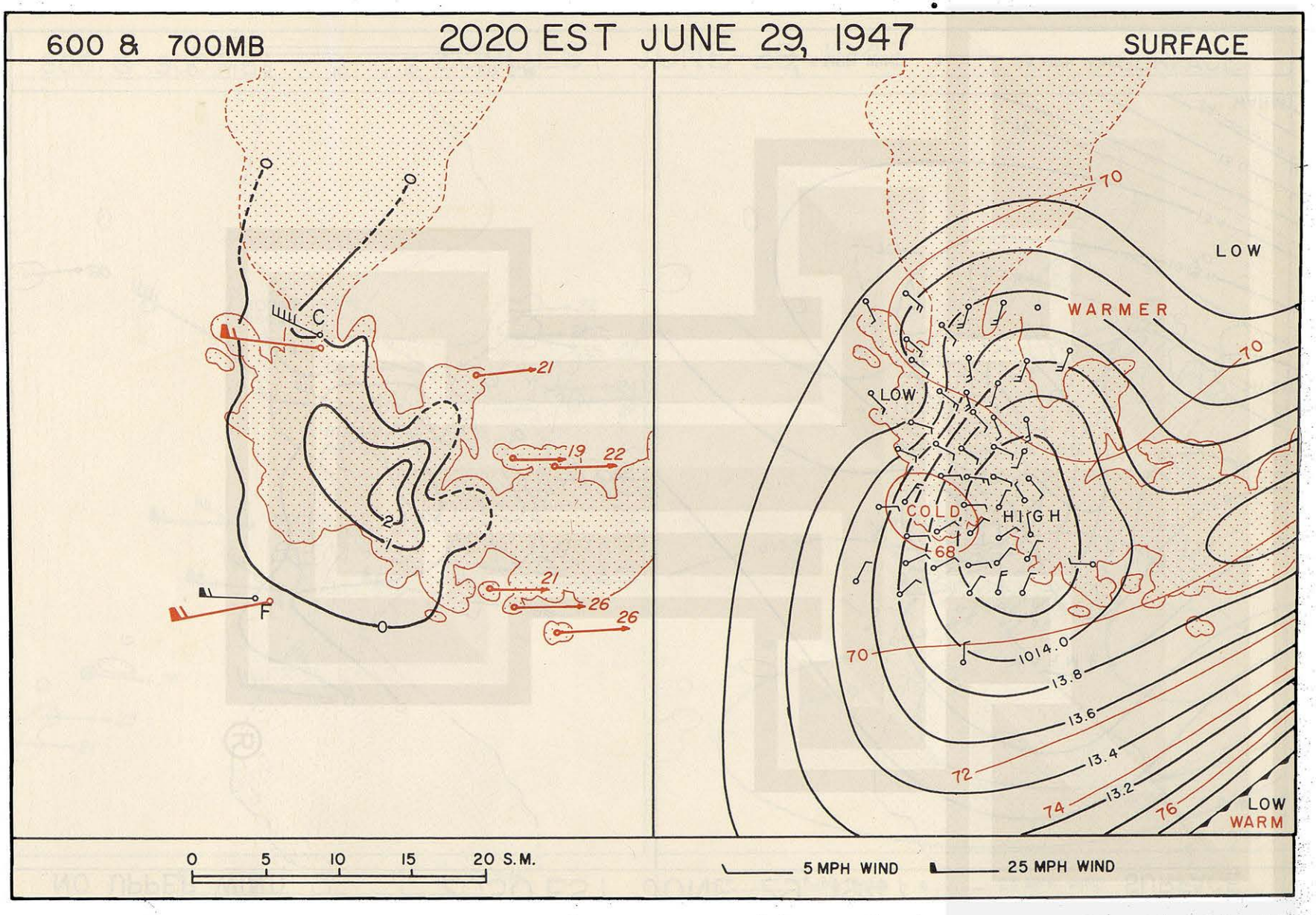
600 & 700MB
2020 EST JUNE 29, 1947
SURFACE
C
F
21
19
22
21
26
26
LOW
WARMER
LOW
COLD
HIGH
68
F
70
70
70
1014.0
13.8
13.6
13.4
13.2
72
74
76
LOW
WARM
0 5 10 15 20 S.M.
5 MPH WIND
25 MPH WIND

FIGURE 41

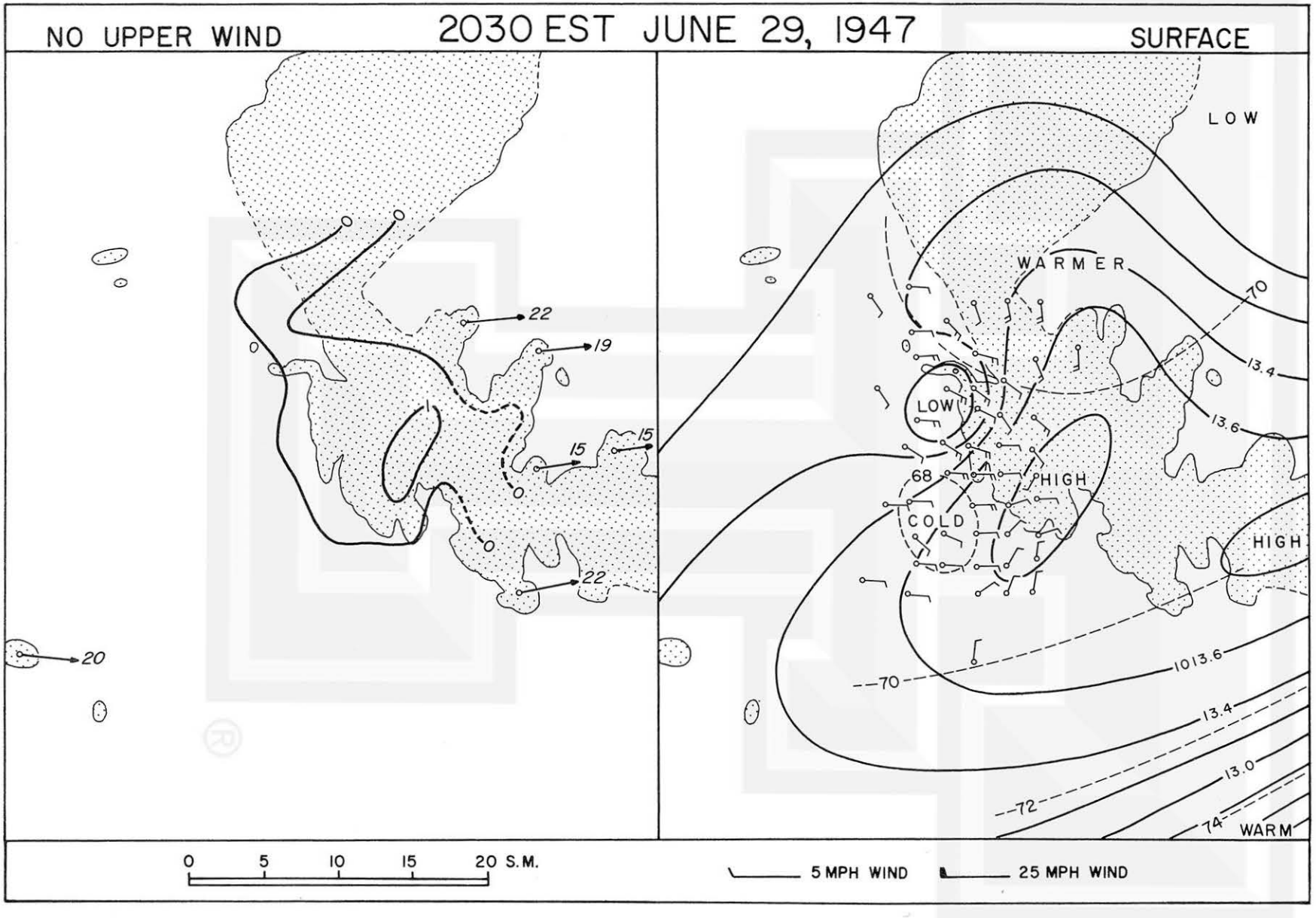
NO UPPER WIND
2030 EST JUNE 29, 1947
SURFACE
LOW
WARMER
70
13.4
13.6
LOW
68
HIGH
COLD
HIGH
1013.6
70
13.4
13.0
72
74
WARM
22
19
15
15
0
22
20
0 5 10 15 20 S.M.
5 MPH WIND
25 MPH WIND

FIGURE 42

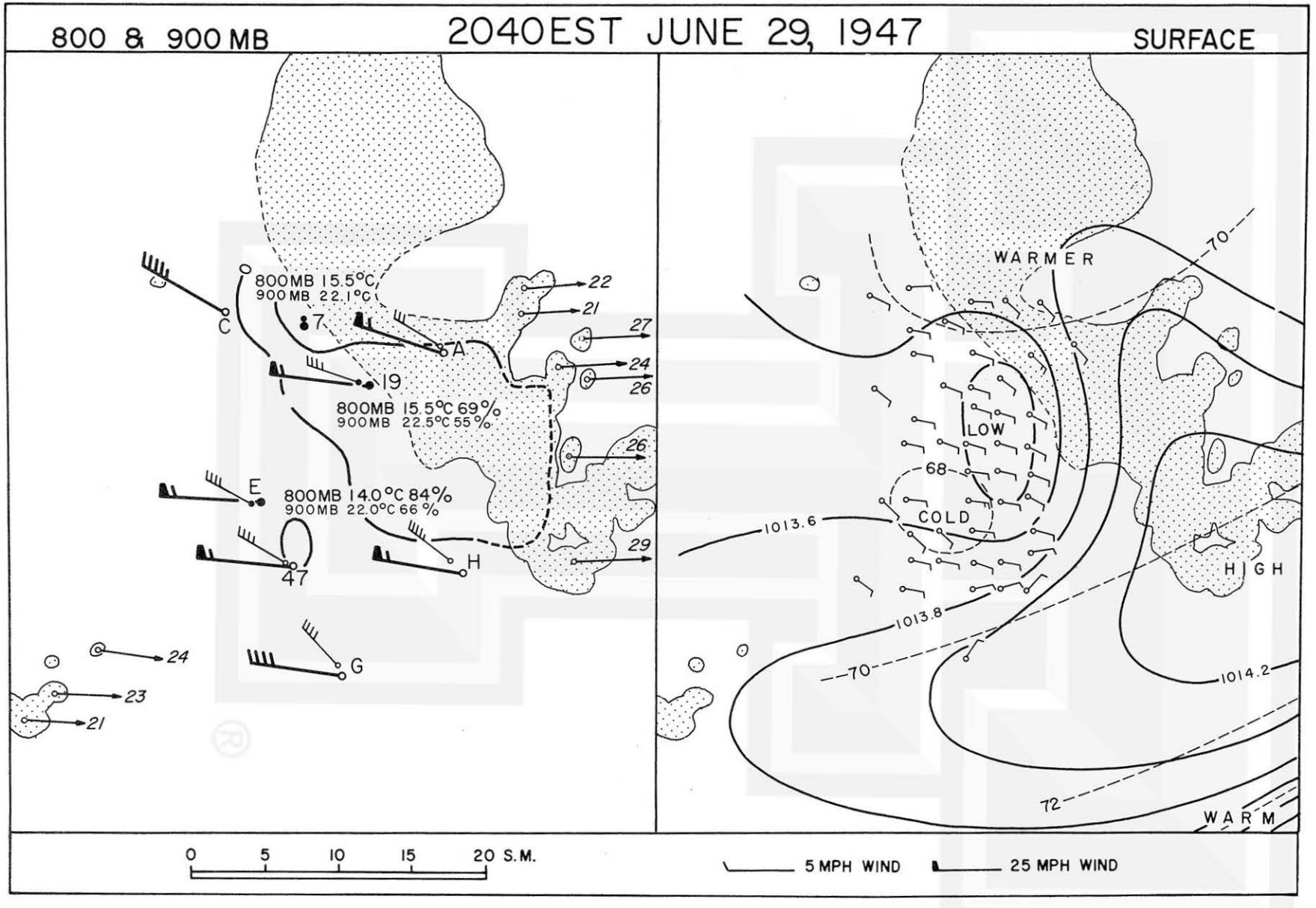
800 & 900 MB
2040 EST JUNE 29, 1947
SURFACE
800MB 15.5°C
900MB 22.1°C
7
C
A
19
800MB 15.5°C 69%
900MB 22.5°C 55%
22
21
27
24
26
26
E
800MB 14.0°C 84%
900MB 22.0°C 66%
47
H
29
G
24
23
21
WARMER
70
LOW
68
COLD
1013.6
1013.8
70
1014.2
HIGH
72
WARM
0 5 10 15 20 S.M.
5 MPH WIND
25 MPH WIND

FIGURE 43

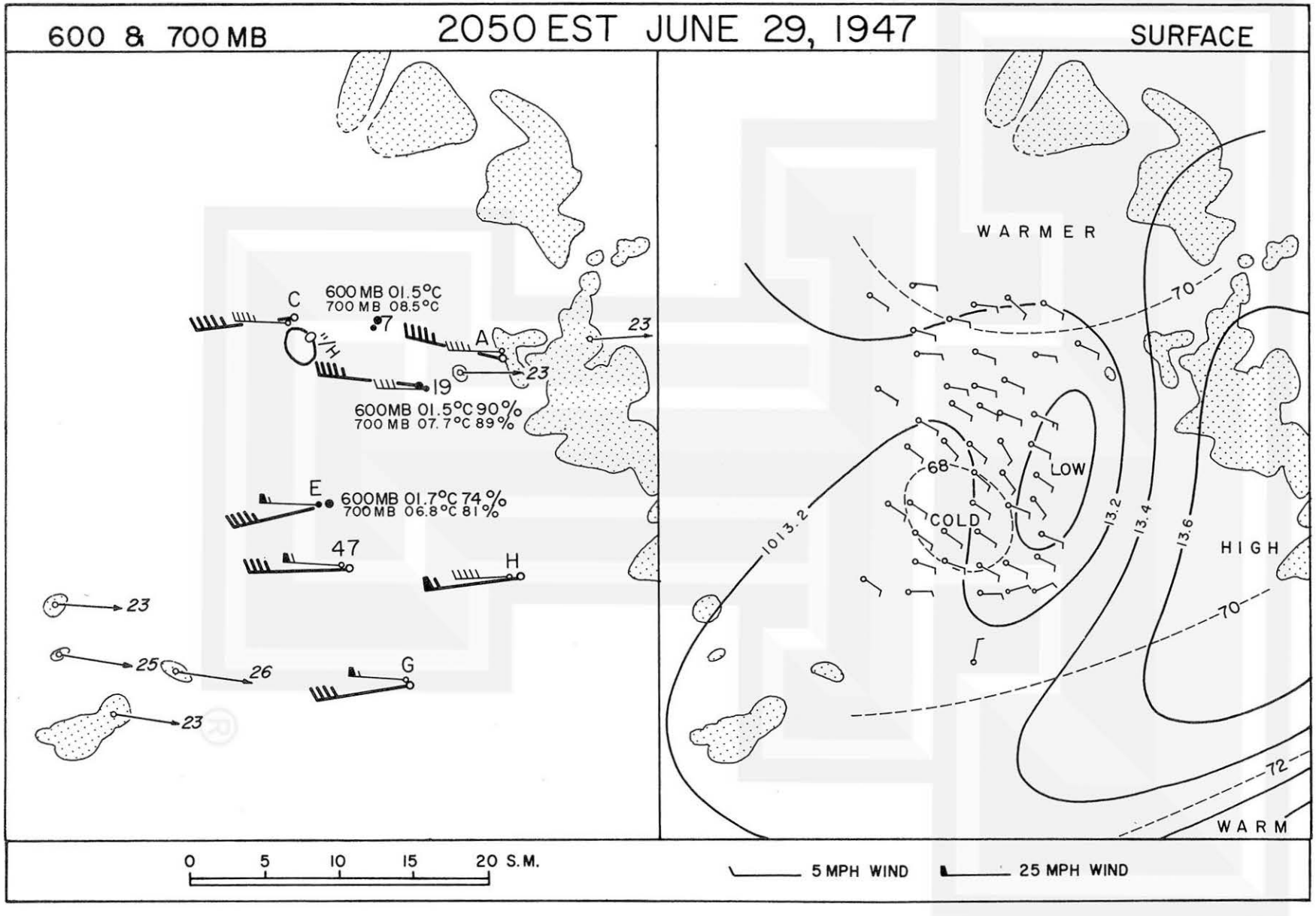
600 & 700 MB
2050 EST JUNE 29, 1947
SURFACE
600 MB 01.5°C
700 MB 08.5°C
C
7
A
23
H
19
23
600MB 01.5°C 90%
700 MB 07.7°C 89%
E
600MB 01.7°C 74%
700 MB 06.8°C 81%
47
H
23
25
26
G
23
WARMER
70
68
LOW
COLD
1013.2
13.2
13.4
13.6
HIGH
70
72
WARM
0 5 10 15 20 S.M.
5 MPH WIND
25 MPH WIND

FIGURE 44

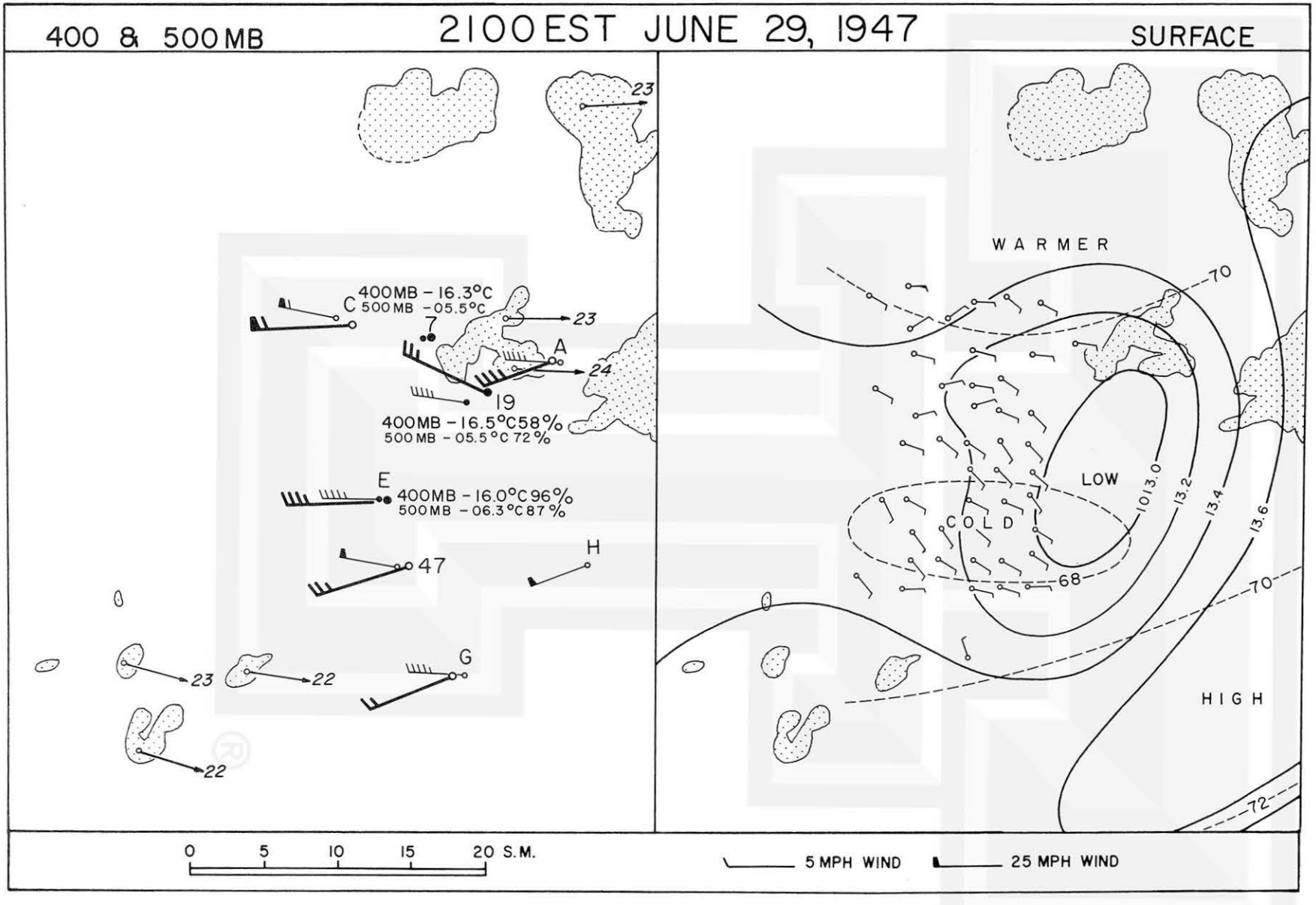
400 & 500 MB
2100 EST JUNE 29, 1947
SURFACE
23
400MB - 16.3°C
C 500MB - 05.5°C
7
23
A
24
19
400MB - 16.5°C 58%
500MB - 05.5°C 72%
E
400MB - 16.0°C 96%
500MB - 06.3°C 87%
47
H
23
22
G
22
WARMER
70
LOW
1013.0
13.2
13.4
13.6
COLD
68
70
HIGH
72
0 5 10 15 20 S.M.
5 MPH WIND
25 MPH WIND

FIGURE 45

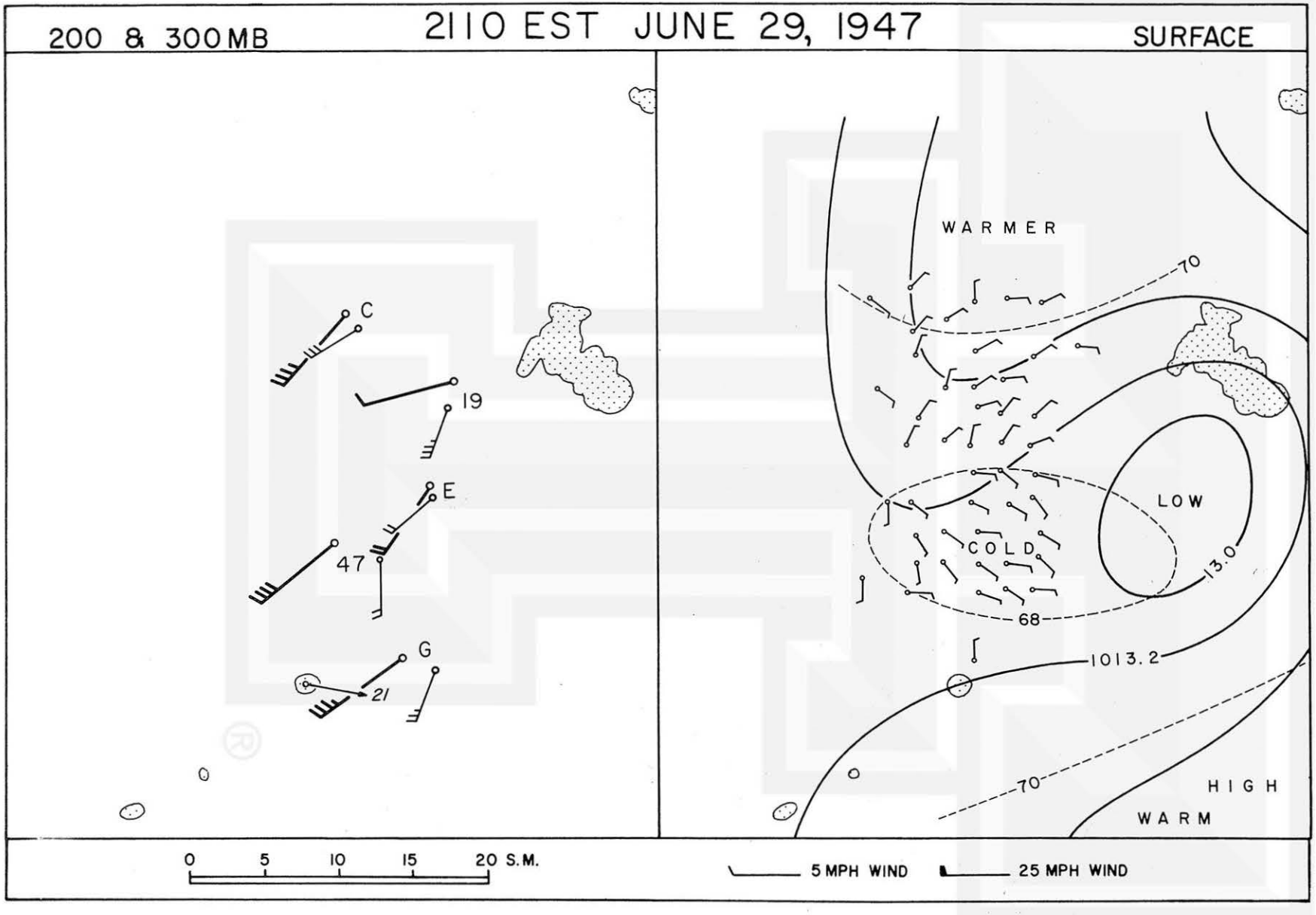
200 & 300 MB
2110 EST JUNE 29, 1947
SURFACE
C
19
E
47
G
21
WARMER
70
LOW
COLD
13.0
68
1013.2
70
HIGH
WARM
0 5 10 15 20 S.M.
5 MPH WIND
25 MPH WIND

FIGURE 46

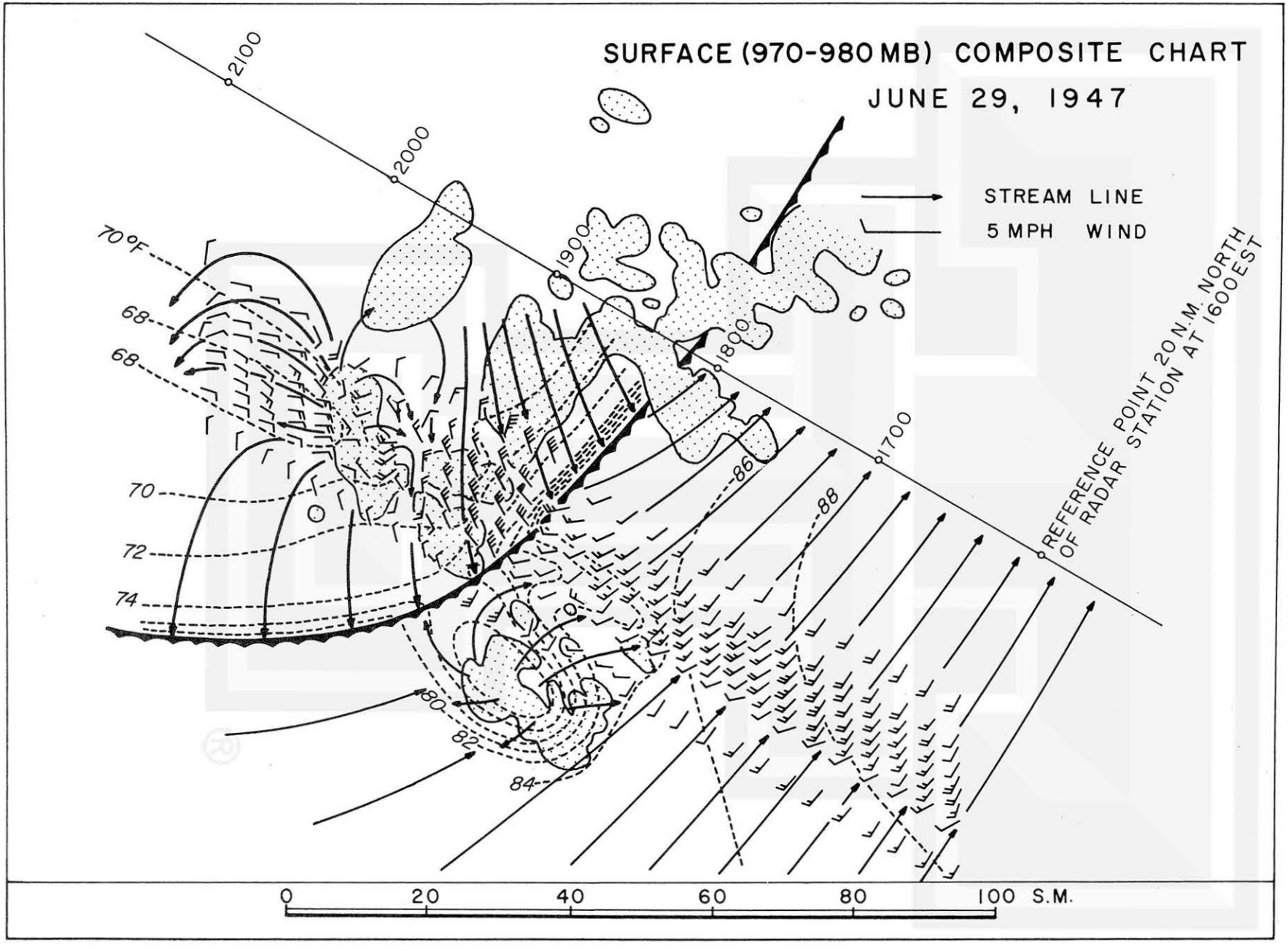
SURFACE (970-980 MB) COMPOSITE CHART
JUNE 29, 1947
STREAM LINE
5 MPH WIND
2100
2000
1900
1800
1700
REFERENCE POINT 20 N.M. NORTH OF RADAR STATION AT 1600 EST
70°F
68
68
70
72
74
80
82
84
86
88
0
20
40
60
80
100 S.M.

FIGURE 47

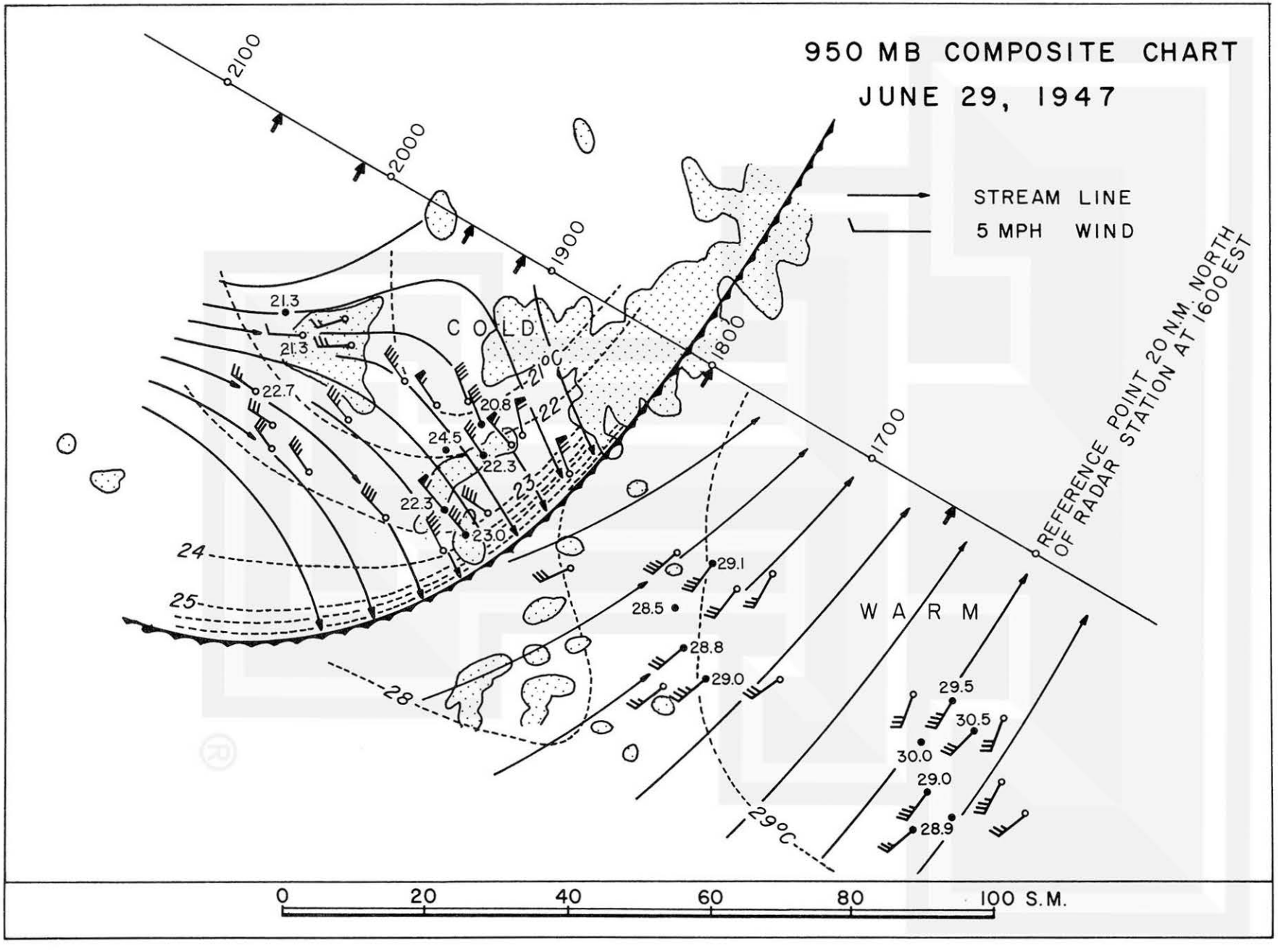
950 MB COMPOSITE CHART
JUNE 29, 1947
STREAM LINE
5 MPH WIND
2100
2000
1900
1800
1700
REFERENCE POINT 20 N.M. NORTH OF RADAR STATION AT 1600 EST
COLD
WARM
21°C
22
23
24
25
28
29°C
21.3
21.3
22.7
20.8
24.5
22.3
22.3
23.0
29.1
28.5
28.8
29.0
29.5
30.5
30.0
29.0
28.9
0
20
40
60
80
100 S.M.

FIGURE 48

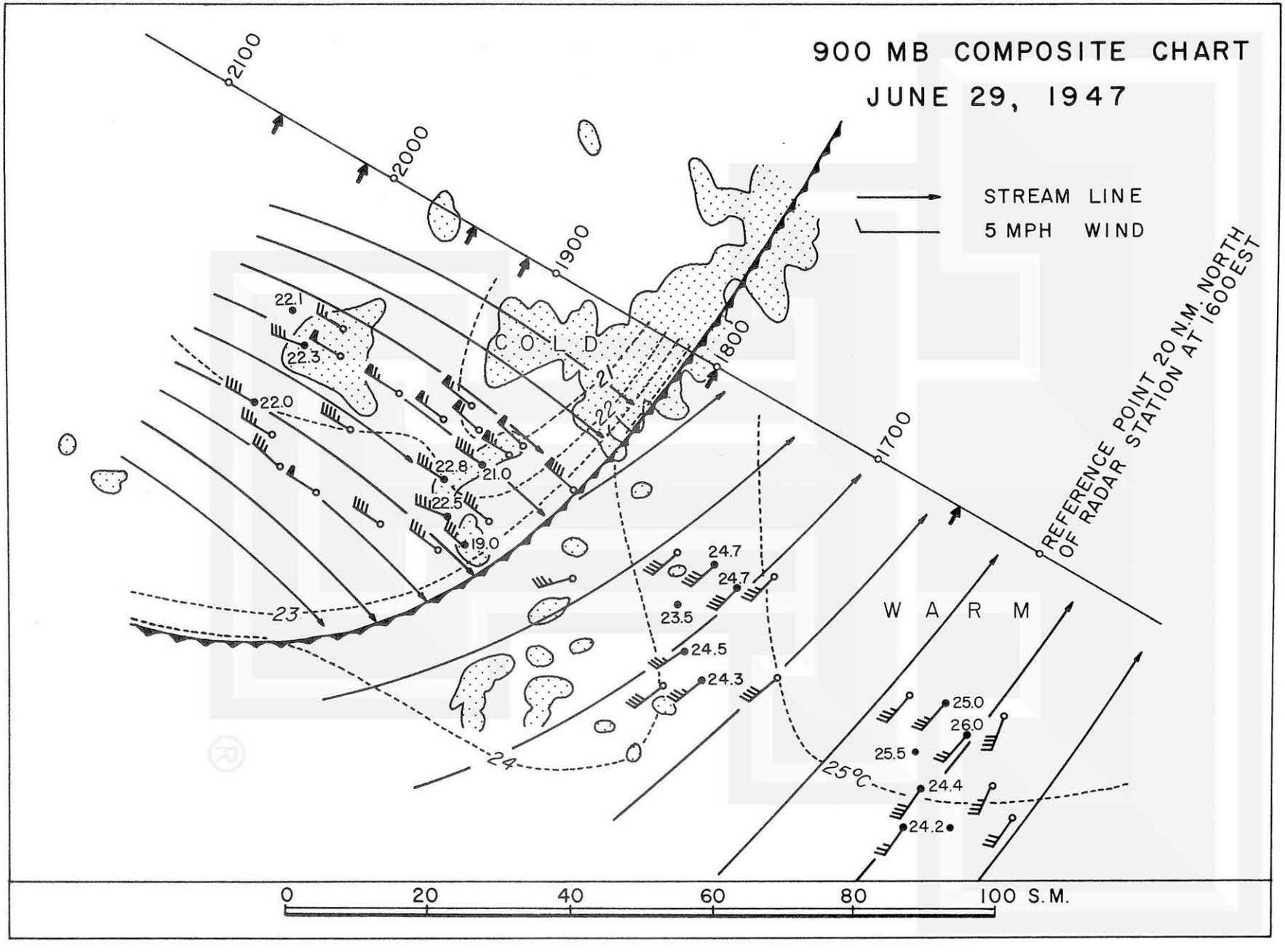
900 MB COMPOSITE CHART
JUNE 29, 1947
STREAM LINE
5 MPH WIND
2100
2000
1900
1800
1700
REFERENCE POINT 20 N.M. NORTH OF RADAR STATION AT 1600EST
COLD
WARM
22.1
22.3
22.0
22.8
21.0
22.5
19.0
21
22
23
24.7
24.7
23.5
24.5
24.3
24
25.0
26.0
25.5
25°C
24.4
24.2
0
20
40
60
80
100 S.M.

FIGURE 49

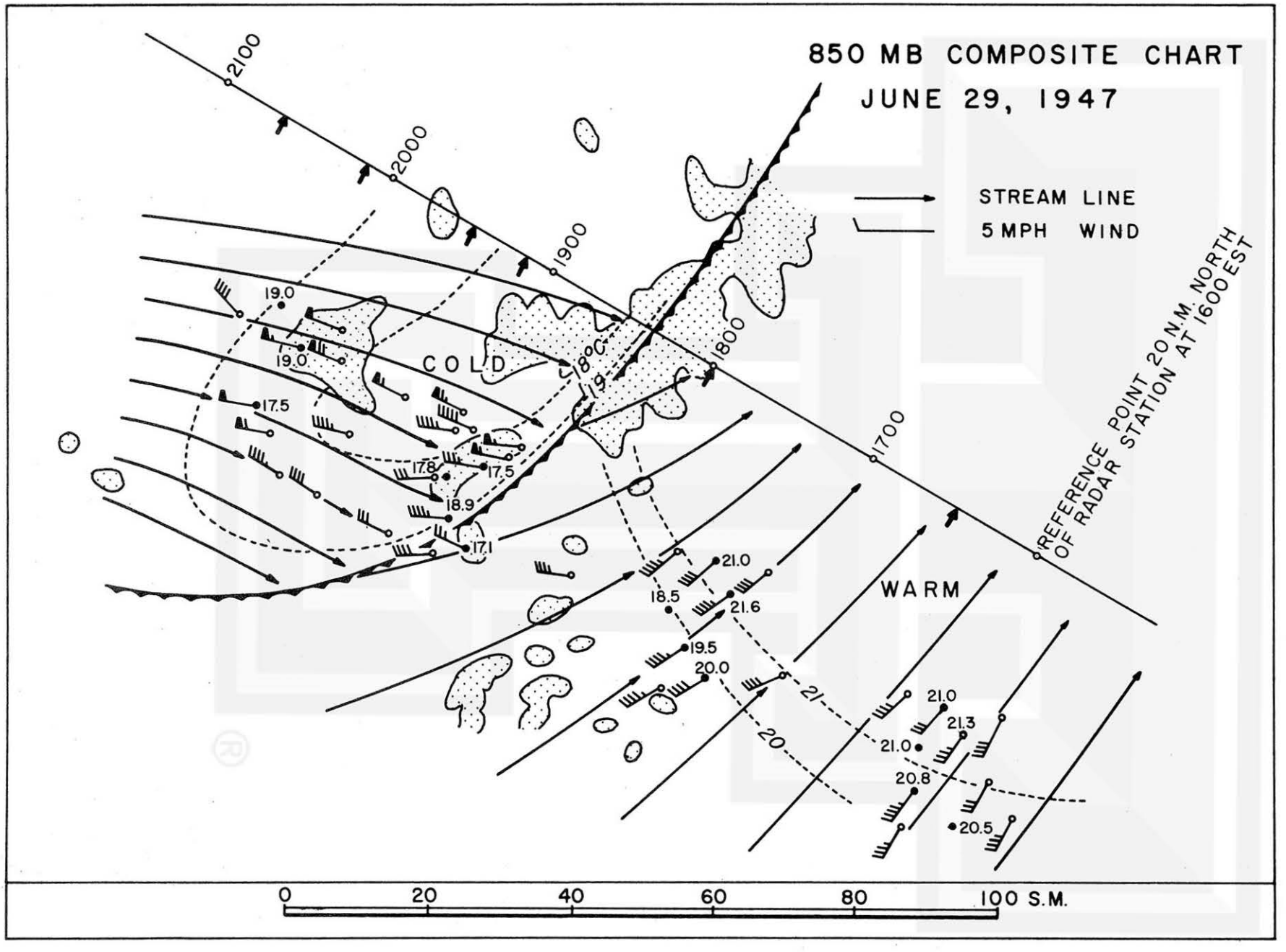
850 MB COMPOSITE CHART
JUNE 29, 1947
STREAM LINE
5 MPH WIND
2100
2000
1900
1800
1700
REFERENCE POINT 20 N.M. NORTH OF RADAR STATION AT 1600 EST
COLD
WARM
18°C
19
19.0
19.0
17.5
17.8
17.5
18.9
17.1
18.5
21.0
21.6
19.5
20.0
21
20
21.0
21.3
21.0
20.8
20.5
0
20
40
60
80
100 S.M.

FIGURE 50

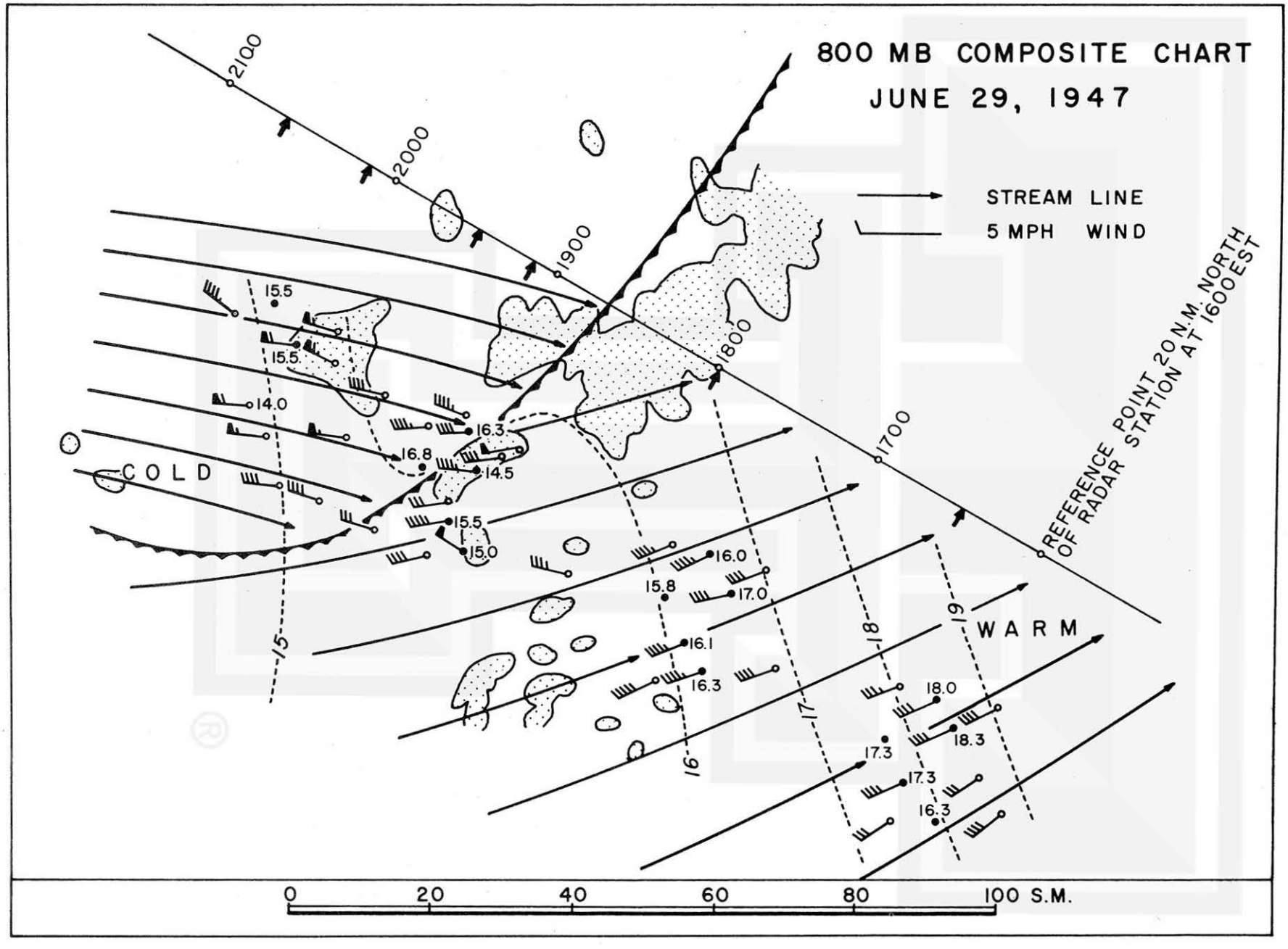
800 MB COMPOSITE CHART
JUNE 29, 1947
STREAM LINE
5 MPH WIND
2100
2000
1900
1800
1700
REFERENCE POINT 20 N.M. NORTH OF RADAR STATION AT 1600 EST
COLD
WARM
15.5
15.5
14.0
16.3
16.8
14.5
15.5
15.0
16.0
15.8
17.0
16.1
16.3
18.0
18.3
17.3
17.3
16.3
15
16
17
18
19
0
20
40
60
80
100 S.M.

FIGURE 51

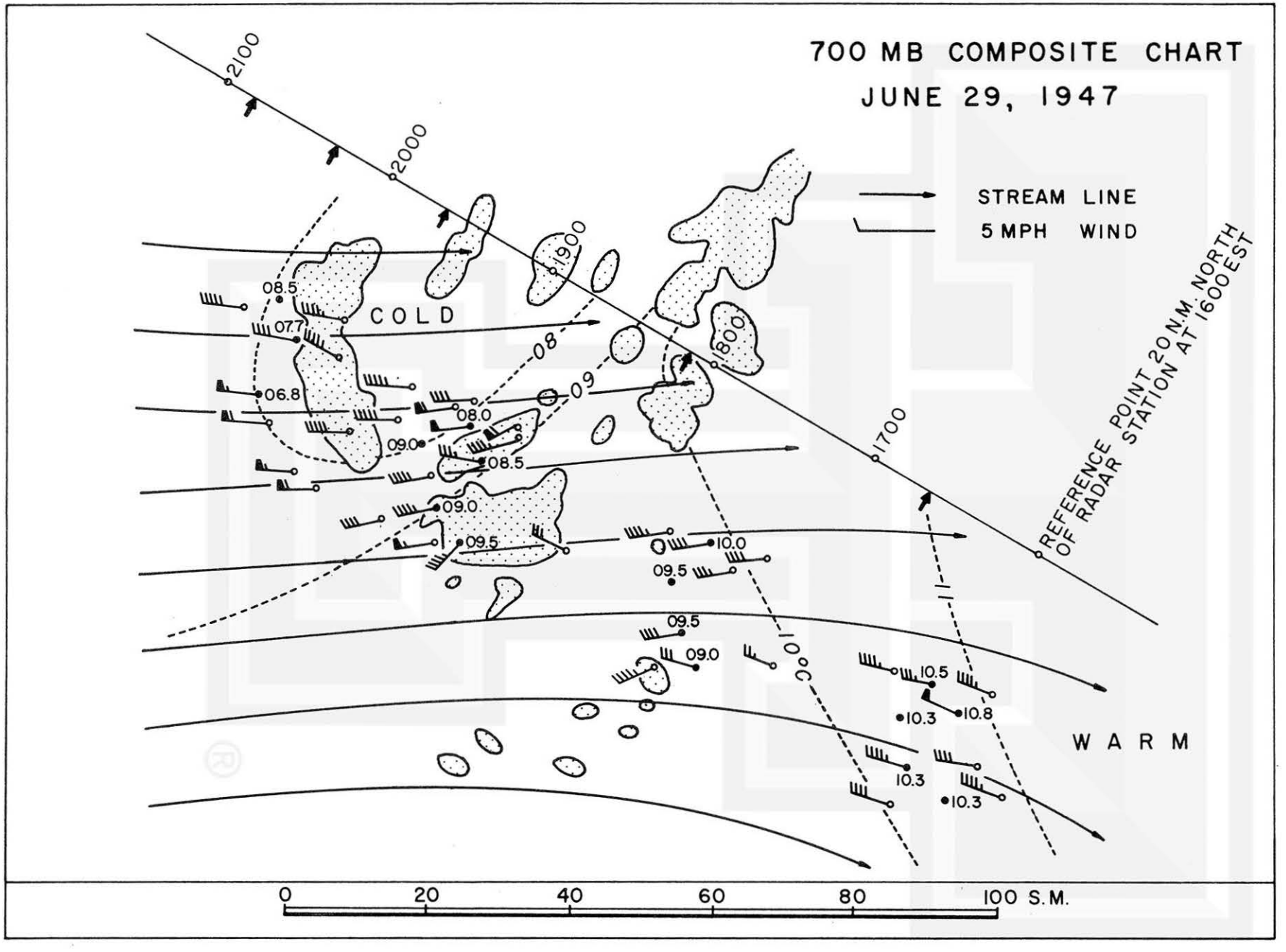
700 MB COMPOSITE CHART
JUNE 29, 1947
STREAM LINE
5 MPH WIND
2100
2000
1900
1800
1700
REFERENCE POINT 20 N.M. NORTH OF RADAR STATION AT 1600 EST
COLD
WARM
08.5
07.7
06.8
08.0
09.0
08.5
09.0
09.5
10.0
09.5
09.5
09.0
10.5
10.3
10.8
10.3
10.3
08
09
10
11
0
20
40
60
80
100 S.M.

FIGURE 52

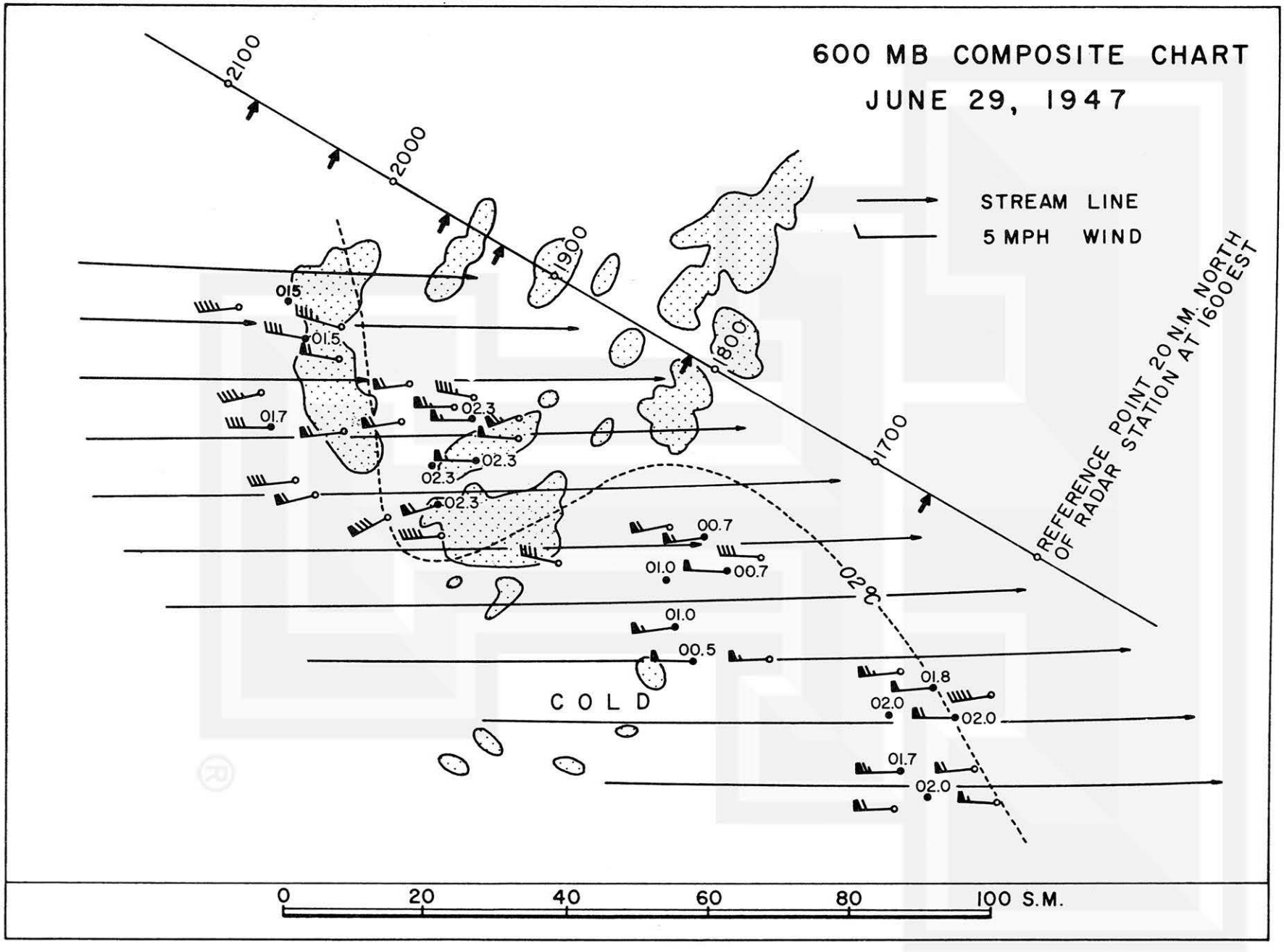
600 MB COMPOSITE CHART
JUNE 29, 1947
STREAM LINE
5 MPH WIND
2100
2000
1900
1800
1700
REFERENCE POINT 20 N.M. NORTH OF RADAR STATION AT 1600 EST
015
01.5
01.7
02.3
02.3
02.3
02.3
00.7
01.0
00.7
01.0
00.5
02C
COLD
01.8
02.0
02.0
01.7
02.0
0
20
40
60
80
100 S.M.

FIGURE 53

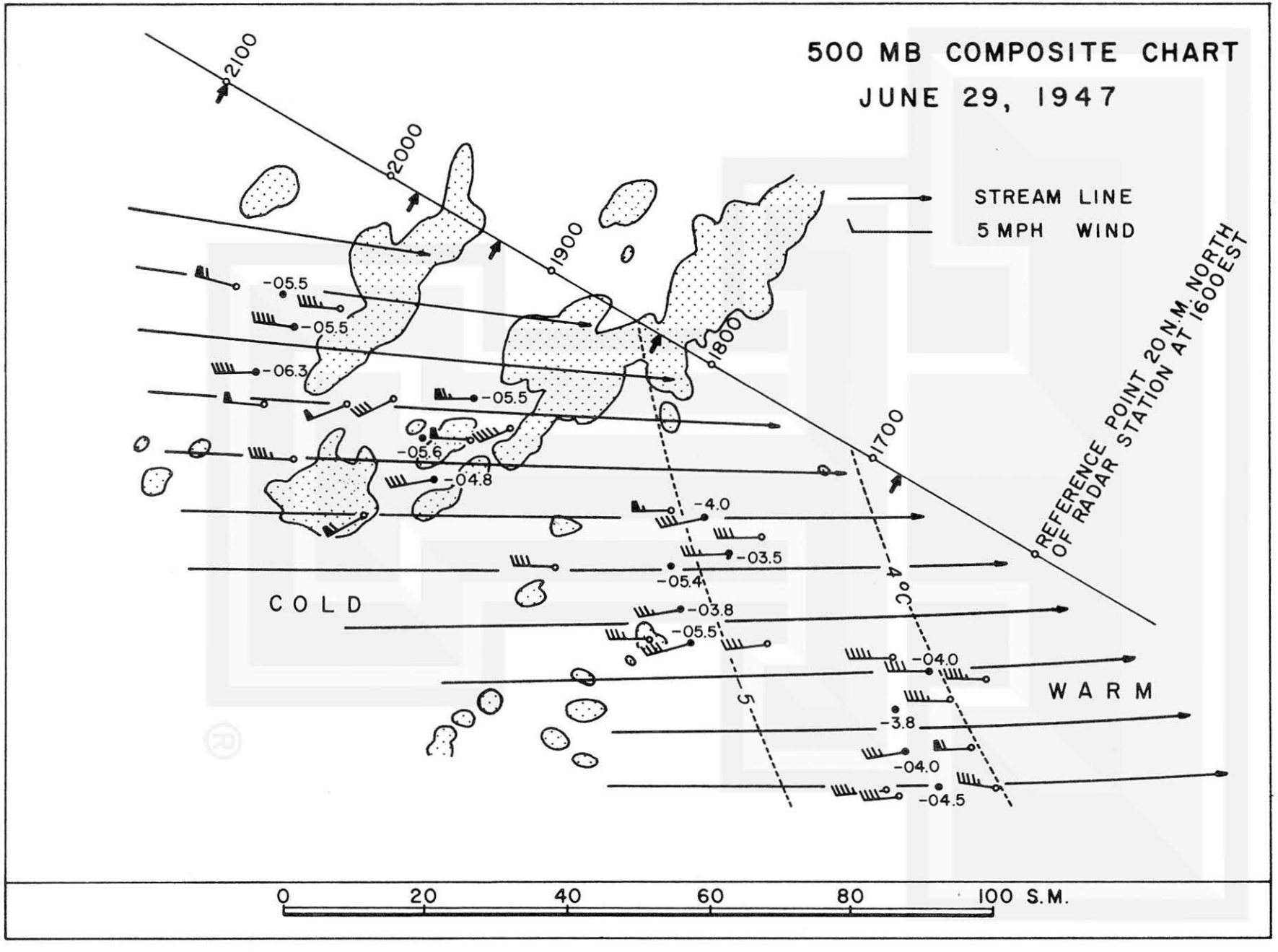
500 MB COMPOSITE CHART
JUNE 29, 1947
STREAM LINE
5 MPH WIND
2100
2000
1900
1800
1700
REFERENCE POINT 20 N.M. NORTH OF RADAR STATION AT 1600 EST
-05.5
-05.5
-06.3
-05.5
-05.6
-04.8
-4.0
-03.5
-05.4
-03.8
-05.5
-04.0
-3.8
-04.0
-04.5
COLD
WARM
-4°C
-5
0
20
40
60
80
100 S.M.

FIGURE 54

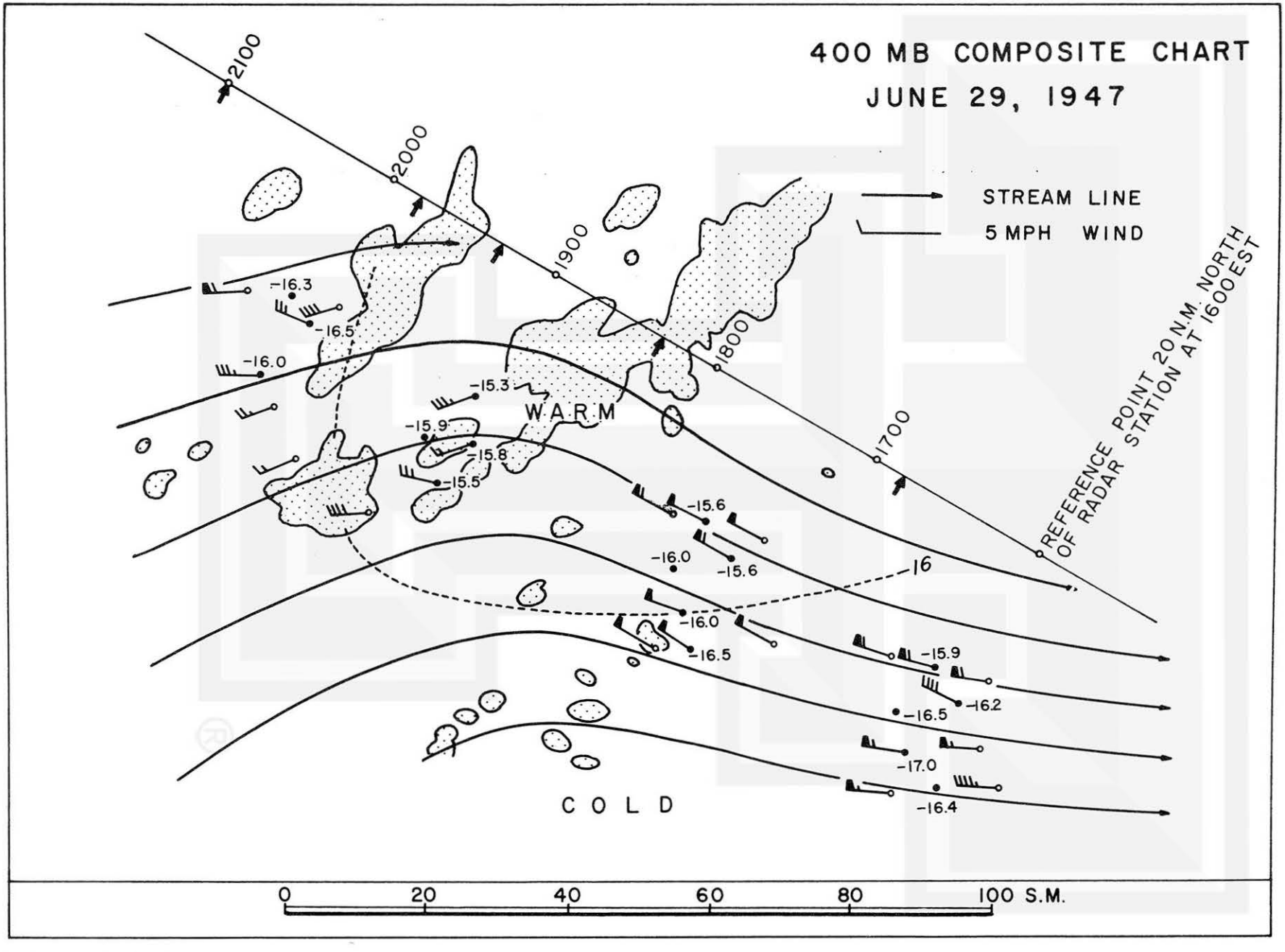
400 MB COMPOSITE CHART
JUNE 29, 1947
STREAM LINE
5 MPH WIND
2100
2000
1900
1800
1700
REFERENCE POINT 20 N.M. NORTH OF RADAR STATION AT 1600 EST
-16.3
-16.5
-16.0
-15.3
-15.9
-15.8
-15.5
WARM
-15.6
-16.0
-15.6
16
-16.0
-16.5
-15.9
-16.2
-16.5
-17.0
-16.4
COLD
0
20
40
60
80
100 S.M.

FIGURE 55

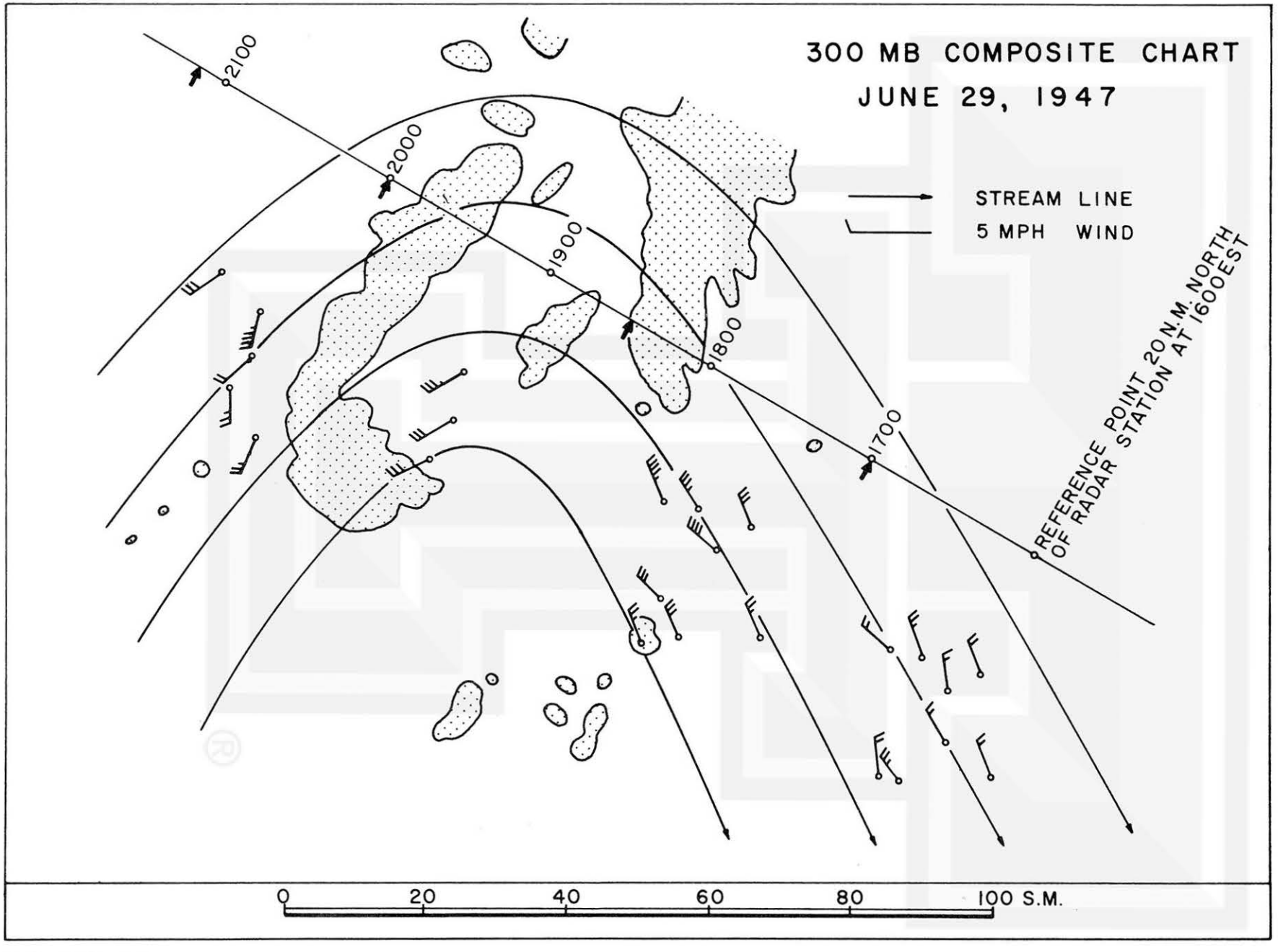
300 MB COMPOSITE CHART
JUNE 29, 1947
STREAM LINE
5 MPH WIND
2100
2000
1900
1800
1700
REFERENCE POINT 20 N.M. NORTH OF RADAR STATION AT 1600EST
0
20
40
60
80
100 S.M.

FIGURE 56

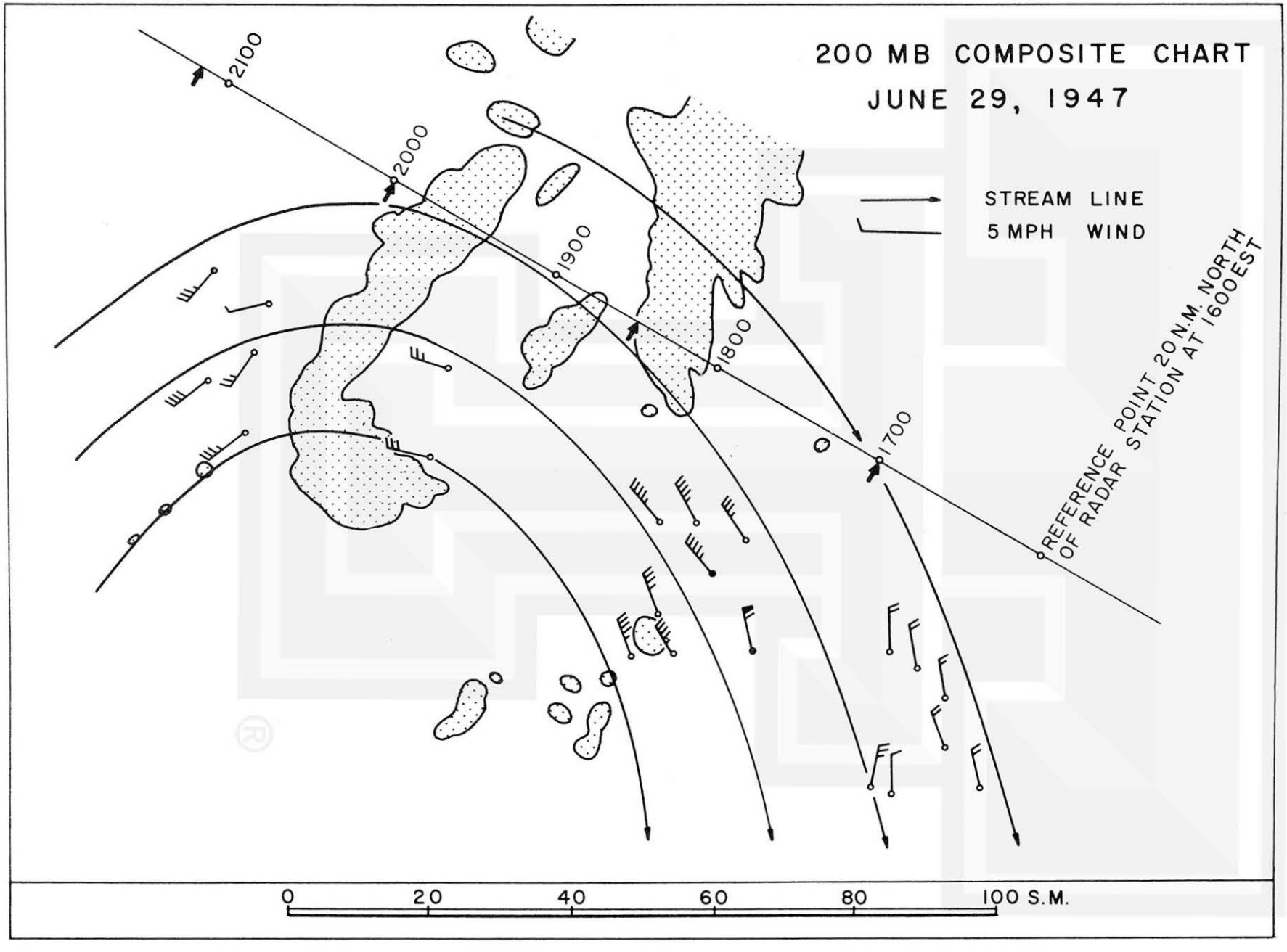
200 MB COMPOSITE CHART
JUNE 29, 1947
STREAM LINE
5 MPH WIND
2100
2000
1900
1800
1700
REFERENCE POINT 20 N.M. NORTH OF RADAR STATION AT 1600 EST
0
20
40
60
80
100 S.M.

FIGURE 57

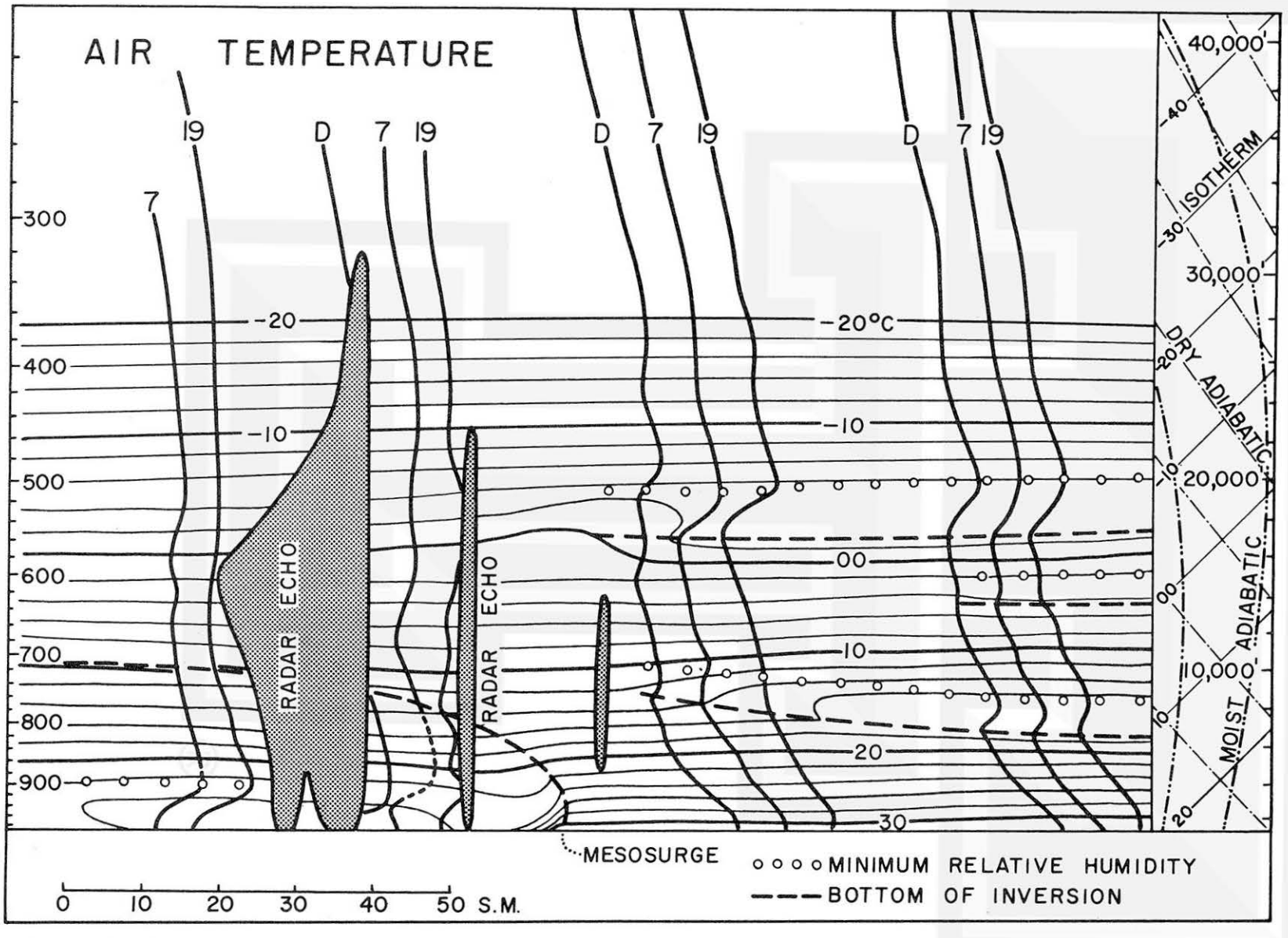
AIR TEMPERATURE
19
D
7
19
D
7
19
D
7
19
7
300
400
500
600
700
800
900
-20
-10
-20°C
-10
00
10
20
30
RADAR ECHO
RADAR ECHO
MESOSURGE
0
10
20
30
40
50 S.M.
MINIMUM RELATIVE HUMIDITY
BOTTOM OF INVERSION
40,000'
40
ISOTHERM
30
30,000
DRY ADIABATIC
20
20,000
00
10
10,000'
MOIST ADIABATIC
10
20

FIGURE 58

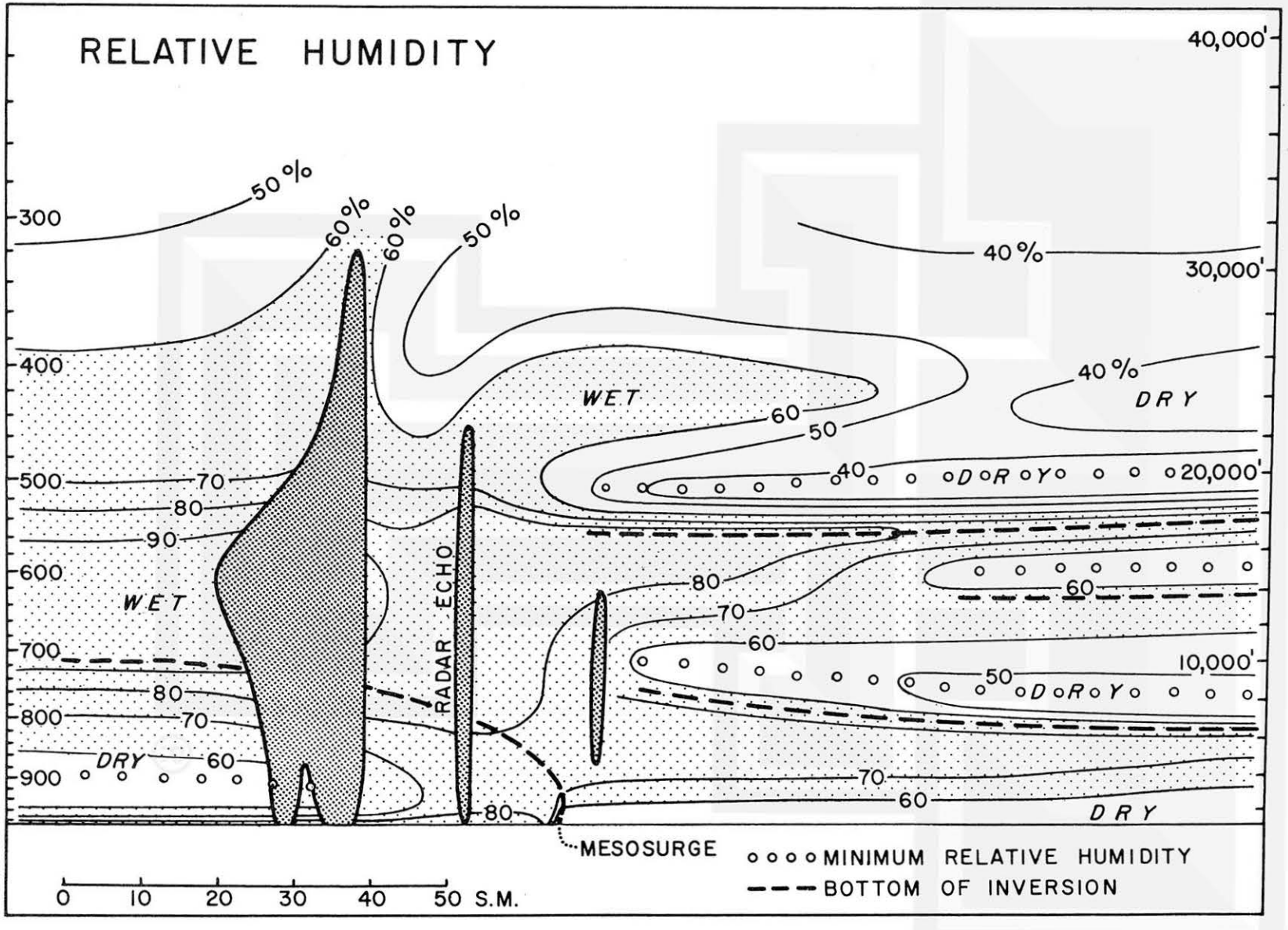
RELATIVE HUMIDITY
40,000'
30,000'
20,000'
10,000'
300
400
500
600
700
800
900
50 %
60 %
60 %
50 %
40 %
40 %
WET
WET
DRY
DRY
DRY
DRY
DRY
60
50
40
70
80
90
80
70
60
80
70
60
50
60
70
60
80
RADAR ECHO
MESOSURGE
0 10 20 30 40 50 S.M.
MINIMUM RELATIVE HUMIDITY
BOTTOM OF INVERSION

FIGURE 59

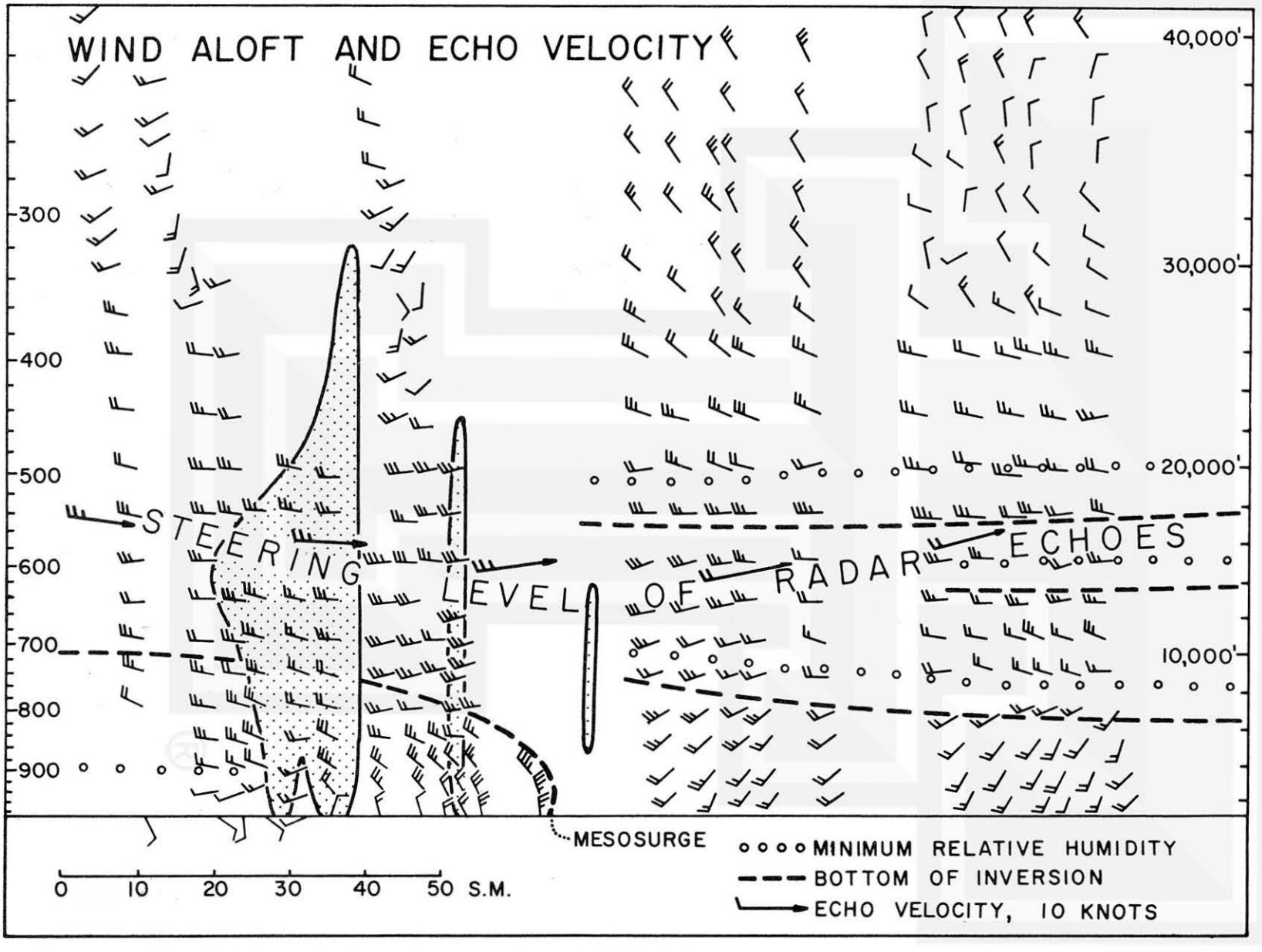
WIND ALOFT AND ECHO VELOCITY
40,000'
30,000'
20,000'
10,000'
300
400
500
600
700
800
900
STEERING LEVEL OF RADAR ECHOES
MESOSURGE
0 10 20 30 40 50 S.M.
MINIMUM RELATIVE HUMIDITY
BOTTOM OF INVERSION
ECHO VELOCITY, 10 KNOTS

FIGURE 60

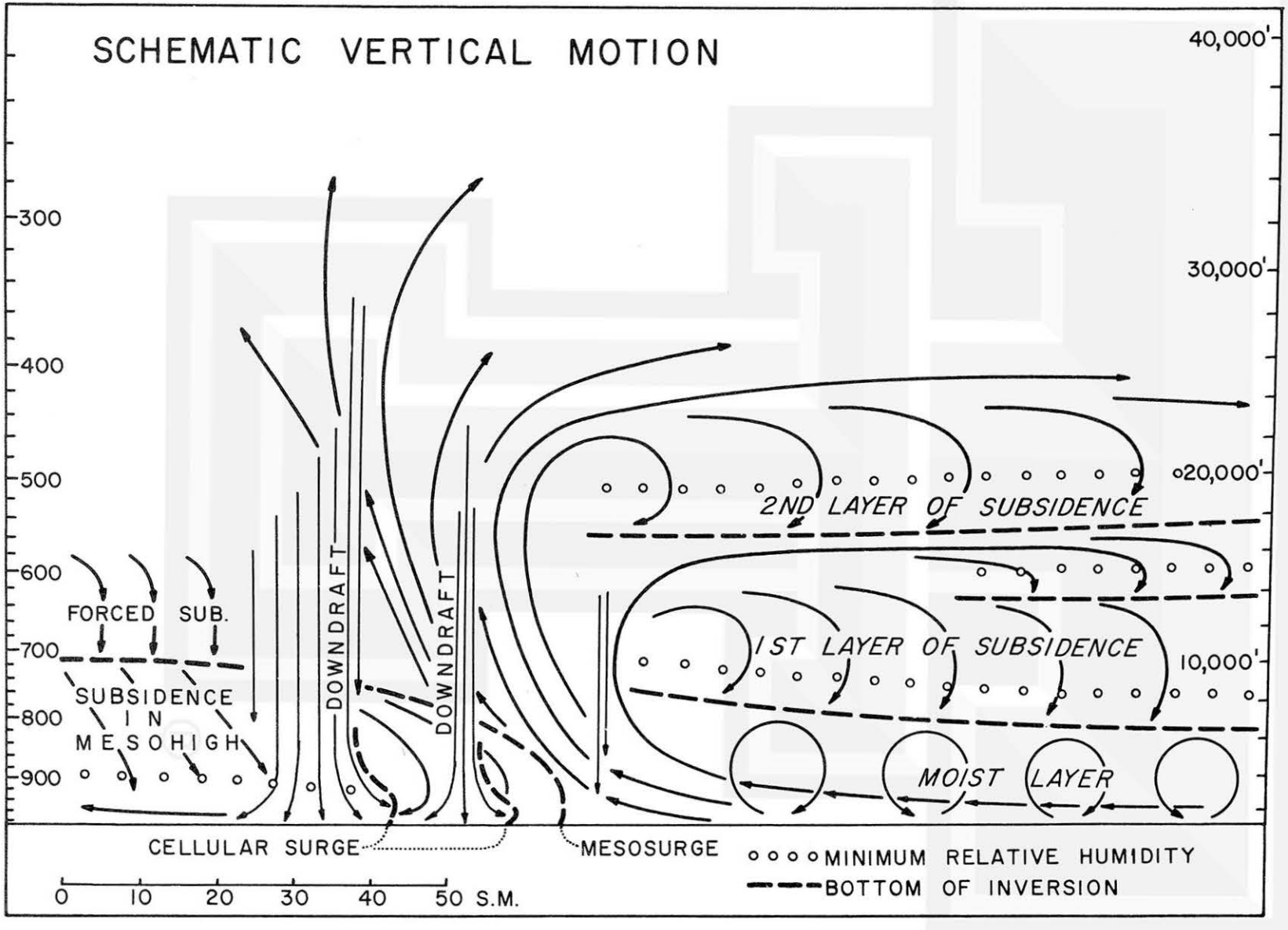
SCHEMATIC VERTICAL MOTION
40,000'
30,000'
20,000'
10,000'
300
400
500
600
700
800
900
FORCED SUB.
SUBSIDENCE IN MESOHIGH
DOWNDRAFT
DOWNDRAFT
2ND LAYER OF SUBSIDENCE
1ST LAYER OF SUBSIDENCE
MOIST LAYER
CELLULAR SURGE
MESOSURGE
MINIMUM RELATIVE HUMIDITY
BOTTOM OF INVERSION
0 10 20 30 40 50 S.M.

FIGURE 61